



University of Kentucky
UKnowledge

Theses and Dissertations--Molecular and
Cellular Biochemistry

Molecular and Cellular Biochemistry

2016

ELUCIDATING BINDING, FUSION AND ENTRY OF HUMAN METAPNEUMOVIRUS

Edita M. Klimyte

University of Kentucky, miss.edita@gmail.com

Digital Object Identifier: <http://dx.doi.org/10.13023/ETD.2016.337>

[Right click to open a feedback form in a new tab to let us know how this document benefits you.](#)

Recommended Citation

Klimyte, Edita M., "ELUCIDATING BINDING, FUSION AND ENTRY OF HUMAN METAPNEUMOVIRUS" (2016). *Theses and Dissertations--Molecular and Cellular Biochemistry*. 28.
https://uknowledge.uky.edu/biochem_etds/28

This Doctoral Dissertation is brought to you for free and open access by the Molecular and Cellular Biochemistry at UKnowledge. It has been accepted for inclusion in Theses and Dissertations--Molecular and Cellular Biochemistry by an authorized administrator of UKnowledge. For more information, please contact UKnowledge@lsv.uky.edu.

STUDENT AGREEMENT:

I represent that my thesis or dissertation and abstract are my original work. Proper attribution has been given to all outside sources. I understand that I am solely responsible for obtaining any needed copyright permissions. I have obtained needed written permission statement(s) from the owner(s) of each third-party copyrighted matter to be included in my work, allowing electronic distribution (if such use is not permitted by the fair use doctrine) which will be submitted to UKnowledge as Additional File.

I hereby grant to The University of Kentucky and its agents the irrevocable, non-exclusive, and royalty-free license to archive and make accessible my work in whole or in part in all forms of media, now or hereafter known. I agree that the document mentioned above may be made available immediately for worldwide access unless an embargo applies.

I retain all other ownership rights to the copyright of my work. I also retain the right to use in future works (such as articles or books) all or part of my work. I understand that I am free to register the copyright to my work.

REVIEW, APPROVAL AND ACCEPTANCE

The document mentioned above has been reviewed and accepted by the student's advisor, on behalf of the advisory committee, and by the Director of Graduate Studies (DGS), on behalf of the program; we verify that this is the final, approved version of the student's thesis including all changes required by the advisory committee. The undersigned agree to abide by the statements above.

Edita M. Klimyte, Student

Dr. Rebecca E. Dutch, Major Professor

Dr. Michael Mendenhall, Director of Graduate Studies

ELUCIDATING BINDING, FUSION AND ENTRY OF HUMAN METAPNEUMOVIRUS

DISSERTATION

A dissertation submitted in partial fulfillment of the
requirements for the degree of Doctor of Philosophy in the
College of Medicine
at the University of Kentucky

By
Edita Klimyte

Lexington, Kentucky

Director: Dr. Rebecca E. Dutch, Professor of Biochemistry

Lexington, Kentucky

2016

Copyright © Edita Klimyte 2016

ABSTRACT OF DISSERTATION

ELUCIDATING BINDING, FUSION AND ENTRY OF HUMAN METAPNEUMOVIRUS

Human metapneumovirus (HMPV) is a respiratory pathogen in the *Paramyxoviridae* family that infects nearly 100% of the world population. This enveloped RNA virus causes severe viral respiratory disease in infants, the elderly, and immunocompromised patients worldwide. Despite its prevalence and importance to human health, no therapies are available against this pathogen. Entry of paramyxoviruses into host cells generally requires the coordinated activity of the attachment glycoprotein, G, which interacts with a cell receptor, and the fusion glycoprotein, F, which promotes subsequent fusion of viral and cellular membranes. However, HMPV F is the primary viral protein mediating both binding and fusion for HMPV. Previous work that showed HMPV F mediates attachment to heparan sulfate proteoglycans (HSPGs), and some HMPV F fusion activity can be promoted by acidic pH. The work presented here provides significant advances in our understanding of the fusion and binding events during HMPV infection. We demonstrated that low pH promotes fusion in HMPV F proteins from diverse clades, challenging previously reported requirements and identifying a critical residue that enhances low pH promoted fusion. These results support our hypothesis that electrostatic interactions play a key role in HMPV F triggering and further elucidate the complexity of viral fusion proteins. Additionally, we characterized the key features of the binding interaction between HMPV and HSPGs using heparan sulfate mimetics, identifying an important sulfate modification, and demonstrated that these interactions occur at the apical surface of polarized airways tissues. We identified differences in particle binding related to the presence or absence of the HMPV G and SH glycoproteins. Lastly, we characterized paramyxovirus infection in cystic fibrosis bronchial epithelial cells, identifying a potential specific susceptibility to HMPV infection in these individuals. The work presented here contributes to our understanding of HMPV infection, from mechanisms of early events of entry to clinical scenarios.

KEYWORDS: Paramyxovirus, Human Metapneumovirus, Fusion Protein
Membrane Fusion, Binding, Heparan Sulfate, Cystic Fibrosis

Edita Klimyte

Student's signature

June 22, 2016

Date

ELUCIDATING BINDING, FUSION AND ENTRY OF HUMAN METAPNEUMOVIRUS

By

Edita Klimyte

Rebecca E. Dutch, Ph.D.

Director of Dissertation

Michael Mendenhall, Ph.D.

Director of Graduate Studies

Dedicated to my parents, for getting me here

Acknowledgements

I am incredibly grateful to my mentor, Dr. Rebecca Dutch, for this training experience in her lab. Becky has been a great role model as a successful scientist, an engaging speaker, and a talented writer. Her guidance and mentorship have inspired my development as a scientist, and I was fortunate to have a mentor that recognized and encouraged my individual goals.

I would like to thank my dissertation committee and outside examiner, respectively: Dr. Wally Whiteheart, Dr. Kathy O'Connor, Dr. Beth Garvy, and Dr. Robin Cooper. I truly appreciate all the suggestions, mentorship, guidance, time, reagents, and equipment you provided to help me complete this work.

I would also like to thank the current and former members of the Dutch Lab, who have contributed to making this a great place to be. Stacy Webb and Dr. Nicolás Cifuentes have been a tremendous source of support, both scientifically as colleagues and day to day as friends. Dr. Farah El Najjar was a constant source of knowledge, support, and friendship during our years together in the lab, and Dr. Andres Chang was incredibly helpful in the short time we were in the lab together. I also would like to say a special thanks to Stacy Smith for allowing the lab to run smoothly. Thank you to all the faculty, postdocs, research and administrative staff, and students in the department for sharing knowledge, reagents, and equipment and for making this department a great place to work.

The work presented here would not have been possible without the help of collaborators: Dr. David Lembo, Dr. Pasqua Oreste, and Dr. John Williams. Their generosity with reagents and input is very appreciated. I am grateful to the Center for Clinical and Translational Science, especially Dr. Tom Kelly and Dr. Vicky King, and the National Institutes of Health for predoctoral funding during my time in the MD/PhD program.

I am forever grateful to my family and friends for their support that has contributed to these achievements. My parents and brother have endured the joys and hardships of this training path with me and have always been supportive during times of celebration and frustration. The friends I have made along the way in Kentucky have made Lexington feel like a home away from home.

Table of Contents

Acknowledgements.....	iii
Table of Contents.....	iv
List of Figures	vii
Chapter 1: Introduction	1
Paramyxoviruses: an overview	1
Human metapneumovirus discovery and clinical relevance	2
Paramyxovirus structure and the functions of surface glycoproteins.....	4
Paramyxovirus attachment and receptor engagement.....	5
Cellular factors required for HMPV binding	6
Membrane fusion promoted by paramyxovirus fusion proteins	11
Mechanisms of viral entry	14
Evidence for HMPV endocytosis.....	16
<i>In vivo</i> viral respiratory lung infection and challenges of <i>in vitro</i> modeling.....	16
Dissertation Overview.....	17
Chapter 2: Materials and Methods.....	23
Cells and tissues	23
Plasmids	23
Antibodies.....	24
Syncytium assay	25
Reporter gene fusion assay.....	25
Surface expression of proteins, metabolic labeling, and immunoprecipitation	26
Homology modeling.....	26
Heparan sulfate mimicking and occluding compounds.....	27
Cell viability assay	27
Virus propagation and titers	27
Cell infection assay.....	29
HAE infection assay.....	29
Cell binding assay.....	30
Statistical Analysis.....	30
Chapter 3: HMPV fusion protein triggering: Increasing complexities by analysis of new strains .	31
Introduction	31
Results.....	33

Different fusion activity of HMPV F proteins.....	33
HMPV F protein surface expression and proteolytic processing.....	34
Sequence differences in HMPV F proteins and role of H434	35
Fusion activity of CAN97-83 F Q434H mutant.....	35
Discussion	36
Chapter 4: Inhibition of HMPV infection by blocking binding to heparan sulfate.....	47
Introduction	47
Results.....	49
Iota-carrageenan inhibits HMPV infection in human respiratory cells	49
O-sulfated K5 polysaccharide derivatives inhibit HMPV infection	51
Heparan sulfate occlusion inhibits HMPV infection and binding	53
Discussion	55
Chapter 5: Novel roles of HMPV G and SH during infection in bronchial epithelial cells.....	69
Introduction	69
Results.....	71
Recombinant ΔG and $\Delta G\Delta SH$ HMPV bind BEAS-2B more efficiently than WT....	71
Recombinant ΔG and $\Delta G\Delta SH$ HMPV do not incorporate cellular actin.....	72
Discussion	73
Chapter 6: HMPV Infection in a Cystic Fibrosis Model	81
Introduction	81
Results.....	83
CFBE cells more permissive to HMPV but not RSV infection than other human lung cells	83
CFBE cells are not permissive to PIV5 infection.....	84
HMPV infection of CFBE cells inhibited by heparan sulfate modulation.....	84
Enhanced HMPV infection is not a result of more particle binding	85
Discussion	86
Chapter 7: Discussion and Future Directions.....	93
Complexity of fusion protein regulation and implications of acidic pH promoted fusion.....	93
Heparan sulfate proteoglycans as a potential receptor for HMPV	96
Sulfated polysaccharides as an antiviral strategy	97
The role of HMPV G in cellular actin recruitment.....	99
HMPV infection in cystic fibrosis	99

HMPV propagation <i>in vitro</i> and future analysis of clinical strains.....	101
Conclusion.....	101
Appendix I: Abbreviations Used in this Document	103
References	105
Vita.....	134

List of Figures

Figure 1. Paramyxovirus family.....	19
Figure 2. HMPV particle structure.	20
Figure 3. HMPV F protein: processing and predicted structures.....	21
Figure 4. Glycosaminoglycans.....	22
Figure 5. HMPV F proteins from different strains exhibit variable fusion activity promoted by low pH.....	39
Figure 6. Amino acid sequence of F proteins of CAN97-83 (A2), TN94-49 (A2), TN96-12 (A1), and TN83-1211 (B2).	41
Figure 7. HMPV F protein expression and cleavage by exogenous trypsin.	42
Figure 8. Partial protein sequence analysis of F from 4 strains of HMPV surrounding key residues at positions (A) 294 and (B) 435.....	43
Figure 9. Q434H mutation results in hyperfusogenic activity in CAN97-83 F promoted by low pH.	44
Figure 10. Mutant F protein expression and cleavage by exogenous trypsin.	45
Figure 11. HMPV F structure homology models highlighting key residues surrounding H435.	46
Figure 12. Representative structures of heparan sulfate and related compounds.....	58
Figure 13. Iota-carrageenan inhibits HMPV infection in cells and tissues by blocking binding.....	59
Figure 14. Iota-carrageenan, SB105-A10 and K5 derivatives do not reduce cell viability.	61
Figure 15. O-sulfated K5 polysaccharide derivatives inhibit HMPV infection in BEAS-2B cells by competing for binding.....	62
Figure 16. Highly sulfated K5 polysaccharide derivatives inhibit HMPV infection in HAE.....	64
Figure 17. Peptide dendrimer SB105-A10 inhibits HMPV infection in human lung cells by inhibiting binding.	65
Figure 18. Treatment of HAE tissues with SB105-A10 reduces HMPV infection.	67
Figure 19. Model for inhibition of HMPV infection by interference between F and heparan sulfate.	68
Figure 20. Recombinant HMPV ΔG and $\Delta G\Delta SH$ bind more efficiently to BEAS-2B cells than WT HMPV.	76
Figure 21. Recombinant HMPV ΔG and $\Delta G\Delta SH$ do not have greater F incorporation compared to WT HMPV.....	78
Figure 22. Electron microscopy imaging of viral particles.	79
Figure 23. Recombinant HMPV ΔG and $\Delta G\Delta SH$ are not associated with β -actin.	80
Figure 24. HMPV infection in Vero and human lung cells.	88
Figure 25. RSV infection in Vero and human lung cells.	89
Figure 26. PIV5 infection in Vero and human lung cells.	90

Figure 27. HS modulation inhibits HMPV infection in CFBE cells.	91
Figure 28. HMPV binding is not more efficient in CFBE cells.....	92

Chapter 1: Introduction

Paramyxoviruses: an overview

Paramyxoviruses are a large family of viruses that cause infections which are a tremendous burden in human and animal worldwide. Paramyxoviruses are primarily spread by aerosols. This family includes a number of human pathogens with effective vaccines available, including the measles (MeV) and mumps (MuV) viruses. MeV was a leading cause of childhood death from infectious diseases, causing an estimated 7-8 million deaths per year, until the development of the measles vaccine in the 1960s. However, despite the initiative of the World Health Organization (WHO), approximately 114,900 people died from MeV infection in 2014 – mostly children under the age of 5 (reported by the WHO). MuV was also a common cause of viral infection during childhood, resulting in serious lifelong complications from initial infection, until the introduction of an effective vaccine in the 1960s. However, the spread of vaccination noncompliance in developed countries, such as the United States, has led to a re-emergence of these viruses in populations where they had been nearly eradicated (1). The paramyxovirus family also includes viruses that are leading causes of respiratory diseases in humans that currently do not have vaccines available. Respiratory syncytial virus (RSV) is the leading cause of respiratory infection in young children worldwide (2, 3). RSV infection is the second largest cause of mortality, after malaria, in infants and causes up to 200,000 deaths per year worldwide and is the leading cause of hospitalization in early childhood in developed nations (4, 5). Closely related to RSV, human metapneumovirus (HMPV), is also recognized as a common causes of viral infection, causing severe respiratory infections in susceptible individuals and is described in more detail in this chapter. Respiratory infections in humans are also caused by paramyxoviruses parainfluenza virus (PIV) types 1-3, which can cause significant disease in immunocompromised patients undergoing organ transplant (6, 7). PIV1 is associated with croup in children (8). Additionally, paramyxoviruses include several emerging zoonotic pathogens, Nipah (NiV) and Hendra (HeV) viruses, transmitted by fruit bats in the *Pteropodidae* family (9, 10). HeV was identified in 1994 as the causative agent of respiratory disease and febrile illness in horses and humans (11). Since its discovery there have been seven human infections of HeV, of which four were fatal (57%) (12). Furthermore, fatality in horses is nearly 70% from HeV infection (12). Outbreaks of NiV infection in humans from infected pigs have been identified in Malaysia, Singapore, Bangladesh and India since 1998, and have caused fatal encephalitis and mortality rates ranging from 43% to 100% (12-15). In addition to infection in horses and pigs by the Henipaviruses, Hev and NiV, respectively,

paramyxoviruses also cause disease in other species. Parainfluenza virus 5 (PIV5), formerly called simian virus 5, can cause kennel cough in dogs and infect other animals (16-18). Sendai virus (SeV) is responsible for a highly transmissible respiratory tract infection in mice, hamsters, guinea pigs, rats, and occasionally pigs (19). Newcastle disease virus (NDV) (20) and avian metapneumovirus (AMPV) (21) cause respiratory disease in domestic fowl, and bovine RSV causes respiratory illness in cattle (22), and atlantic salmon paramyxovirus (ASP) in fish (23), leading to huge economic losses in poultry and livestock industries.

All paramyxoviruses are enveloped, negative sense, single-stranded RNA viruses (24). Based on morphological characteristics, protein function, and sequence homology, this large family of approximately 36 species of diverse viruses is divided into 18 distinct genera, which are grouped into two subfamilies, *paramyxoviridae* and *pneumovirinae* (Fig. 1). The *pneumovirinae* subfamily consists of two genera, which include RSV and HMPV. The remaining genera are classified in the *paramyxoviridae* subfamily, and include the viruses: MeV, MuV, PIV, HeV, NiV, NDV, ASP, and reptilian viruses in the ferlaviruses genus (Fig. 1) (25-27). Several recently discovered paramyxoviruses such as J virus, Mossman virus, and Salem virus have not yet been classified within a subfamily (24).

Human metapneumovirus discovery and clinical relevance

HMPV is a ubiquitous pathogen that causes respiratory disease worldwide (28-30). HMPV was first identified in 2001 in the Netherlands from nasopharyngeal aspirates of sick children (31). Since its identification, HMPV is now known to be the cause of respiratory infections in humans since at least 1958 (31). HMPV strains have been phylogenetically classified into two genetic lineages (A and B) with distinct sublineages (A1, A2, B1, and B2) (32). While concurrent circulation of all four subtypes is common, a single, usually different, subtype usually predominates each year (33-36).

Nearly every person is exposed to HMPV in the first decade of life; sero-conversion occurs on average by the age of five and nearly 100% of individuals test seropositive for antibody reactivity to HMPV antigens by age ten (7). HMPV is the second most common cause of lower respiratory infection in children, following the closely related respiratory syncytial virus (RSV) (37, 38). Importantly, up to 70% of infants hospitalized for severe RSV bronchiolitis were also co-infected with HMPV, suggesting HMPV co-infection leads to more severe disease during RSV infection (39-41). Prematurity is a risk factor for developing severe illness from HMPV later in

childhood, more so than for RSV illness (42). While infants are considered the most vulnerable population to developing illness from HMPV, adults can foster severe respiratory infection as well, especially elderly and immunocompromised patients (43-45). Even previously healthy adults can develop severe respiratory disease that requires hospitalization (46). Long-term care residents over the age of 65 are particularly at risk, as HMPV can cause illness in as many as 72% of patients during outbreaks (47-49). Individuals with congenital heart defects are also at high risk of developing severe disease (38, 50, 51). Furthermore, one study found the burden of hospitalization for HMPV associated respiratory disease was 5.4 fold greater in HIV-infected compared to HIV-uninfected children (52). Also HIV-infected children had greater bacterial coinfection and a higher mortality rate than did uninfected children due to HMPV respiratory infection (52). One study showed that children with cancer had a nearly 50% rate of hospitalization due to HMPV infection (53). Individuals with chronic respiratory diseases, such as chronic obstructive pulmonary disease and asthma, are also at risk for serious disease from HMPV infection (54, 55). HMPV infection is also thought to be a significant cause of exacerbations and pulmonary decline in individuals with cystic fibrosis (56-58). However it is not known how the pathophysiology that results in cystic fibrosis promotes HMPV infection.

Most viral respiratory infections in healthy adults are contained in the upper respiratory tract, resulting in symptoms associated with the ears, nose, throat, and sinuses. These symptoms are often grouped together in association as the “common cold”, although there are numerous distinct viruses that can cause this, including HMPV. However, respiratory infection can spread to the lower respiratory tract, causing more severe disease. Complications of respiratory infection associated with HMPV include pneumonia, bronchiolitis, and febrile seizures (44, 59). Such complications can be life threatening in susceptible individuals. It has also been suggested that severe acute respiratory infection from HMPV may have lifelong consequences such as asthma and hyperresponsiveness of the airway (60, 61). While HMPV infection has been thought to be restricted to the respiratory epithelium and lungs, there have been several reports of fatal encephalitis with HMPV the only detected pathogen in both lung and brain tissue (62-64). There are several other paramyxoviruses that are known to cause neurological disease in humans, including measles (65, 66) and Nipah virus (14, 67, 68). Furthermore, HMPV infection has been associated with acute myocarditis, or swelling of the heart myocardium commonly caused by viral infection (69). Heart involvement has also been documented for mumps virus and human parainfluenza viruses 2 and 3 (70). It is not known what viral or host genetic factors contribute to

HMPV tropism outside of the respiratory tract. Even though primary infection occurs during childhood in the majority of cases, repeat infections are common throughout life, likely due to strain variations and incomplete immunity. Despite HMPV prevalence and clinical relevance, there are no specific antiviral treatments or vaccines available.

Paramyxovirus structure and the functions of surface glycoproteins

The genome of paramyxoviruses consists of six to ten genes and varies in size from 13 to 19 kb (71). The viral envelope, derived from the plasma membrane of the host, surrounds the single-stranded RNA genome, contained within the nucleocapsid. The nucleocapsid is composed of the nucleocapsid protein (N), the phosphoprotein (P) and the large polymerase protein (L). Of the six to ten genes, only two or three of encoded proteins are expressed at the surface of the virus. The surface glycoproteins are available to interact with the target cell during entry and serve functions in attachment and membrane fusion to deliver the nucleocapsid to the cytoplasm. The matrix protein (M) functions in particle assembly and is thought to be closely associated with the viral membrane, surface glycoproteins, and nucleocapsid. The rest of the encoded proteins are primarily involved in viral genome transcription, replication, or assembly. Some reptilian viruses, including Fer-de-Lance virus, in the Ferlavirus genus have an additional gene encoding the unknown protein (U) of approximately 20 kDa that has no counterpart in other paramyxoviruses or any similarity to other reporter sequences (26, 27, 72). The order of genes in the genome of HMPV is as follows: HMPV (3'-N-P-M-F-M2-SH-G-L-5') (31, 73, 74).

The main viral glycoproteins at the surface of the paramyxoviruses are the attachment protein (H, HN, or G) and the fusion protein (F) (Fig. 2) (24). The nomenclature of the attachment proteins varies due to differences in receptor binding and neuraminidase activity. The attachment proteins of rubulaviruses, respiroviruses, and avulaviruses have both hemagglutinin, which binds sialic acid, and neuraminidase, sialic acid cleaving, functions and are called HN proteins. The attachment proteins of morbilliviruses lack neuraminidase activity but can bind sialic acid, and are called H. *Pneumovirinae* and Henipaviruses do not bind sialic acid, and their attachment proteins are referred to as G, for glycoprotein. Thus, the attachment of HMPV is referred to as G (Fig. 2). The attachment and fusion proteins mediate viral entry by coordinated activity in most paramyxoviruses and are discussed in more detail in subsequent sections (75). In addition to the fusion and attachment glycoproteins on the viral surface, three of the seven genera of paramyxoviruses, including members of rubulaviruses, pneumoviruses, and the unclassified J

virus, also express a third viral surface glycoprotein, the small hydrophobic protein (SH). Unlike the fusion and attachment proteins, the SH protein is much less conserved across the family. Some SH proteins are type I proteins, which contain a single transmembrane region (69), and some, like that of PIV5 and the *pneumovirinae*, are type II, with multiple transmembrane domains (76). The exact role of SH proteins in the paramyxovirus life cycle is not well understood, as most mutant viruses lacking of this protein replicate efficiently *in vitro* (76-79). However, the deletion of the SH proteins of RSV and avian metapneumovirus (AMPV) reduced replication and pathogenicity in animal models (80-82). Furthermore, recombinant HMPV lacking the SH gene was found to replicate in both hamster (76) and nonhuman primate models less efficiently in the lower respiratory tract than wild-type HMPV (83). These findings suggest SH may play a role in immune modulation *in vivo*, and indeed, studies with RSV (84), PIV5 (85, 86), and mumps (87) suggest that SH antagonizes the induction of apoptosis and, like HMPV (88), may also block the activity of NF- κ B (89). Furthermore, all HMPV isolates to date have the SH gene, indicating its presence is required for fitness (90). Additionally, several functions of HMPV SH have been identified recently. Like the SH of RSV (91), the HMPV SH protein exhibits viroporin activity, serving as channel to allow small molecules to pass across the membrane (92). Furthermore, HMPV SH can regulate the cell-to-cell fusion activity of F (92). Additionally, HMPV SH, in addition to HMPV G, can inhibit macropinocytosis of HMPV in dendritic cells, further supporting that the SH protein contributes to immune evasion (93).

Paramyxovirus attachment and receptor engagement

All paramyxovirus attachment proteins characterized to date are homotetrameric type II integral membrane proteins (24). They are made up of a membrane-proximal stalk and a large c-terminal globular head domain anchored by a single-pass N-terminal transmembrane domain (24). From the solved crystal structures of the globular head domains of several paramyxovirus attachment proteins, it has been shown the attachment protein globular head is composed of four six-blade β -propeller fold monomers arranged in a four-fold symmetry (94-100). The stalk domain of the paramyxovirus attachment protein is like a helical coiled-coil that generally interacts with the fusion protein (101-105). For most HN attachment proteins, the sialic acid binding site is located at the top of the globular head (96), although some HN proteins, NDV (106, 107) and PIV3 (108-110), have a second binding site to sialic acid that is important for fusion promotion.

Most paramyxoviruses engage the cellular receptors for binding by the attachment protein. As previously described, rubulaviruses, respiroviruses, and avulaviruses have HN attachment proteins, and bind sialic acid with various degrees of affinity (111). The H proteins of morbilliviruses generally bind sialic acid, and use additional cellular proteins, such as nectin-4 (112, 113), CD46 (88), and CD150/SLAM (88) in the case of MeV, as receptors for attachment. The G proteins of HeV and NiV bind to cellular Ephrin B2/B3 (114-116), and the G proteins of *pneumovirinae* have been reported to bind heparan sulfate proteoglycans (HSPGs) (117, 118). However, it has been shown that the HMPV fusion protein is necessary and sufficient for binding to HSPGs (79), and that $\alpha V\beta 1$ integrin plays an important role in promoting HMPV infection (79, 119, 120). Additionally, it has been reported that the RSV fusion protein mediates attachment to the cell surface via nucleolin (121). Nevertheless, HMPV G can inhibit macropinocytosis of HMPV in dendritic cells and reduce activation of CD4+ helper T cells, suggesting HMPV G can regulate particle uptake and contribute to immune evasion (93). RSV also produces a soluble form of the G protein that plays a role in immune modulation (122). These findings suggest that, unlike members of the *paramyxoviridae* subfamily, receptor binding activity for members of the *pneumovirinae* subfamily can occur through the F protein and receptor interactions with the G protein are not essential.

In addition to mediating the initial attachment of the virus to a cell, the attachment proteins of most paramyxoviruses also have fusion promoting activity. Interaction of the attachment protein of most paramyxoviruses with its receptor results in triggering of the fusion protein to undergo a series of conformational changes that drives fusion of the viral envelope and a lipid membrane of the target cell. The co-expression of the homotypic attachment and fusion proteins is required for membrane fusion and viral spread to occur of most paramyxoviruses (101, 123-131). However, studies have shown that both RSV and HMPV are infectious in the absence of the G protein (74, 76, 77, 132, 133). Furthermore, cell-to-cell fusion promoted by the F protein (Fig. 3) of HMPV CAN97-83 (A2) occurs without co-expression of HMPV G (133-136). These findings suggest HMPV G does not contribute to membrane fusion as in the trigger of the fusion protein that is typical of attachment proteins found in paramyxoviruses.

Cellular factors required for HMPV binding

Unlike most paramyxoviruses, the binding of HMPV to target cell is mediated by the fusion protein. Our group showed that HMPV requires the glycosaminoglycan heparan sulfate for

binding and infectivity, as cells deficient in heparan sulfate synthesis or treated with heparinases were not able to bind HMPV (79). Heparan sulfate is ubiquitously expressed on the cell surface and extracellular matrix of almost all cell types as heparan sulfate proteoglycans (HSPGs) (137, 138). Proteoglycans belong to a large class of diverse surface glycoproteins that mediate numerous cell functions, including signaling, growth and adhesion (139-143). Heparan sulfate is one of four glycosaminoglycans found on the surface of mammalian proteins. The biosynthesis of glycosaminoglycans, their distinct structural feature, and different types of heparan sulfate proteoglycans are described in detail in other sections.

Additionally, integrin $\alpha\text{V}\beta\text{1}$ has been identified as a binding factor and required for efficient infection. Integrins are a large family of cell adhesion proteins that are expressed in all cell types and have critical roles in the regulation of cell-to-cell, cell-to-matrix adhesion (144), growth, differentiation, attachment, migration, thrombus formation, and apoptosis (reviewed in (145, 146)). Integrins are transmembrane heterodimers, composed of at least 18 different α and 10 different β subunits. Integrins serve an important role by conveying signals from the outside to the inside of cells and vice versa, through interactions between the cytoplasmic domains of the α and β integrin subunits with a variety of intracellular proteins (147-149). Additionally, some integrins are known to be promiscuous and bind a variety of ligands (150), and other have specific domains for binding many different proteins, including HSPGs (151), and proteins expressing the amino acid sequence arginine-glycine-asparagine (RGD) (152, 153). It has reported that the HMPV fusion protein binds through an RGD motif (119, 120). Importantly, it has been shown that integrins such as $\alpha\text{5}\beta\text{1}$, can play an important role in the regulation of cell signaling through receptor-mediated endocytosis and the recycling of many surface proteins (154). Integrins are receptors for some picornaviruses, papillomaviruses, adenoviruses, and hantaviruses (148, 155, 156). Integrin $\alpha\text{V}\beta\text{1}$ has been identified as a binding factor and required for efficient infection of HMPV (79, 119, 120).

Glycosaminoglycans biosynthesis and distinct structural features

Cell surface proteoglycans consist of a diverse family of core proteins heavily modified by sugars called glycosaminoglycans (GAGs). GAGs are divided into four major forms based on the specific sugars that make up the repeating disaccharide units of the polysaccharide chains: heparan sulfate, chondroitin sulfate, dermatan sulfate and keratan sulfate (Fig. 4). The steps of biosynthesis are similar for the different forms of GAGs, although they are distinct from one

another by the specific sugar moieties found in the repeating disaccharide units. The GAG addition to transmembrane proteins occurs in the Golgi either by O-linked glycosylation at serine/threonine residues or N-linked glycosylation at asparagine residues. A three or four-sugar linkage, referred to as an oligosaccharide bridge, is created between the core protein and the terminal glycosaminoglycan, a linear polysaccharide consisting of repeating disaccharide units, an amine sugar and an uronic acid, with the exception of keratan. The amino sugars in the repeating disaccharide units include N-acetyl-D-glucosamine, N-acetyl-D-galactosamine, and in the case of keratan, N-acetyl-D-lactosamine (Fig. 4). Typically only one type of amino sugar is found in a GAG polysaccharide chain, but several types of GAGs may modify a single proteoglycan. The hydroxyl groups of the amino sugars can further be modified by O-sulfation. Uronic acids are a form of oxidized sugars, where the terminal primary alcohol is enzymatically oxidized to a carboxylic acid; the two forms found in GAGs are glucuronic acid and iduronic acid. These epimers may both be found in a single GAG chain.

To synthesize both the oligosaccharide bridge and GAG polysaccharide chain, specific glycosyltransferases found in the Golgi add respective uridine diphosphate (UDP) activated sugars initially to the protein core at one of the previously mentioned residues (Ser/Thr or Asn) and then subsequently to the growing polysaccharide chain. After the GAG backbone is formed, the chain can be modified by sulfation and/or epimerization of uronic acids, catalyzed by sulfotransferases and epimerases respectively. The sulfotransferases utilize 3'-phosphoadenosine-5'-phosphosulfate, an activated sulfate, for the addition of sulfate groups. Because of this modification, GAGs are often highly negatively charged.

Heparan sulfate (HS) is ubiquitously expressed in most mammalian tissues. HS chains are linked to the core protein by a tetrasaccharide bridge via O-glycosylation of a serine residue. The first step involves the addition of a xylose to the serine, followed by two galactose molecules, and glucuronic acid. The subsequent addition of N-acetylglucosamine commits this biosynthesis pathway to make HS; the alternative addition of N-acetylgalactosamine would result in chondroitin sulfate synthesis (Fig. 4). Evidence has shown that the specific glycosyltransferase that adds N-acetylglucosamine in this fate-determining step recognizes acidic residues around the serine being modified. Interestingly, HS can be modified by sulfation like other GAGs, but HS is uniquely found to be sulfated in clusters, as opposed to uniformly throughout the chain like in CS and DS. Greater than 80% of HS glucosamine is N-sulfated, and even a greater percent is O-sulfated (157). HS modification allows for diverse products, but analysis of HS types have found

the HS produced is more specific to cell type rather than core proteins; therefore, different proteoglycans produced by a single cell type express HS with a similar pattern of chain modification, potentially contributing to tissue tropism of the viruses that bind HS. Heparan sulfate has been identified as a binding factor for numerous viruses, including retroviruses, herpesviruses, filoviruses, paramyxoviruses, human papilloma virus, hepatitis C virus, Dengue virus, and baculoviruses (79, 117, 142, 158-177).

Chondroitin sulfate (CS) is primarily expressed in the central nervous system (178-181). CS shares the first four steps of biosynthesis with HS; however, committed step to CS synthesis involves the addition of N-acetylgalactosamine instead of N-acetylglucosamine (Fig. 4). To date, CS has been implicated as a binding receptor for only two viruses, for porcine circovirus 2 (167) and herpes simplex virus (182), although it has reported antiviral activity against Japanese encephalitis (183) virus and Dengue virus (184) *in vitro*. Dermatan sulfate (DS) is primarily expressed in skin tissue and is released into the extracellular matrix during wound repair (185, 186). DS has been previously been characterized as a type of CS (sometimes referred to CS type II), although this organization has been recently questioned. Like CS, the amino sugar in the disaccharide repeat is also N-acetylgalactosamine. However, DS contains almost exclusively iduronic acid as the second sugar, whereas most CS contain primarily glucuronic acid (Fig. 4). Otherwise, the synthesis of DS is similar to that that of HS and CS. Unlike other GAGs, keratan sulfate (KS) consists of a sulfated poly-N-acetyllactosamine chain; instead of alternating amino sugar and uronic acid, the two repeating units are N-acetylglucosamine and galactose (Fig. 4). KS modification on proteins is found in distinct tissues, including cartilage and the cornea of the eye (187). The residue of KS attachment also can vary. Type I KS is linked to the protein by N-glycosylation at an asparagine residue through a three-sugar oligosaccharide bridge (Fig. 4); type II KS is linked to the protein by O-glycosylation at a serine or threonine residue directly through N-acetylgalactosamine (not shown). To date, neither DS nor KS have been associated with function as a viral receptor.

Heparan sulfate proteoglycans (HSPGs) implicated in viral entry

Heparan sulfate proteoglycans (HSPGs) encompass a diverse class of proteins defined by the substitution with HS polysaccharide chains. Because HS has been identified as the most common type of GAG associated with attachment function for viruses, HSPGs have been investigated in their role in attachment for numerous viruses. Indeed, the identification of HS as

a required binding factor for HMPV infection suggests HSPGs may serve as an attachment factor for infection. HSPGs are found both as secreted proteins in the extracellular matrix, as well as membrane associated proteins at the cell surface of all tissues. The membrane bound HSPGs, which could serve as a potential receptor, include two main families of cell surface proteins, syndecans and glypicans, as well as other proteoglycans including neuropilin and betaglycan. Syndecans and glypicans regulate a wide spectrum of biological activities, including cell proliferation, morphogenesis, wound repair, and host defense by binding proteins in the extracellular environment as well as other plasma membrane proteins via heparan sulfate chains.

The syndecans comprise a family of four distinct genes encoding integral membrane proteins (SDC 1-4) expressed in a cell and tissue specific manner. Structurally, syndecans are similar in the organization of protein domains: the protein is anchored by a single transmembrane domain, with a large extracellular domain and shorter cytoplasmic tail, which consists of two conserved regions surrounding a variable domain (188). SDC-1 is the predominant HSPG in mammary epithelia and has been identified as an attachment factor for herpes simplex virus type 1 (158, 164) and human papilloma virus (171, 175, 189). SDC-2 is primarily expressed on fibroblasts and cells of the vasculature (190-192). Dengue virus (168) and herpes simplex virus type 1 (158) have been shown to use SDC-2 for attachment. SDC-3 is primarily expressed in the nervous system, the adrenal gland, and the spleen (193). Finally, SDC-4 is expressed in focal adhesions of adherent cells. Both SDC-1 and SDC-4 have been identified as mediators of HCV attachment (165, 172). SDC-2 (194), SDC-3 (161), and SDC-4 (160) have been implicated in HIV-1 entry (reviewed in (195)). Syndecans have been identified as receptors or coreceptors for several HS-binding viruses, possibly in part due to the fact that HS chains are attached to the ectodomains distal to the plasma membrane on syndecan proteins, making them available for interaction. Chondroitin sulfate chains are also found on SDC-1 and SDC-4, although closer to the plasma membrane than the HS chains.

The glypicans are a family of at least six proteins (GPC1-6) that are linked to the cell membrane via a glycosylphosphatidylinositol (GPI) anchor (196-199). The size of the core protein of glypicans is similar (60–70 kDa), with moderate homology among most glypicans (200). The position of 14 cysteine residues that form disulfide bonds in the folded protein is conserved, suggesting that the three-dimensional structure of glypicans is very similar (200). Heparan sulfate is the only GAG that has been found on glypicans, and heparan sulfate chain attachment sites are restricted to the last 50 amino acids in the C-terminus, placing the chains close to the cell

membrane (200). Glypicans are involved in mediating signaling during development, morphogenesis, and growth. GPC3 is mutated in patients with an overgrowth syndrome, Simpson-Golabi-Behmel syndrome (SGBS) (201). Glypican expression is also cell and tissue specific, and most glypicans are expressed predominantly in the central nervous system. However, GPC-1 is widely expressed in other tissues including the epidermis and hair follicles (202, 203). Because glypicans are attached to the outer membrane leaflet via a lipid anchor, they can be removed from the cell surface using a phospholipase, specifically phospholipase C. Unlike syndecans, glypicans have not been identified to function as receptors for viral entry until very recently. Using a targeted RNA interference entry screen, GPC-5 was identified as a common host cell entry factor for hepatitis B and delta viruses (204). Whether HMPV recognizes a specific HSPG for binding remains to be determined.

Membrane fusion promoted by paramyxovirus fusion proteins

The merger of two membranes is a thermodynamically favored process, but has a high kinetic barrier; thus, enveloped viruses utilize fusion proteins to mediate this process. All paramyxoviruses discovered to date express a homotrimeric type I fusion protein, which are also found in influenza, Ebola and HIV. Paramyxovirus F proteins have distinct domains that consist of a hydrophobic fusion peptide (FP), two heptad repeat regions (HRA and HRB), a single-pass transmembrane domain (TM), and a C-terminal cytoplasmic tail (Fig. 3A) (205). Paramyxovirus fusion proteins are synthesized as a biologically inactive F₀ precursor form which must then be cleaved into the fusogenically active F₁+F₂ metastable prefusion form (Fig. 3A). Most paramyxovirus fusion proteins are cleaved by intracellular proteases, including furin (206-208) or cathepsin L (209-211), but for the HMPV fusion protein (F), this can be achieved by the addition of exogenous trypsin (134). During endogenous infection *in vivo*, it is thought that secreted host proteases cleave HMPV F. Upon triggering, the paramyxovirus fusion protein undergoes extensive and essentially irreversible conformational changes (Fig. 3B) that result in the repositioning of the heptad repeat regions to form a stable six-helix bundle (6-HB), with the released energy proposed to drive the fusion process (75, 212). Premature activation can result in inactivation of the attachment and fusion machinery, resulting in a defective particle no longer able to infect cells (213). Paramyxovirus fusion proteins can promote cell-to-cell fusion when expressed at the plasma membrane by transfection or infection, resulting in the formation of giant, multinucleated cells called syncytia (24, 214, 215). For HMPV, studies of mutant viruses and recombinant proteins

showed that the F protein is the major protective antigen (216-218), and the *pneumovirinae* fusion protein is a common target for vaccine and antiviral development (219).

The paramyxovirus fusion proteins are minimally conserved at the amino acid level, however structural and biochemical analysis suggest a similar structure among paramyxovirus fusion proteins (Fig. 3B). Obtaining the prefusion conformation of the soluble globular head domain has been challenging as most paramyxovirus fusion proteins are not stable in this form without the transmembrane domain, thus different strategies, including the addition of a trimerization domain (220-222), have been employed. A crystal structure of the prefusion form of PIV5 F (222) and a partial structure of the prefusion form of HMPV F with a bound antibody (221) have been solved. In the metastable, prefusion conformation, PIV5 F consists of a large globular head domain and a three-helix, coiled-coil stalk domain composed of three HRB domains proximal to the membrane (222). The HRA domain is located at the top of the globular head, and the hydrophobic fusion peptide is buried between subunits of the trimer, leaving the cleavage site exposed (222). Additionally, the postfusion fusion protein structures of three paramyxoviruses, PIV3 F (223), NDV F (224), and RSV F (225), have been solved, and the formation of the 6-HB is conserved in the solved postfusion conformation structures. Thus, it is hypothesized that refolding of the fusion protein to form the 6-HB results in formation of the fusion pore to release the nucleocapsid into the cytoplasm. However, it is likely multiple fusion trimers are required to accomplish this, as cells expressing PIV5 HN and very low amounts of PIV5 F were unable to promote membrane fusion (226).

The protein refolding that takes place to change from the prefusion to the postfusion conformation is essentially irreversible. Therefore, the paramyxovirus fusion protein needs to be triggered at the right time and place. For most paramyxoviruses, it is thought that interaction of the attachment protein with cell surface receptors, and with the fusion protein, is required for triggering (24, 227), and studies have shown that the attachment protein and the fusion protein interact for a number of paramyxoviruses and that these specific interactions are required for triggering (123-125, 127-129, 228-230). The interaction occurs between the globular head region of the fusion protein (126) and different domains of the attachment protein, including the globular head domain (229, 231, 232), the stalk domain (103-105, 130, 228, 233), and the TM domain (234, 235). It is hypothesized that the attachment protein undergoes a conformational change upon receptor binding, which results in the interaction with the fusion protein that triggers fusion (95, 99, 106, 228). The fusion proteins of PIV5 and Sendai virus can promote fusion

without the attachment protein, however the expression of the attachment protein dramatically enhances the fusion activity (226, 236). Furthermore, the fusion proteins of *paramyxoviridae* can be triggered by raising the temperature without the presence of the attachment protein (237, 238). The fusion proteins of RSV and HMPV can promote cell-to-cell fusion without the attachment protein (134, 136, 239-242). HMPV F from CAN97-83 (A2) promotes fusion without the G protein, with brief exposure to low pH (134, 136, 243), and co-expression of HMPV G with this F protein does not enhance its fusion activity (134). Furthermore, recombinant RSV and HMPV without the attachment protein are still infectious *in vitro* and *in vivo* (76, 79, 93, 134, 240, 244). Thus, while most paramyxoviruses require the attachment protein to trigger the fusion protein, viruses in the *pneumovirinae* subfamily may utilize a different mechanism.

HMPV Fusion protein

HMPV F is a homotrimeric surface glycoprotein synthesized as a 539 residue precursor that undergoes proteolytic cleavage at the arginine at position 102 to the activated form, which is linked by a disulfide bridge (Fig. 3A) (245). The majority of paramyxovirus F proteins are cleaved by intracellular proteases prior to being packaged into newly formed virions (208, 210); however, HMPV requires exogenous trypsin to be grown efficiently in cell culture, suggesting HMPV F may be cleaved after viral budding *in vivo* by an extracellular protease such as TMPRSS2 (31, 246, 247). The F protein, in the activated, or cleaved, form sits in the viral membrane as a homotrimer in a metastable conformation until an environmental trigger causes a large conformational change in protein structure (Fig. 3B) (221). Similarly to other paramyxovirus fusion proteins, it is predicted that the globular head and stalk of the prefusion conformation of HMPV F refold to extend the hydrophobic fusion peptide into the target membrane in the intermediate form. In the final post-fusion conformation the protein folds back on itself resulting in the formation of a 6-HB, which promotes fusion between the two membranes (Fig. 3C) (205). The final protein conformation is the lowest energy state, making this process essentially irreversible. Therefore, the initial environmental trigger is a critical step that must be temporally and spatially coordinated for fusion to take place (248-250).

The role of acidic pH in HMPV F triggering

The requirement for acidic pH to trigger fusion protein activity has been well described for the fusion proteins of influenza and the rhabdovirus vesicular stomatitis virus (VSV) (251-254).

For fusion proteins that can be triggered to fuse by low pH, it is thought that electrostatic repulsive forces that arise between residues, often involving histidines that become protonated at low pH and nearby basic residues contribute to the destabilization of the prefusion conformation of the fusion protein, which then leads to refolding to the postfusion conformation (255-257). During entry, influenza A (258-260) and VSV (261-269) require acidification of the endosome to escape into the cytoplasm and establish infection.

The majority of paramyxovirus fusion proteins promote cell-to-cell fusion when they are co-expressed with their respective attachment proteins, without exposure to acidic pH (24, 270-272). However, HMPV F proteins can promote membrane fusion without G, and the F proteins from some strains of HMPV can be triggered to fuse by brief exposure to low pH (134, 136, 241-243). In the HMPV F protein, a conserved histidine residue at position 435 is thought to serve as a pH sensor, and its protonation at pH values below the pKa (approximately 6.04) contribute to triggering F (136, 242, 243). H435 is in close proximity to 3 conserved basic residues, K295, R396, and K438, based on a homology model of the prefusion conformation, and is therefore proposed to lead to electrostatic repulsion that results in triggering of F and fusion (136, 243). An initial analysis of HMPV F proteins from a single prototype strain from each clade suggested low pH triggered fusion is rare among HMPV strains (241, 242). Specifically, glycine 294 was identified as a requirement for low pH triggered fusion, and this residue is not commonly found in HMPV F proteins and had not been previously identified in a Clade B HMPV (241). Furthermore, additional analysis identified residues at positions 296, 396, and 404 as the main determinants of fusion activity among HMPV F proteins (242). HMPV F proteins that were triggered to promote cell-to-cell fusion at both pH 5 and pH 7, and thus characterized as pH independent, became low pH dependent for fusion after mutagenesis at these positions (242). These findings suggest acidic pH is not a general factor in HMPV F trigger, however few HMPV F proteins have been studied in each clade. Furthermore, it has only been shown that fusion activity of HMPV F is not enhanced by the co-expression of the attachment protein G for CAN97-83 (A2) F (134). Whether acidic pH has biological significance in the context of endocytic entry for all HMPV strains is not clear.

Mechanisms of viral entry

The fusion proteins of most paramyxoviruses promote fusion at neutral pH, and this, in large part, has led to the hypothesis that membrane fusion occurs at the plasma membrane. Thus, it had generally been thought paramyxovirus entry occurs by direct viral envelope fusion to the

plasma membrane (75). However, several members of the paramyxovirus family have been shown to utilize complex entry pathways, including different types of endocytosis and macropinocytosis.

Endocytosis is a process to internalize substances from the extracellular environment following activation of a surface protein, and is primarily classified as clathrin-dependent or caveolin-dependent. Clathrin-dependent endocytosis utilizes the proteins in the AP-2 complex and Eps15 to form a protein network around an area of the plasma membrane that invaginates to become a vesicle (273). The GTPase dynamin is required for the final formation of the clathrin-coated vesicle (273). Many viruses, including Influenza (274-277), VSV (278), and Dengue virus (279, 280), can enter cells by clathrin-mediated endocytosis. Furthermore, the paramyxoviruses RSV (281) and HMPV (282) have also been shown to enter cells by this route. The second major endocytic route is caveolin-dependent endocytosis, whereby vesicles lined with the protein caveolin-1 form from small invaginations of the plasma membrane rich in cholesterol (283, 284) in a dynamin-dependent manner (283-285). BK virus, echovirus-1, and the paramyxovirus NDV (286, 287) have been shown to enter cells in a caveolin-dependent manner (288-290). Both clathrin-mediated and caveolin-mediated vesicles transport cargo into acidified endosomes (291), where cargo is sorted and delivered to the target compartments. Many viruses utilize the acidity of the endocytic pathway to their advantage to trigger their fusion proteins and deliver their genomic content to the cytoplasm of the cell (261, 292-294).

Distinct from endocytic vesicle formation, macropinocytosis is a process of non-selective internalization of large quantities of solute and membrane that has been associated with viral entry (295, 296). Macropinocytosis involves actin-mediated membrane ruffling of the plasma membrane, with formation of lamellipodia that fold back to fuse with the membrane to form large, irregularly shaped vesicles called macropinosomes (reviewed in (297)). In most cell types, macropinocytosis is a signal-dependent process that normally occurs in response to growth factor stimulation (295), however, some specialized cell types, such as antigen-presenting cells, are capable of constitutive macropinocytosis (298, 299). After formation, macropinosomes undergo maturation that is associated with a reduction in surface area and acquisition of the marker of late endosomes, Rab 7, eventually fusing with lysosomes (300). Macropinocytosis has been implicated as the entry route for some viruses, including vaccinia virus (301), adenovirus type 3 (302), filamentous influenza (303), RSV (304), and HMPV (93), often in a cell type-dependent

manner. Whether macropinocytosis is an entry route utilized by HMPV in non-antigen presenting cells remains to be determined.

Evidence for HMPV endocytosis

Although not all strains of HMPV are associated with low pH promoted fusion proteins, HMPV likely enters cells of the airway epithelium by clathrin-mediated endocytosis (282). A recent study has shown that HMPV viral envelope fusion occurs in endosomal compartments of human bronchial epithelial cells (282), and HMPV infection was inhibited by chlorpromazine treatment, an inhibitor of clathrin-mediated endocytosis (136). Additionally, HMPV entry requires the GTPase dynamin, as the inhibitor dynasore inhibited HMPV infection (136, 282). Furthermore, lysosomotropic agents that disrupt the acidification of endosomes, such as bafilomycin A, concanamycin A, inhibited HMPV infection to varying degrees (136, 242, 282). However, the extent of inhibition of HMPV infection by these agents was strain dependent, and may be associated with the requirement for acidic pH for fusion (136, 242, 282). Therefore, it likely that most, if not all, HMPV strains enter airway epithelium cells by clathrin-mediated endocytosis, and the fusion events may take place in various stages of endosomal maturation depending on acidic pH requirements of each strain.

***In vivo* viral respiratory lung infection and challenges of *in vitro* modeling**

The human respiratory tract is a complex histological environment in the different anatomical regions through which air, and any potential viral pathogens, flow: from the nasal epithelium of the nose, to the pharynx, to the bronchi and lastly the terminal alveoli where gas exchange occurs. The respiratory epithelium is primarily lined with pseudostratified ciliated columnar epithelium with mucus-producing goblet cells on a lamina propria. The respiratory tract is involved in the critical function of gas exchanges, delivering oxygen to alveoli and removing carbon dioxide waste. Additionally, the respiratory epithelium serves an important immune function: beating cilia help to clear any potential pathogens trapped in mucus that has antimicrobial proteins.

Because of this complexity, one of the biggest challenges of studying human respiratory viruses is the shortage of physiologically relevant models without the use of animals. Most *in vitro* studies investigating paramyxoviruses to date have been done in monolayer cell cultures derived from immortalized animal and human cell lines. However, technical advances in manipulating cells

to reverse cellular differentiation in order to derive tissue specific stem cells has led to the development of the airway epithelium three-dimensional cultures. Polarized epithelium with pseudostratified, mucociliary epithelium, as well as apical and basolateral surfaces, allow us to investigate directional responses to pathogen exposure *in vitro*. The airway tissue system represents a model of intact normal human airway epithelial cells, and has been promoted as a valid animal-alternative model to study respiratory pathogens and testing potential therapeutic agents (305). Human airway epithelium (HAE) has been utilized to study respiratory pathogens *haemophilus influenza*, *streptococcus pneumonia*, influenza virus A, and HRSV (306-308). HMPV infection at the apical surface of HAE tissues has been reported previously (El Najjar, submitted) although features of binding and entry have not be evaluated in this model. Heparan sulfate has been identified as a required cellular factor for HMPV binding; however, several reports have concluded that HSPGs are not localized on the ciliated apical side of fully differentiated bronchial epithelial cells cultured at the air-liquid interface or tracheal tissue sections (142, 309-311). HAE presents an opportunity to apply what has been learned about HMPV since its discovery in a physiologically relevant system. This culture system allows us to ask *in vivo* questions regarding cellular responses to viral infection and conveniently answer them utilizing an *in vitro* system.

Dissertation Overview

Human metapneumovirus (HMPV) is an enveloped RNA virus that causes severe respiratory disease in infants, the elderly, and immunocompromised patients worldwide. Despite its prevalence and importance to human health, no therapies are available against this pathogen. Key features of early events in HMPV infection have been identified. However, many important aspects of binding and fusion events remain unknown. This body of work characterized critical aspects HMPV F protein triggering by low pH, which has biological relevance for endocytic entry. It was previously demonstrated low pH can promote fusion activity of the F protein from some strains of HMPV, but analysis of a limited number of other strains suggested this is a rare characteristic and requires specific residues. Analysis of F proteins from phylogenetically diverse HMPV strains showed low pH triggered fusion, challenging previously thought requirements, and led to the identification of a critical residue that enhances low pH promoted fusion. These results support our hypothesis that electrostatic interactions play a key role in HMPV F triggering by low pH and further elucidate the complexity of viral fusion proteins.

Previous work showed HMPV F mediates attachment to HSPGs. We characterized the key features of the binding interaction between HMPV and HSPGs using heparan sulfate mimetics, identifying an important sulfate modification, and demonstrate that these interactions occur at the apical surface of polarize airways tissues. These results significantly advance our understanding of HMPV infection in the human airway and identify an antiviral strategy. Furthermore, in our analysis of HMPV F mediated binding to HSPGs, we identified regulatory roles of HMPV glycoproteins G and SH that affect binding mediated by F and a potential novel function for HMPV G in actin recruitment. These results contribute to our understanding of the HMPV G and SH, which often do not share the same functional roles of analogous proteins found in viruses of the same family.

While a majority of the work presented here examined mechanisms of early events of entry, we also characterized HMPV infection in a clinical scenario using cystic fibrosis bronchial epithelial (CFBE) cells. Compared to paramyxoviruses RSV and PIV5, CFBE were specifically more permissive to HMPV infection, which correlates to the limited number of epidemiological studies of virus infection in cystic fibrosis patients. Our results identified a potential specific susceptibility to HMPV infection, which has not been previously reported. Therefore, the work presented here contributes to our understanding of HMPV infection over a broad breadth, from mechanisms of early events of entry to a clinical model of chronic respiratory disease.

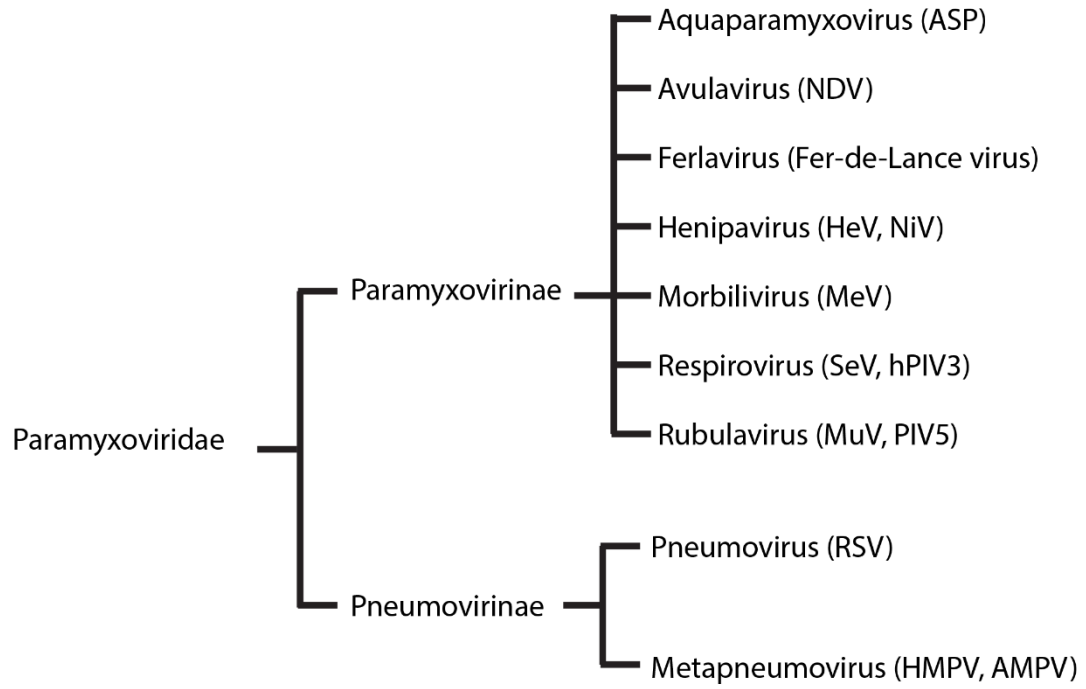


Figure 1. Paramyxovirus family.

Figure is adapted from (312).

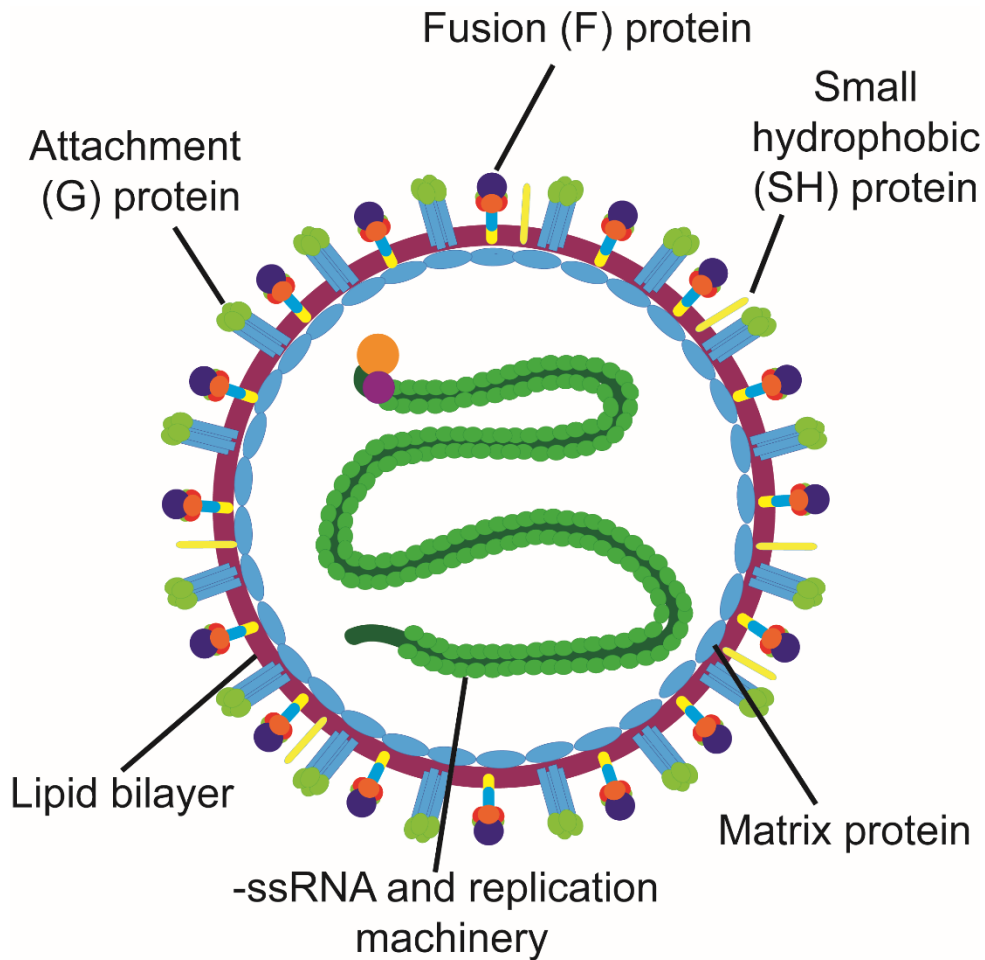


Figure 2. HMPV particle structure.

The three glycoproteins found on the surface of HMPV include the attachment protein (G), the homotrimeric fusion protein (F), and the small hydrophobic (SH) protein. The viral envelope (red) is derived from host cell plasma membrane in part due to the assembly of the matrix protein (blue ovals), which closely associated with the inner leaflet of the viral envelope. The nucleocapsid surrounds the negative sense, single stranded RNA genome and contributes to the replication machinery required during infection.

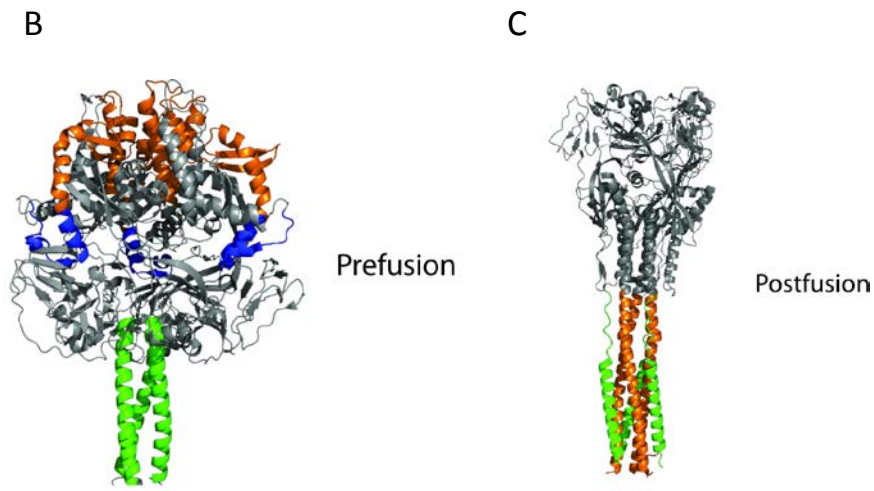
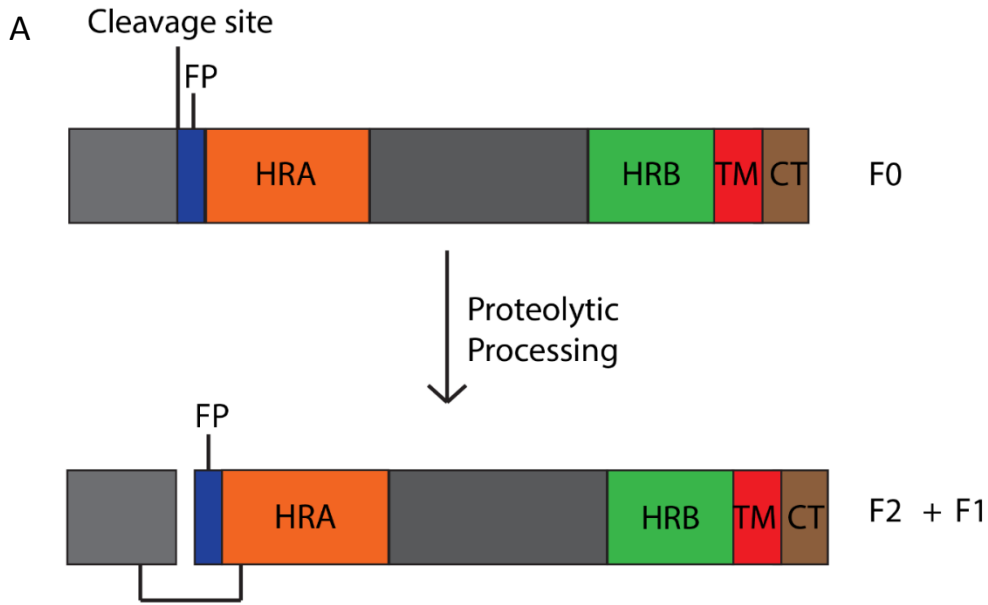


Figure 3. HMPV F protein: processing and predicted structures

(A) The HMPV F protein includes: a hydrophobic fusion peptide (blue), heptad repeat A (HRA) (orange) and heptad repeat B (HRB)(green) domains, the transmembrane (TM) domain (red), and the cytoplasmic tail (brown). The inactive precursor F0 undergoes proteolytic cleavage, resulting in protein fragments F1 + F2 linked by a disulfide bridge. (B) Structures of the uncleaved form of PIV5 F in its prefusion conformation (222) and (C) the hPIV3 F in its postfusion conformation (223), adapted from (312).

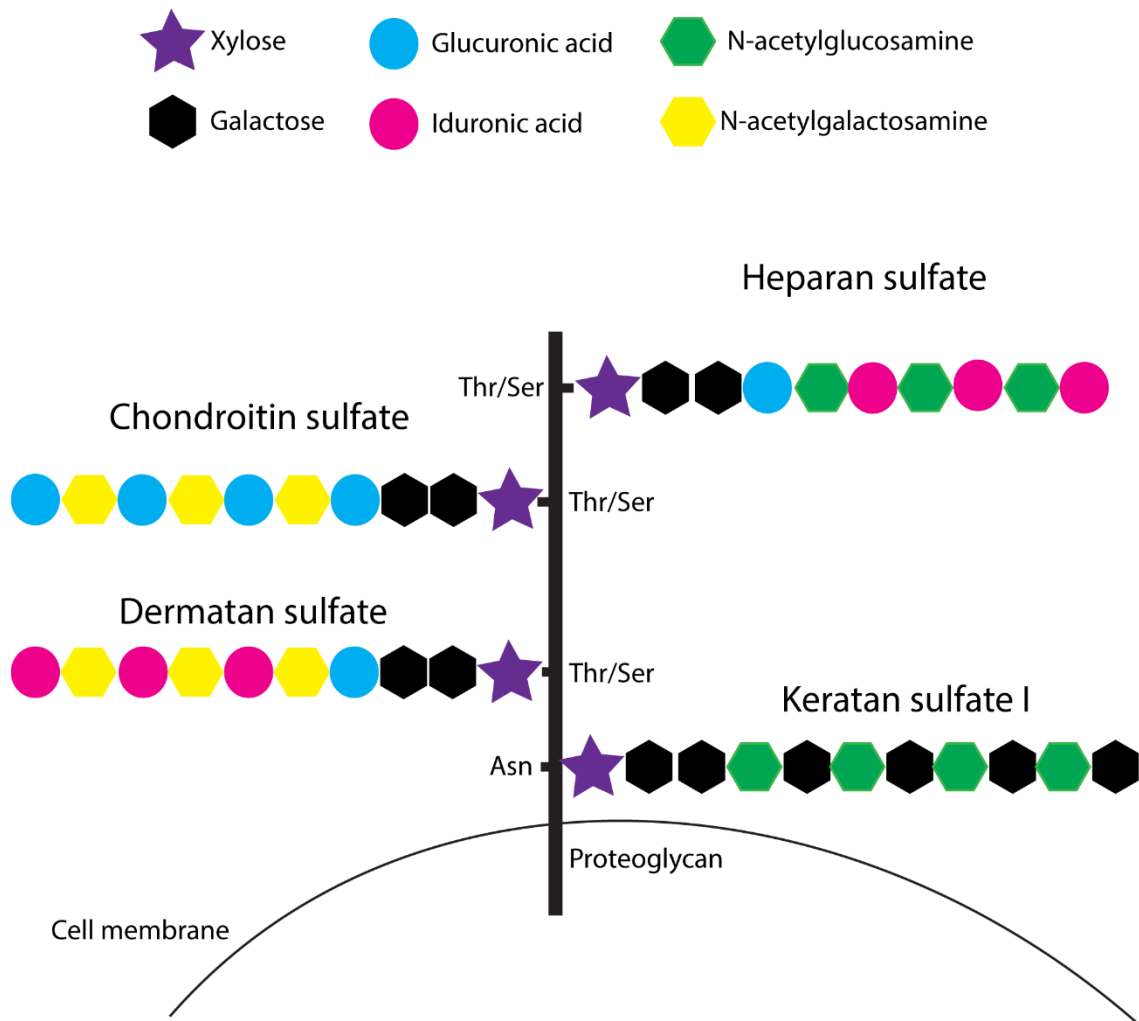


Figure 4. Glycosaminoglycans

Representative structures of glycosaminoglycans (GAGs) heparan sulfate, chondroitin sulfate, dermatan sulfate, and keratin sulfate type I. All four types of GAGs can be further modified by N-sulfation and O-sulfation.

Chapter 2: Materials and Methods

Cells and tissues

Vero cells were grown in Dulbecco's Modified Eagle's Medium (DMEM; Gibco) supplemented with 10% fetal bovine serum (FBS). BSR cells (provided by Karl-Klaus Conzelmann, Max Pettenkofer Institut) were grown in DMEM supplemented with 10% fetal bovine serum and 1% penicillin and streptomycin (P/S). The medium of the BSR cells was supplemented with 0.5 mg/ml G-418 sulfate (Gibco Invitrogen, Carlsbad, CA) every third passage to select for T7 polymerase-expressing cells. A549 cells were grown in Roswell Park Memorial Institute medium (RPMI; Lonza) supplemented with 10% FBS. BEAS-2B cells, a human bronchial epithelial cell line, obtained from ATCC, were maintained in BEGM medium containing all the recommended supplements (Lonza) in flasks coated with bovine collagen (Sigma), bovine fibronectin (VWR Scientific) and bovine serum albumin (EMD Millipore). Cystic fibrosis bronchial epithelial (CFBE) cells were kindly supplied by Carolyn Coyne from the University of Pittsburg. CFBE cells were grown in DMEM supplemented with 10% FBS, 1 mM of non-essential amino acids (Gibco), and 1 mM of sodium pyruvate (Invitrogen). All cells were grown at 37°C under 5% CO₂.

Well-differentiated (transepithelial resistance >1000 Ohm) primary normal bronchial human airway epithelial (HAE) tissue cultures were purchased from MatTek Corp. (Ashland, MA, USA). Cell culture inserts were placed atop two washers (MatTek) in 6-well plates with 5 mL AIR 100 growth medium (MatTek) in contact with the basal surface and incubated at an air-liquid interface at 37°C and 5% CO₂. Tissues were maintained for 5-7 days for differentiation after arrival by washing the apical surface with 0.9% sodium chloride and changing the media every 48 hours prior to initiation of infection experiments.

Plasmids

HMPV virus strains were kindly provided by the designated sources: CAN97-83 (Ursula J. Buchholz, NIAID), TN83-1211 (BEI Resources), TN94-49 and TN96-12 (John Williams, U. of Pittsburg). RNA was isolated from viruses propagated in Vero cells as by phenol-chloroform extraction. Briefly, 100 µL of virus solution was resuspended in 800 µL Tripure and incubated at room temperature for 5 min. Next 200 µL chloroform was added and the sample was shaken vigorously for 15 sec and let stand for 15 min. The sample was centrifuged for 15 min at 12,000xg at 4°C. The top (colorless) layer containing the RNA was transferred to a new tube and 500 µL

isopropanol added. The RNA was allowed to precipitate for 10 min at room temperature and pelleted by centrifugation for 10 min at 12,000 x g, at 4°C. 1mL 75% ethanol was added to the pellet. After inverting to mix, the samples were centrifuged for 5 min at 7,500 x g at 4°C. The supernatant was discarded and the pellet air-dried overnight. The RNA was resuspended in 50µL DEPC treated water.

The F genes were amplified from RNA using the following primers designed with EcoR1 restriction sites upstream and downstream of the gene: forward primer 5'AAAGAATTCGCTAGCAATCAAGAACGGGACAAATAAAAATGTCTTGGAAAGTGGTGATCATTTTTTCAT TGC and reverse primer 5'AAAAAGAATTCTTTAATTAATACTAA-CTGTGTGGTATGAAGCC. Using the SuperscriptIII One Step RT-PCR system (Invitrogen) according to manufacturer's protocol, the gene was amplified using the following thermocycler settings: 1 cycle at 55°C for 30 min, 1 cycle at 94°C for 2 min, 40 cycles of the following three steps: 94°C for 15 sec, 60°C for 2 min, 68°C for 1 min, then 1 cycle at 68°C for 5 minutes. The amplified product was held at 15°C until it was confirmed by gel electrophoresis, and bands corresponding to F (1600bp) were excised and purified. The inserts were digested with EcoR1 and ligated into alkaline phosphatase-treated pCAGGs overnight at 16°C using T4 DNA Ligase (New England BioLabs). Competent E coli cells were transformed with ligation product and plated on plates with Ampicillin. After 12-18 hr of growth at 37°C, colonies were screened for an insert. Correct orientation of insert in pCAGGS was determined by digestion with Pac1 (restriction site in forward primer) and Xba1 (restriction site in pCAGGS) digestion, with proper orientation giving bands of sizes 1754 bp and 4651 bp. The CAN97-83 434H F mutant was created using the gene in pGEM-3Zf(+) using QuikChange site-directed mutagenesis (Stratagene) and subcloned back into pCAGGS. All F expression plasmids were sequenced in their entirety and BioEdit was used for sequence analysis.

Antibodies

A rabbit polyclonal antibody against avian metapneumovirus (AMPV) C matrix (M) protein supplied by Dr. Sagar Goyal (University of Minnesota) with cross reactivity to HMPV M was used to detect HMPV M protein by Western blot (313). All other antibodies were purchased from the following companies: β-actin (Sigma), Peroxidase AffiniPure Goat Anti-Rabbit IgG and Peroxidase AffiniPure Goat Anti-Mouse IgG (Jackson Immuno Research). Antipeptide antibodies to HMPV F (Genemed Synthesis, San Francisco, CA) were generated using amino acids 524 to 538 of HMPV F (314).

Syncytium assay

Subconfluent monolayers of Vero cells in 6-well plates were transiently transfected with a total of 2 µg of DNA consisting of pCAGGS-HMPV F derived from CAN97-83, CAN97-83 mutant 434H, TN83-1211, TN49-49 or TN96-12, or the empty pCAGGS vector, using Lipofectamine Plus reagents (Invitrogen) according to the manufacturer's instructions. The next morning, confluent cell monolayers were washed with PBS (phosphate buffered saline; Invitrogen) and incubated at 37°C in Opti-MEM (Gibco) with 0.3 µg/ml TPCK (l-1-tosylamide-2-phenylethyl chloromethyl ketone)-trypsin (Sigma) for 1 hr. Then the cells were rinsed once with PBS (pH 7.2) before PBS of the indicated pH, buffered with 10 mM HEPES and 5 mM MES (2-(*N*-morpholino)ethanesulfonic acid hemisodium salt), was added. Cells were incubated for 4 min at 37°C with PBS pH 5 or pH 7, and then the media was replaced again with Opti-MEM with 0.3 µg/ml TPCK-trypsin. The pH pulse was repeated three more times (2 hr apart) throughout the day. Vero cells were incubated overnight at 37°C to allow syncytia formation to take place. Digital photographs of syncytia were then taken with a Nikon Coolpix995 camera mounted on a Nikon TS100 inverted phase-contrast microscope using a 5X objective. Quantification of syncytia formation is reported as a fusion index, as previously reported (315). Briefly, the fusion index was calculated using the equation $f = [1 - (C / N)]$ where *c* is the number of cells in a field after fusion and *n* the number of nuclei. Six fields were scored per condition representative of 3 independent experiments.

Reporter gene fusion assay

Vero cells in 6-cm dishes were transfected using Lipofectamine Plus reagents (Invitrogen) with 1.5 µg pCAGGS-HMPV F derived from CAN97-83, TN83-1211, TN49-49 or TN96-12 or CAN97-83 mutant 434H or empty pCAGGs control, and 1.5 µg T7 control plasmid (Promega) containing luciferase cDNA under the control of the T7 promoter. The following day Vero cells in one 6-cm dish were lifted with trypsin, a process which also efficiently cleaved the HMPV F protein. The cells were resuspended in DMEM plus 10% FBS and overlaid onto two 35-mm dishes of confluent BSR cells, which constitutively express the T7 polymerase. The combined cells were incubated at 32°C for 2 hr. The cells were then rinsed once with PBS (pH 7.2) before adding pH 5 or 7 PBS buffered with 10 mM HEPES and 5 mM MES (morpholineethanesulfonic acid). The cells were incubated for 4 min at 37°C under the indicated pH conditions, and then Opti-MEM with 0.3 µg/ml TPCK-trypsin was added. The cells were again incubated at 32°C for 1 hr, and then the cells were treated with pH 5 or 7 PBS as before. DMEM with FBS was added after this treatment, and the

cells were incubated at 37°C for 4 hr. Finally, the cell lysates were analyzed for luciferase activity using a luciferase assay system (Promega) according to manufacturer's protocol. Light emission was measured using an Lmax luminometer (Molecular Devices, Sunnyvale, CA).

Surface expression of proteins, metabolic labeling, and immunoprecipitation

Vero cells were transiently transfected with 4µg pCAGGS expression vectors using Lipofectamine Plus reagent. At 18 to 24 hr posttransfection, the cells were starved in methionine- and cysteine-deficient DMEM for 30 min and then metabolically labeled with Tran³⁵S-label (100 µCi/ml; MP Biomedicals) for 3 hr with or without the presence of 0.3 µg/ml TPCK-trypsin. The cells were washed three times with cold pH 8 PBS and incubated with 1 mg/ml EZ-Link Sulfo-NHS-Biotin (Pierce, Rockford, Ill.) diluted in pH 8 PBS for 15 min of rocking at 4°C and then 30 min at room temperature. The cells were washed twice with PBS before being lysed with radioimmunoprecipitation assay buffer containing 100 mM Tris-HCl (pH 7.4), 150 mM NaCl, 0.1% sodium dodecyl sulfate (SDS), 1% Triton X-100, 1% deoxycholic acid, protease inhibitors (1 Kallikrein inhibitory unit of aprotinin, [Calbiochem, San Diego, Calif.] and 1 mM phenylmethylsulfonyl fluoride [Sigma, St. Louis, Mo.]), and 25 mM iodoacetamide (Sigma). The lysates were centrifuged at 136,500 × *g* for 10 min at 4°C, and the supernatants were collected. Antipeptide sera and protein A-conjugated Sepharose beads (Amersham, Piscataway, N.J.) were used to immunoprecipitate the F proteins as previously described (316). The beads were boiled twice in 10% SDS for 10 min to release the proteins. Ten percent of the total protein was removed for analysis, and the remaining 85% was incubated with immobilized streptavidin (Pierce) for 1 hr at 4°C. Then biotin-labeled protein bound to streptavidin was pulled down and released by boiling with loading buffer. The immunoprecipitated F proteins were analyzed via SDS-15% polyacrylamide gel electrophoresis (SDS-PAGE) and visualized using the Typhoon imaging system.

Homology modeling

The DeepView/Swiss-PdbViewer v3.7 (www.expasy.org/spdbv/) was used to generate homology models of the HMPV F protein in prefusion and postfusion conformations as previously described (136, 243). The prefusion model of HMPV F was created by threading the amino acid sequence onto the crystal structure of PIV5 F in its metastable prefusion form (222). The postfusion homology model of HMPV F was created by threading the amino acid sequence of HMPV into the crystal structure of Newcastle Disease Virus F in its postfusion conformation (317).

Heparan sulfate mimicking and occluding compounds

Iota-carrageenan was purchased from Sigma (Invitrogen). Peptide dendrimer SB105-A10 ([H-ASLRVRIKK]₄ Lys₂-Lys-β-Ala-OH) was synthesized by Lifetein with a purity of >95%. *Escherichia coli* K5 polysaccharides derivatives were provided by David Lembo and Glycores 2000 (318).

Cell viability assay

Approximately 10,000 BEAS-2B or A549 cells were grown in triplicate overnight in a 96 well plate. BEAS-2B cells were either incubated with 2 μM SB105-A10 for 1 hr, 40 μg/mL iota-carrageenan for 4 hr, or 10 μM of each of the K5 derivatives for 4 hr at 37°C. A549 cells were incubated with 2 μM SB105-A10 for 1 hr at 37°C. Control cells were incubated with OptiMEM, which was used to dilute all of the compounds. Then 3-(4, 5-Dimethylthiazol-2-yl)-2, 5-diphenyl-2H-tetrazolium bromide (MTT; Fisher Scientific) (5 mg/mL) was added and incubated for 3 hr at 37°C. The media was removed from the cells by tapping the plate and blotting excess liquid. Next, 100 μL of stop solution (90% isopropyl alcohol, 10% DMSO) was added and the plate was incubated at room temperature for 20 minutes in the dark with rocking. Absorbance was read at 590 nm using a plate reader. Absorbance of treated cells was normalized to the untreated control.

Virus propagation and titers

Recombinant, green fluorescent protein (GFP)-expressing HMPV (rgHMPV) strain CAN97-83 (genotype group A2) and the mutant viruses HMPV ΔG and HMPV ΔG/ΔSH with a codon-stabilized SH gene (319) were kindly provided by Peter L. Collins and Ursula J. Buchholz (NIAID, Bethesda, MD). The viruses were propagated in Vero cells (starting multiplicity of infection [MOI], 0.01 to 0.03) and incubated at 37°C with Opti-MEM, 200 mM l-glutamine, and 0.3 μg/ml tosylsulfonyl phenylalanyl chloromethyl ketone (TPCK)-trypsin (Sigma), replenished every day. On the fifth day, or when cytopathic effects were observed in at least 25% of the cells, cells and medium were collected and subjected to centrifugation at 2,500 × g for 10 min at 4°C in a Sorvall RT7 tabletop centrifuge. The supernatant was then stored in 1× sucrose phosphate glutamate (SPG) (218 mM sucrose, 0.0049 M l-glutamic acid, 0.0038 M KH₂PO₄, 0.0072 M K₂HPO₄), and aliquots were flash frozen in liquid nitrogen and thawed twice prior to storage at -80°C. To achieve more concentrated rgHMPV for HAE tissue experiments, supernatants of harvested cells and medium were subjected to centrifugation on a 20% sucrose cushion for 3 hr at 27,000 × g at

4°C using a SW28 swinging-bucket rotor on a Beckman Optima L90-K ultracentrifuge. Following centrifugation, the supernatant was removed, and the pellet was resuspended in 100 µl Opti-MEM per T75 flask harvested, and left at 4°C overnight. Aliquots were stored at -80°C by flash freezing in liquid nitrogen.

Recombinant GFP-expressing parainfluenza virus 5 (rgPIV5) was kindly provided by Robert Lamb (Howard Hughes Medical Institute, Northwestern University) (136). rgPIV5 was propagated in MDBK cells as described previously (316) and stored in 1× SPG. Aliquots were frozen in liquid nitrogen and thawed twice prior to storage at -80°C. Recombinant GFP-expressing respiratory syncytial virus (rgRSV) was provided by Mark Peebles (The Ohio State University).

For GFP-expressing viruses (rgHMPV, rgPIV5, and rgRSV), viral titers were calculated by creating serial dilutions of the viral samples in Opti-MEM. Vero cells were seeded on a 96-well plate overnight and infected in serial dilution (10^{-1} to 10^{-12}) with 50µL of virus solution in duplicate. The number of GFP-expressing cells was counted in wells demonstrating 25-100 GFP-positive cells the following day. Average titer was calculated based on the dilution of the virus solution in the wells counted.

For non-GFP expressing viruses (HMPV Δ G and HMPV Δ G/ Δ SH) viral particles were estimated using serial dilutions of viral samples assessed for M protein content using Western blot and compared to protein levels of an rgHMPV standard of known titer. Volumes of untitered virus and the rgHMPV standard of known titer (2, 4, and 8 µL in duplicate) were resolved on 15% SDS-PAGE, and the proteins were transferred to a PVDF membrane (Fisher) at 50 volts for 80 min. The membrane was blocked with Odyssey Blocking Buffer (Li-Cor) at 4°C overnight and incubated with anti-AMPV M antibody (1:500) in PCT (PBS; phosphate buffered saline (Invitrogen) with casein and 0.2% Tween-20) for 3 hr at room temperature. The membrane was washed with t-TBS (0.2% Tween-20 in 1X TBS (Tris buffered saline)) and incubated with Peroxidase AffiniPure Goat Anti-Rabbit secondary antibody (1:10,000) in PCT for 1 hr at room temperature. The membrane was washed with t-TBS and incubated with SuperSignal West Pico Chemiluminescent Substrate (Fisher) for 10 min in the dark prior to development by ECL. Densitometry was quantified using ImageQuantTL, and an average density units of M protein per µL of virus input was calculated for each sample. Titer was determined by comparing to the standard of known titer.

Cell infection assay

BEAS-2B cells were grown to low confluency (approximately 50,000 cells per well; as recommended by ATCC) in a 24 well plate overnight. Iota-carrageenan solution was freshly prepared in PBS at 0.7 mg/mL by incubating at 55°C with brief vortexing. Virus was pretreated with iota-carrageenan or K5 polysaccharide derivatives diluted in OptiMEM for 30 min at 4°C with rocking. Cells were washed two times with PBS and 200µL of virus solution was added at MOI of 1. For SB105-A10 experiments, BEAS-2B or A549 cells were washed 2 times with PBS, and incubated with 200µL of SB105-A10 diluted in Opti-MEM at variable concentrations at 37°C for 1 hour. Cells were washed once with PBS and infected with 200 µL of virus solution in OptiMEM at an MOI of 1. For all treatments, cells were incubated with the infection media in duplicate for 2 hours at 37°C with rocking every 30 min. After 2 hr, cells were washed twice with PBS, and infection media was replaced. For GFP expressing virus, following an overnight incubation, cells were resuspended, fixed in 2% formaldehyde diluted in PBS with 50 mM EDTA, and analyzed with a BD FACS Calibur flow cytometer, for which the GFP expression of at least 10,000 cells were determined. Data analysis was performed using FCS Express software, and data presented in graphs represent the percentage of GFP-expressing cells as a percentage of the untreated control as previously described (79).

HAE infection assay

HAE tissues were maintained according to the manufacturer's recommendations for 5-7 days after arrival. Tissues were transferred to a new 6-well plate with 1 ml of HEPES buffered saline (HBS; 150 mM NaCl, 20 mM HEPES pH 7.5, 1 mM MgCl₂ and 1 mM CaCl₂) and washed with 400 µL of sterile 0.9% NaCl. The apical surface was washed 3 times with 75 µg/mL lysophosphatidyl choline (LPC; Sigma) in HBS for 10 min at room temperature (320). LPC was removed from the apical surface, and HBS from the basal surface of the tissues, and 1mL of AIR 100 Growth Medium was added to the basal side. To measure the effects of heparan sulfate mimics, rgHMPV or rgPIV5 at MOI of 5 (calculation was based on 0.8×10^6 cells per tissue according to manufacturer) was pretreated either with 40 µg/mL iota-carrageenan, 10µM K5-N,OS (H) or 10µM K5-OS(H) (untreated control received Opti-MEM) in a total volume of 100 µL. For SB105-A10, the tissues were treated with 2 µM SB105-A10 in Opti-MEM for 1 hr at 37°C prior to infection (untreated control tissue was incubated with Opti-MEM). The infection solution (100 µL at MOI of 5) was added to the apical surface of the tissues drop-wise, and the tissues were incubated at

37°C for 2 hours with rocking every 30 min. After 2 hr, the infection media was aspirated, and the apical surface washed 1X with 200µL of HBS. Fresh AIR 100 Growth Medium with 0.3 µg/ml TPCK-trypsin was added to each well and incubated at 37°C. After 48 hr, the apical surface of the tissues was imaged for GFP expression using an Axiovert-100 (3 fields per tissue) at 5X magnification. The number of infected cells was determined by counting GFP-expressing cells and averaged per tissue. The results are reported as a percent infection of the untreated control.

Cell binding assay

Approximately 250,000 BEAS-2B cells were cultured overnight in a 6-well plate. rgHMPV was pretreated with iota-carrageenan at 40 mg/mL or 1µM of the K5 polysaccharide derivatives diluted in Opti-MEM for 30 minutes at 4°C with rocking. For SB105-A10 treatment, cells were washed two times with PBS and incubated in a 200 µL solution of SB105-A10 diluted in Opti-MEM at 37°C for 1 hour. For all treatments, cells were washed twice with cold PBS and infected with 500µL of virus solution at an MOI of 1 for 2 hr at 4°C with rocking to prevent internalization. Cells were washed with PBS 3 times, lysed using 45 µl of RIPA buffer with 0.15 M NaCl with a complete protease inhibitor cocktail tablet (Fisher), and frozen at -80°C. Cells were thawed and scraped on ice, and lysates were cleared by centrifugation for 10 min at 55,000 rpm at 4°C (Sorvall *Discovery* M120). Western blot analysis for M to quantify bound HMPV was carried out as described above.

Statistical Analysis

All data are presented as mean +/- standard deviation. A standard Student's *t*-test or one-way ANOVA was performed when appropriate to analyze the differences between the individual experiments with statistical significance set as $p \leq 0.05$. Post-hoc Bonferroni's multiple comparison test (GraphPad Prism) was used within one-way ANOVA to identify specific differences between groups.

Chapter 3: HMPV fusion protein triggering: Increasing complexities by analysis of new strains

*This work was completed with the help of Andres Chang, who cloned the fusion proteins from HMPV CAN97-83, TN94-49 and TN96-12 and designed the primers for this construct. Andres Chang also created the homology model for the prefusion and postfusion structures of HMPV F and identified the exposed basic residues on the surface of HMPV F that may contribute to interaction with heparan sulfate. Viruses TN94-49 and TN96-12 were kindly provided by John Williams (University of Pittsburg).

Introduction

Human metapneumovirus (HMPV), an enveloped, negative-sense, single-stranded RNA virus in the Paramyxoviridae family, is a common cause of both upper and lower respiratory tract infections (30, 31, 321). First identified in 2001 in the Netherlands, HMPV is now known to be the cause of respiratory infections in humans since at least 1958 (31). HMPV strains have been phylogenetically classified into two genetic lineages (A and B) with distinct sublineages (A1, A2, B1, and B2) (32). Nearly all people are initially infected with HMPV in early childhood, and reinfection throughout life is common (7). Respiratory disease caused by HMPV can vary in severity, from mild cold-like symptoms to severe lower respiratory tract infection such as pneumonia and bronchiolitis (321, 322). Infants, immunocompromised and geriatric patients are most likely to foster severe infection (37, 38, 43-45). There is no vaccine or antiviral treatment against HMPV.

To infect cells, enveloped viruses fuse the viral envelope with membranes of the target cell, a process mediated by one or more surface viral glycoproteins. For HMPV, this process can occur in endosomes (282) and is mediated by the fusion protein (F). HMPV F proteins, like all paramyxovirus F proteins, are trimeric type I fusion proteins. To become active, paramyxovirus F proteins undergo proteolytic cleavage of the precursor form of the protein (F₀) into an active, disulfide-linked form (F₁+F₂) (75, 212). For HMPV F, this can be achieved by the addition of exogenous trypsin (134), although it is thought secreted host proteases cleave F during infection *in vivo*.

The paramyxovirus F protein undergoes an essentially irreversible conformational change during the process of membrane fusion, with the released energy proposed to drive the fusion process. The triggering event that drives these conformational changes for the majority of

paramyxovirus F proteins is hypothesized to occur following attachment of the virus to its receptor, requiring the coordinated activity of an attachment protein and a fusion protein (reviewed in (212)). However, HMPV attachment and fusion is dependent on F alone (79, 134, 136). Furthermore, HMPV F promotes cell-to-cell fusion without the putative attachment protein, G (134, 136, 241, 242). This suggests HMPV F is triggered to fuse by environmental and host factors in the right time and place.

There is direct evidence HMPV can enter target cells by endocytosis in epithelial and endothelial cells. Antigen presenting cells of the immune system can take up HMPV by micropinocytosis (93). However, HMPV particles are internalized via clathrin-mediated endocytosis in human bronchial epithelial cells (282), which requires dynamin (136, 282). Furthermore, viral membrane fusion has been shown to take place in endosomes (282). Our group and others have shown HMPV infection for at least some strains can be inhibited by interfering with acidification of endosomes, suggesting low pH can contribute to HMPV infection (136, 242, 282). Many paramyxovirus F proteins can promote fusion at neutral pH (75). However, low pH can trigger the fusion of activity of HMPV F from some strains, including HMPV strain CAN97-83 (clade A2) (134, 136). For fusion proteins that can be triggered to fuse by low pH, it is thought that electrostatic repulsive forces that arise between residues, often involving histidines that become protonated at low pH and neighboring basic residues contribute to the destabilization of the prefusion conformation of F, which then leads to refolding to the postfusion conformation (255-257). In HMPV F, a conserved histidine residue (H435) in the heptad repeat B linker domain is thought to serve as a pH sensor and contribute to triggering F (136, 242). H435 is in close proximity to 3 conserved basic residues, K295, R396, and K438, based on a homology model of the prefusion conformation, and is therefore proposed to lead to electrostatic repulsion that results in triggering of F and fusion (136, 243). Studies with recombinant HMPV with mutations in this region confirmed its importance for virus infectivity (243).

While the trigger of CAN97-83 (A2) F by acidic pH has biological significance in the context of endocytic entry, low pH is not required for fusion activity for F proteins for all strains of HMPV. An initial analysis of F proteins from a single prototype strain from each clade revealed low pH triggered fusion is rare among HMPV (241). Specifically, glycine 294 was identified as a requirement for low pH triggered fusion, and this residue is not commonly found in HMPV F proteins (241). Furthermore, additional analysis identified residues at positions 296, 396, and 404 as the main determinants of fusion activity among hMPV F proteins (242). These findings suggest

acidic pH is not a general factor in HMPV F trigger, however few HMPV F proteins have been studied in each clade.

In this study, we analyzed the different fusion activity of HMPV F proteins from three unique strains: TN83-1211 (Clade B2), TN94-49 (Clade A2), and TN96-1211 (Clade A1). We identified an F protein from TN83-1211 (B2) that promotes greatly enhanced fusion after low pH pulses compared to CAN97-83 (A2) F, and determined the specific residue, H434, is a key contributor to this hyperfusogenic phenotype, supporting the hypothesis that electrostatic interactions in this region play a key role in HMPV F triggering. Furthermore, we characterized an F protein from strain TN94-49 (A2) that promotes cell-to-cell fusion after low pH pulses without residue G294, which has been previously thought to be required for low pH promoted fusion. Lastly, we identified an F protein from TN96-12 (A1) that failed to fuse in cell-to-cell fusion assays, suggesting additional host factors are required for triggering for this HMPV F. Taken together, these results further elucidate the complexity of HMPV F proteins and provide insights to how fusion is regulated in endosomal compartments to establish infection.

Results

Different fusion activity of HMPV F proteins

We previously showed that the fusion protein (F) derived from HMPV strain CAN97-83 (A2) could be triggered to promote membrane fusion by short exposure to low pH (134, 136). However, fusion by F proteins from other strains, specifically those in the B genetic lineage, were not low pH triggered in studies from other groups, suggesting low pH is not a requirement for fusion for F proteins of all strains of HMPV (241, 242). However, F proteins from only a small number of strains within each clade have been examined. We therefore characterized the fusion activity of F proteins from several additional strains and determine how these results fit with the current understanding of essential residues involved in low pH triggered HMPV F (136, 241, 242, 314). The F genes were cloned from the following strains of HMPV, with the respective clades indicated in parentheses: TN83-1211 (B2), TN94-49 (A2), and TN96-1211(A1). Because the primer design also included short intergenic upstream and downstream of F, CAN97-83 (A2) F was also cloned using the same expression construct so that activities between the different F proteins could be directly compared. To determine if the F proteins could be triggered to promote membrane fusion by low pH exposure, Vero cells transiently expressing the different F constructs, or the control expression plasmid without F, were exposed to a series of pulses of buffer at pH

5 or 7. The cells were visualized for cell-to-cell fusion, syncytium formation, the following day. In addition to imaging the cells, the fusion index was calculated for each strain (315). As previously reported, CAN97-83 (A2) F promoted cell-to-cell fusion after brief exposure to low pH pulses, as did TN94-49 (A2) to a same degree (Fig. 5A). Interestingly, TN96-12 (A1) F failed to fuse with low pH or neutral pH exposure, whereas TN83-1211 (B2) caused robust syncytia formation that was more extensive than that observed with CAN97-83 (A2) F at low pH (Fig. 5A and 5B). While the fusion index serves as a representative quantitation of syncytia formation, we used a luciferase reporter gene assay as quantitative measure of cell-to-cell fusion by the F proteins (134). Vero cells transfected with the F construct and a plasmid encoding the luciferase enzyme under a T7 promoter were overlaid on BSR cells, which are stably transfected to express the T7 polymerase. Cells were treated with pH 5 or 7 buffer and cell lysates were analyzed for luciferase activity. As observed with the syncytia assay, TN94-49 (A2) F exhibited similar fusion activity as CAN97-83 (A2) F under low pH conditions, and TN83-1211 (B2) F exhibited fusion activity nearly 500% of CAN97-83 (A2) F (Fig. 5C). Fusion activity of TN96-12 (A1) was not observed above background (Fig. 5C).

HMPV F protein surface expression and proteolytic processing

To verify that the varying fusion activity observed for F proteins from the different strains were not a results of changes in surface expression, we performed surface biotinylation. The antibody used to recognize F for immunoprecipitation is a polyclonal antibody generated using amino acids 524 to 538 of CAN97-82 (A2) F and all 4 of the F proteins in these studies are completely conserved in this region (Fig. 6). There was no significant difference in total (Fig. 7A) and surface expression (Fig. 7B) of F from the different strains (Fig. 7C).

While HMPV F is synthesized as a single protein (F0), it must be cleaved into fragments F1 and F2, which are linked by disulfide bonds, to be fusogenically active. In cell assays exogenous trypsin is added to cells to cleave F (34, 73, 90, 323). Although we found equivalent surface expression of the different F constructs, it was possible they are not recognized by trypsin to the same degree. To determine if the different F proteins were not being cleaved by trypsin with the same efficiency, we examined the ratio of surface expression of cleaved F (F1) compared to total F, cleaved (F1) and uncleaved F (F0). Incubation of the cells with trypsin during metabolic labeling revealed the four F constructs are processed to similar efficiency (Fig. 7D, which suggests

differences in trypsin cleavage at the plasma membrane do not account in the variable fusion activity.

Sequence differences in HMPV F proteins and role of H434

Because the surface expression and cleavage efficiency of the F proteins did not differ among the F proteins from different strains, we examined the nucleotide and amino acid sequences to identify potential residues that could explain the different fusion activities. HMPV F is highly conserved, thus sequence analysis revealed only a small number of differences at the amino acid level (Fig. 6). While there were 37 nucleotide differences between CAN97-83 (A2) and TN94-49 (A2), these only resulted in 6 amino acid differences. One key difference was noted at residue 294, as TN94-49 (A2) did not have a glycine but rather lysine at this position (Fig. 8A). Therefore, TN94-49 (A2) F does not require G294 for low pH triggering, in contrast to the previous suggestion that G294 is required for clade A F proteins for low pH triggering (241, 242). Comparison of CAN97-83 (A2) and TN96-12 (A1) revealed 86 nucleotide differences and 9 differences at the amino acid level, though the role of each of these residues in fusion is still unclear. TN96-12 (A1) F lacks G294, previously hypothesized to be critical for low pH triggering, but this residue is also absent in TN94-49 (A2) F, which is low pH triggered. Despite a greater than 400% increase in fusion activity promoted by low pH, TN83-1211 (B2) F differs from CAN97-83 by only 3 nucleotides, which result in differences at two amino acid positions, R175S and Q434H (Fig. 8B). Histidine 434 specifically was noted because it is immediately adjacent to conserved histidine 435, which is required for fusion activity of CAN97-83 (A2) F and is thought to play a critical role in electrostatic repulsion with neighboring cationic residues after protonation at low pH (134, 136, 243).

Fusion activity of CAN97-83 F Q434H mutant

Based on these findings, we hypothesized the additional histidine in this region of F results in hyperfusogenic activity at low pH. To confirm that this residue is essential for the observed hyperfusogenic phenotype, a point mutation was introduced to CAN97-83 (A2) F at this position by site directed mutagenesis and verified by sequencing. To characterize the fusion activity of the CAN97-83 F 434H mutant, Vero cells were transfected with the expression plasmids and treated to pH pulses to promote fusion. Compared to the wild-type CAN97-83 (A2) F, the Q434H mutant F induced dramatic syncytia formation in cells treated with PBS at pH 5, similar to TN83-1211 (B2)

F (Fig. 9A and 9B). Quantification of fusion activity of the 434H mutant using a reporter gene assay showed the same fusion activity of the mutant compared to TN83-1211 (B2) F, which is significantly greater than that of wild-type CAN97-83 (A2) F at pH5 (Fig. 9C). Immunoprecipitation to determine overall protein expression (Fig. 10A) and specifically surface expression (Fig. 10B) of the proteins revealed similar expression levels (Fig. 10C). However, the cleavage efficiency of surface F by exogenous trypsin was increased in CAN97-83 Q434H, which may contribute to the hyperfusogenic phenotype (Fig. 10D). Further studies in surface expression and proteolytic processing are necessary to determine if these factors, in addition to H434, contribute to the fusion activity of this mutant. Altogether, these results show the introduction of an additional histidine in this region of F, adjacent to histidine 435, resulted in greater overall fusion activity as well as increased sensitivity to low pH to promote fusion.

The results of this study reveal significant differences in the fusion activity of F proteins derived from diverse strains of HMPV that challenge the previous understanding the residues that are involved in low pH triggered fusion for HMPV F. We identified a B2 clade HMPV F protein that can be triggered to fuse by low pH, suggesting that this characteristic can be seen outside of clade A viruses. High fusion activity promoted by low pH of TN83-1211 F was attributed to H434, supporting that this region of F can contribute to the triggering of the conformational changes in F to drive membrane fusion. Furthermore, TN94-49 (A2) F with K294 was triggered to fuse by low pH, suggesting G294 is not an absolute requirement of clade A HMPV F for low pH-mediated fusion. These findings demonstrate the complexity of HMPV F activity and regulation.

Discussion

In this study we characterized the fusion activity of the F derived from 3 different strains of HMPV, TN94-49 (A2), TN96-12 (A1) and TN83-1211 (B2), compared to CAN97-83 (A2). Treatment with low pH promoted fusion in cells expressing F proteins from three of the four strains, with dramatic fusion observed by TN83-1211 (B2), whereas TN96-12 (A1) F failed to fuse under standard assay conditions. The hyperfusogenic activity of TN83-1211 (B2) F was recreated with the introduction of 434H in CAN97-83 (A2) F, supporting that this region of F plays a critical role in low pH-induced triggering of membrane fusion.

We have previously reported low pH promoted membrane fusion by CAN97-83 (A2) F (134, 136). However, others have reported that low pH does not promote fusion for strains outside of the A clade (241, 242). Here we show low pH promoted fusion by an F protein from

another A2 HMPV, TN94-49, as well as an F protein from the B2 clade, TN83-1211, suggesting low pH promoted fusion activity is not exclusive to any phylogenetic group. The specific residue G294 has been reported as a requirement for low pH promoted fusion by clade A F proteins (241). However, TN94-49 (A2) F, which fuses under low pH conditions, does not have this residue but rather K294. Interestingly, genetic variability analysis of HMPV F revealed position 294 is one of two positively selected sites in the gene, with relaxed selective constraints for amino acids G, K, and E (324). This suggests the residue at this position, as long as it is G, K, or E, does not affect virus fitness. Furthermore, it was reported that no lineage B HMPV F sequences have G294, suggesting acidic pH is not a general trigger of HMPV F proteins for activity (241). In this study we found TN83-1211 (B2) F does have the residue G294, indicating it is not exclusive to clade A viruses. Additional residues at positions 296, 396, and 404 have also been shown to affect F sensitivity to low pH (242). However, these positions are completely conserved in the F proteins of the four strains analyzed here despite variable response to low pH (Fig. 6). Altogether, these results suggest fusion protein activity is highly complex, and identification of specific residues from prototype strains that are associated with low pH promoted fusion may be challenging.

Sequence analysis revealed TN83-1211 (B2) F is nearly identical to CAN97-83 (A2) F in amino acid sequence, with a notable difference at position 434 in the hyperfusogenic protein. The H434 residue lies adjacent to a conserved histidine at position 435, which has been shown to participate in potential electrostatic interactions with surrounding positive residues K295, R396, and K438, that drive the conformational change during triggering of the protein (243). We generated a prefusion homology model for HMPV F (Fig. 11A) based on the solved crystal structure of prefusion parainfluenza virus 5 F (222). Although the partial structure of the prefusion form of HMPV F has been solved, it only includes residues to amino acid 430, and thus is lacking the key residues examined in this study (221). Based on this model, H434 and H435, exposed on the prefusion protein for solvent protonation, are surrounded by basic residues K295, R396, and K438 (Fig. 11B). We propose the addition of a second histidine that can become protonated in this critical region may contribute to lower prefusion stability due to charge-charge repulsion with these surrounding basic residues (Fig. 11B), which is supported by the distribution of these residues in the postfusion model (Fig. 11C).

Interestingly, examination of over 120 known HMPV F amino acid sequences revealed no other HMPV F sequences with H434. This suggests a high level of fusion may not enhance fitness of HMPV during endogenous infection. It has been shown for the attachment and fusion

machinery of PIV3 that enhancement of receptor binding and fusion in monolayer cell culture is detrimental to growth and replication in HAE culture and in cotton rats (325). Thus, some viruses with high activity F are less competent to establish infection in an *in vivo* model. Alternatively, mutant RSV with F proteins of high fusion activity caused higher viral loads, severe lung histopathology, and weight loss in mice compared to controls (326). Therefore, the impact of fusion activity on viral fitness may depend on complex factors beyond the fusion protein alone. Because H434 is not found in any other known F from HMPV aside from TN83-1211 (B2), it is possible hyperfusogenic activity does not confer a fitness advantage in the population HMPV.

Under standard syncytia and reporter gene assay conditions, TN96-12 (A1) F failed to fuse at low or neutral pH despite surface expression and processing equivalent to other variants analyzed. These results suggest that TN96-12 (A1) F requires additional cellular or viral factors to trigger fusion activity that are not present at the plasma membrane. It has recently been shown HMPV can fuse in endosomes, which may have host factors available to trigger F that are not present at the plasma membrane (282). While F protein activity independence from an attachment protein has been characterized for CAN97-83 (A2) F (134), it is possible TN96-12 (A2) F requires interaction with other viral proteins that are not present in these fusion assays. It has been shown HMPV G can affect particle entry in dendritic cells (93) and also the small hydrophobic protein can also modulate fusion activity (92). Lastly, existing methodologies to study HMPV F limit detection of specific prefusion and postfusion conformations. Therefore, TN96-12 (A1) F when solely expressed at the plasma membrane without other viral glycoproteins may be unstable in its prefusion form and prematurely trigger resulting in the absence of fusion activity.

HMPV F fusion activity is a true balancing act between prefusion stability and triggering of F to fuse membranes and establish infection. Tipping too far in either direction appears to be a detriment to viral fitness. The results in this study highlight the diversity in HMPV F activity in response to low pH and the challenges of identifying specific residues that correlate with low pH promoted fusion. Further studies are necessary that take into account the complex regulatory interactions in the context of an intact infectious viral particle.

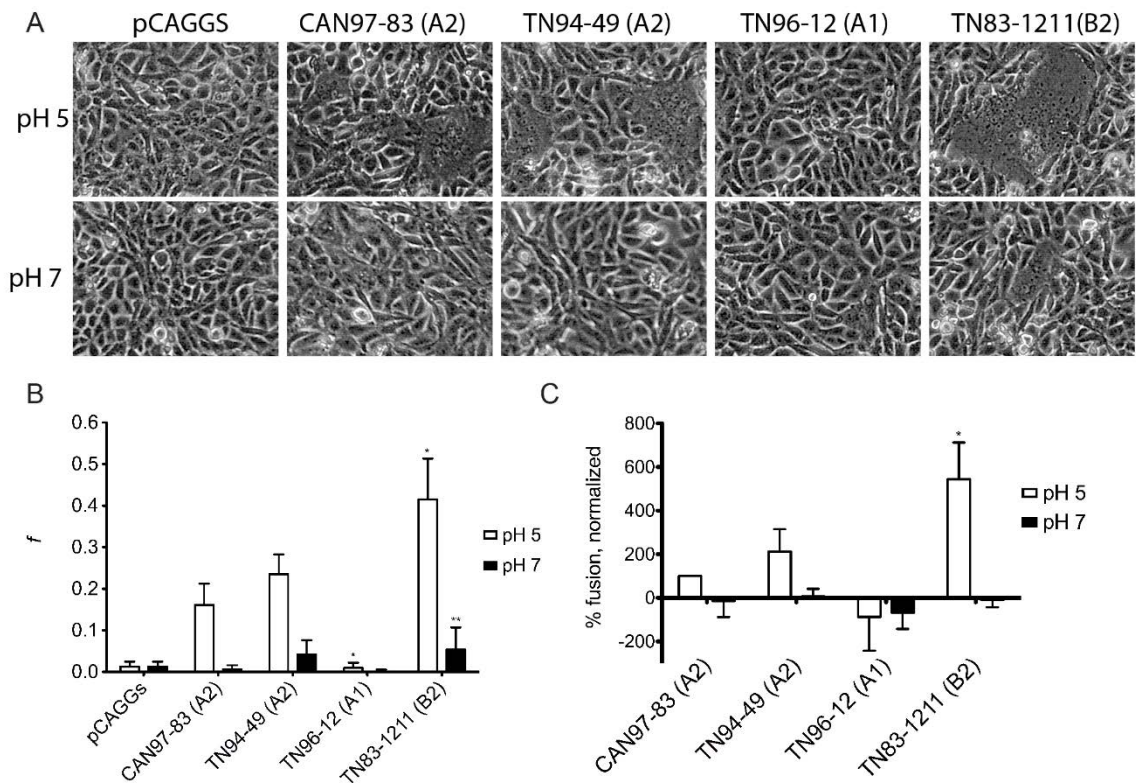


Figure 5. HMPV F proteins from different strains exhibit variable fusion activity promoted by low pH.

(A) Representative images of syncytium formation of cells expressing the HMPV F proteins after pulses at pH 5 or pH 7 (n = 3). (B) The fusion index was calculated using the equation $f = [1 - (C / N)]$ where c is the number of cells in a field after fusion and n the number of nuclei. Six fields were scored per condition representative of 3 independent experiments. * Indicates statistically significant compared to f for CAN97-83 (A2) F after pH 5 pulses, ** Indicates statistically significant compared to f for CAN97-83 (A2) F after pH 7 pulses (n=3) (C) Luciferase reporter gene assay of Vero cells transfected with HMPV F that were used to overlay BSR cells and subjected to two pH pulses. Data are presented as percentages of CAN97-83 (A2) F luminosity (fusion) at pH 5 (n = 3) +/- standard deviation. * Indicates statistically significant compared to f for CAN97-83 (A2) F after pH 5 pulses.

```

          10          20          30          40          50
...|...|...|...|...|...|...|...|...|...|
CAN97-83 (A2) MSWKVVIIFSLLITPQHGLKESYLEESCSTITEGYLSVLRGTGWYTNVFTL
TN94-49 (A2) MSWKVVIIFSLLITPQHGLKESYLEESCSTITEGYLSVLRGTGWYTNVFTL
TN96-12 (A1) MSWKVVIIFSLLITPQHGLKESYLEESCSTITEGYLSVLRGTGWYTNVFTL
TN83-1211 (B2) MSWKVVIIFSLLITPQHGLKESYLEESCSTITEGYLSVLRGTGWYTNVFTL
*****

          60          70          80          90          100
...|...|...|...|...|...|...|...|...|...|
CAN97-83 (A2) EVGDVENLTCSDGPSLIKTELDTKSALRELKTVSADQLAREEQIENPRQ
TN94-49 (A2) EVGDVENLTCADGPSLIKTELELTKSALRELKTVSADQLAREEQIENPRQ
TN96-12 (A1) EVGDVENLTCADGPSLIKTELDTKSALRELRTVSADQLAREEQIENPRQ
TN83-1211 (B2) EVGDVENLTCSDGPSLIKTELDTKSALRELKTVSADQLAREEQIENPRQ
*****:*****:*****:*****

          110         120         130         140         150
...|...|...|...|...|...|...|...|...|...|
CAN97-83 (A2) SRFVLGAIALGVATAAAVTAGVAIAKTI RLESEVTAIKNALKTTNEAVST
TN94-49 (A2) SRFVLGAIALGVATAAAVTAGVAIAKTI RLESEVTAIKNALKTTNEAVST
TN96-12 (A1) SRFVLGAIALGVATAAAVTAGVAIAKTI RLESEVTAIKNALKTTNEAVST
TN83-1211 (B2) SRFVLGAIALGVATAAAVTAGVAIAKTI RLESEVTAIKNALKTTNEAVST
*****

          160         170         180         190         200
...|...|...|...|...|...|...|...|...|...|
CAN97-83 (A2) LGNGVRVLATAVRELKDFVSKNLTRAINKNKCDIDDLKMAVFSQFNRRF
TN94-49 (A2) LGNGVRVLATAVRELKDFVSKNLTRAINKNKCDIDDLKMAVFSQFNRRF
TN96-12 (A1) LGNGVRVLATAVRELKDFVSKNLTRAINKNKCDIADLKMAVFSQFNRRF
TN83-1211 (B2) LGNGVRVLATAVRELKDFVSKNLTSAINKNKCDIDDLKMAVFSQFNRRF
*****

          210         220         230         240         250
...|...|...|...|...|...|...|...|...|...|
CAN97-83 (A2) LNVVRQFSDNAGITPAISLDLMTDAELARAVSNMPTSAGQIKLMLENRAM
TN94-49 (A2) LNVVRQFSDNAGITPAISLDLMTDAELARAVSNMPTSAGQIKLMLENRAM
TN96-12 (A1) LNVVRQFSDNAGITPAISLDLMTDAELARAVSNMPTSAGQIKLMLENRAM
TN83-1211 (B2) LNVVRQFSDNAGITPAISLDLMTDAELARAVSNMPTSAGQIKLMLENRAM
*****

          260         270         280         290         300
...|...|...|...|...|...|...|...|...|...|
CAN97-83 (A2) VRRKGFILIGVYGSSVIYMQVQLPIFGVIDTPCWIVKAAPSCSGKKNYA
TN94-49 (A2) VRRKGFILIGVYGSSVIYMQVQLPIFGVIDTPCWIVKAAPSCSKKKNYA
TN96-12 (A1) VRRKGFILIGVYGSSVIYMQVQLPIFGVIDTPCWIVKAAPSCSEKKNYA
TN83-1211 (B2) VRRKGFILIGVYGSSVIYMQVQLPIFGVIDTPCWIVKAAPSCSGKKNYA
*****

          310         320         330         340         350
...|...|...|...|...|...|...|...|...|...|
CAN97-83 (A2) CLLREDQGWYQONAGSTVYYPNEKDCETRGDHVFCDTAAGINVAEQSKEC
TN94-49 (A2) CLLREDQGWYQONAGSTVYYPNEKDCETRGDHVFCDTAAGINVAEQSKEC
TN96-12 (A1) CLLREDQGWYQONAGSTVYYPNEKDCETRGDHVFCDTAAGINVAEQSKEC
TN83-1211 (B2) CLLREDQGWYQONAGSTVYYPNEKDCETRGDHVFCDTAAGINVAEQSKEC
*****

```

```

          360          370          380          390          400
    . . . | . . . | . . . | . . . | . . . | . . . | . . . | . . . | . . . |
CAN97-83 (A2) NINISTTNYPCKVSTGRHPISMVALSPLGALVACYKGVSCSIGSNRVGII
TN94-49 (A2) NINISTTNYPCKVSTGRHPISMVALSPLGALVACYKGVSCSIGSNRVGII
TN96-12 (A1) NINISTTNYPCKVSTGRHPISMVALSPLGALVACYKGVSCSIGSNRVGII
TN83-1211 (B2) NINISTTNYPCKVSTGRHPISMVALSPLGALVACYKGVSCSIGSNRVGII
*****

          410          420          430          440          450
    . . . | . . . | . . . | . . . | . . . | . . . | . . . | . . . |
CAN97-83 (A2) KQLNKGCSYITNQDADTVTIDNTVYQLSKVEGEQHVIKGRPVSSSFDPVK
TN94-49 (A2) KQLNKGCSYITNQDADTVTIDNTVYQLSKVEGEQHVIKGRPVSSSFDPVK
TN96-12 (A1) KQLNKGCSYITNQDADTVTIDNTVYQLSKVEGEQHVIKGRPVSSSFDPVK
TN83-1211 (B2) KQLNKGCSYITNQDADTVTIDNTVYQLSKVEGEHHVIKGRPVSSSFDPVK
*****:*****:*

          460          470          480          490          500
    . . . | . . . | . . . | . . . | . . . | . . . | . . . | . . . |
CAN97-83 (A2) FPEDQFNVALDQVFENIENSQALVDQSNRILSSAEKNTGFIIVIIILIAV
TN94-49 (A2) FPEDQFNVALDQVFENIENSQALVDQSNRILSSAEKNTGFIIVIIILIAV
TN96-12 (A1) FPEDQFNVALDQVFESIENSQALVDQSNRILSSAEKNTGFIIVIIILIAV
TN83-1211 (B2) FPEDQFNVALDQVFENIENSQALVDQSNRILSSAEKNTGFIIVIIILIAV
*****.*****

          510          520          530
    . . . | . . . | . . . | . . . | . . . | . . . | . . . |
CAN97-83 (A2) LGSSMILVSIFIIKKTKKPTGAPPEL SGVTNNGFIPHS
TN94-49 (A2) LGSSMILVSIFIIKKTKKQTGAPPEL SGVTNNGFIPHS
TN96-12 (A1) LGSTMILVSVFIIKKTKKPTGAPPEL SGVTNNGFIPHS
TN83-1211 (B2) LGSSMILVSIFIIKKTKKPTGAPPEL SGVTNNGFIPHS
***:*****:***** *****

```

Figure 6. Amino acid sequence of F proteins of CAN97-83 (A2), TN94-49 (A2), TN96-12 (A1), and TN83-1211 (B2).

Sequence alignment was generated using ClustalW. The asterisk “*” indicates identical residues, “.” indicates conserved substitutions and “.” semi-conserved substitutions.

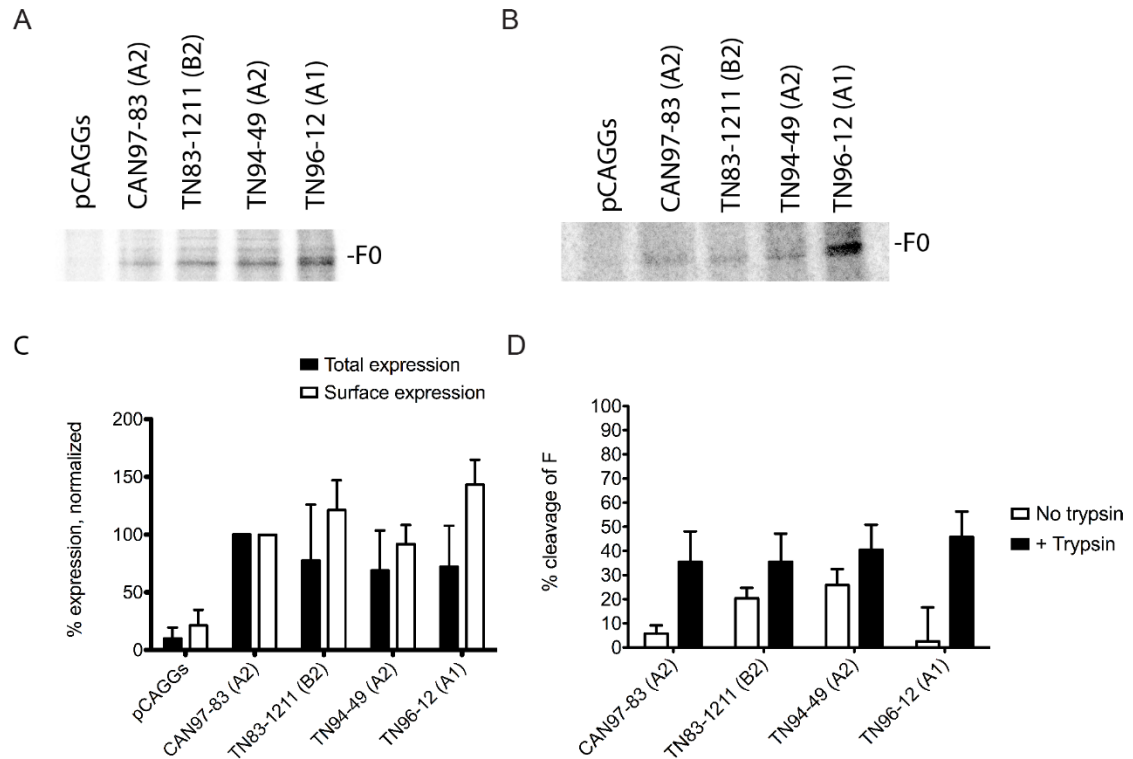


Figure 7. HMPV F protein expression and cleavage by exogenous trypsin.

Representative gel of (A) total and (B) surface protein expression in metabolically labeled Vero cells expressing CAN97-83 (A2) F, TN94-49 (A2) F, TN96-12 (A1) F, and TN83-1211 (B2) F. (C) Quantification of the total and surface expression of the F₀ form in metabolically labeled Vero cells expressing CAN97-83 (A2) F, TN94-49 (A2) F, TN96-12 (A1) F, and TN83-1211 (B2) F. Data are presented as percentages of CAN97-83 (A2) F expression, which was set to 100% (n = 3). (D) Trypsin cleavage efficiency of surface expression of CAN97-83 (A2) F, TN94-49 (A2) F, TN96-12 (A1) F, and TN83-1211 (B2) F in the presence or absence of 0.3 μg/ml of TPCK-trypsin was quantified by the following equation: percent cleavage = F₁/(F₁ + F₀) (n = 3). Error bars show standard deviation.

A

	290	300
	
CAN97-83 (A2)	TPCWIVKAAPSCSGKKGNYA	
TN94-49 (A2)	TPCWIVKAAPSCSKKKGNYA	
TN96-12 (A1)	TPCWIVKAAPSCSEKKGNYA	
TN83-1211 (B2)	TPCWIVKAAPSCSGKKGNYA	
	*****	*****

B

	430	440
	
CAN97-83 (A2)	DNTVYQLSKVEGEQHVIKGR	
TN94-49 (A2)	DNTVYQLSKVEGEQHVIKGR	
TN96-12 (A1)	DNTVYQLSKVEGEQHVIKGR	
TN83-1211 (B2)	DNTVYQLSKVEGEHHVIKGR	
	*****	*****

Figure 8. Partial protein sequence analysis of F from 4 strains of HMPV surrounding key residues at positions (A) 294 and (B) 435.

Sequence alignment was generated using ClustalW. The asterisk "*" indicates identical residues and "." indicates conserved substitutions.

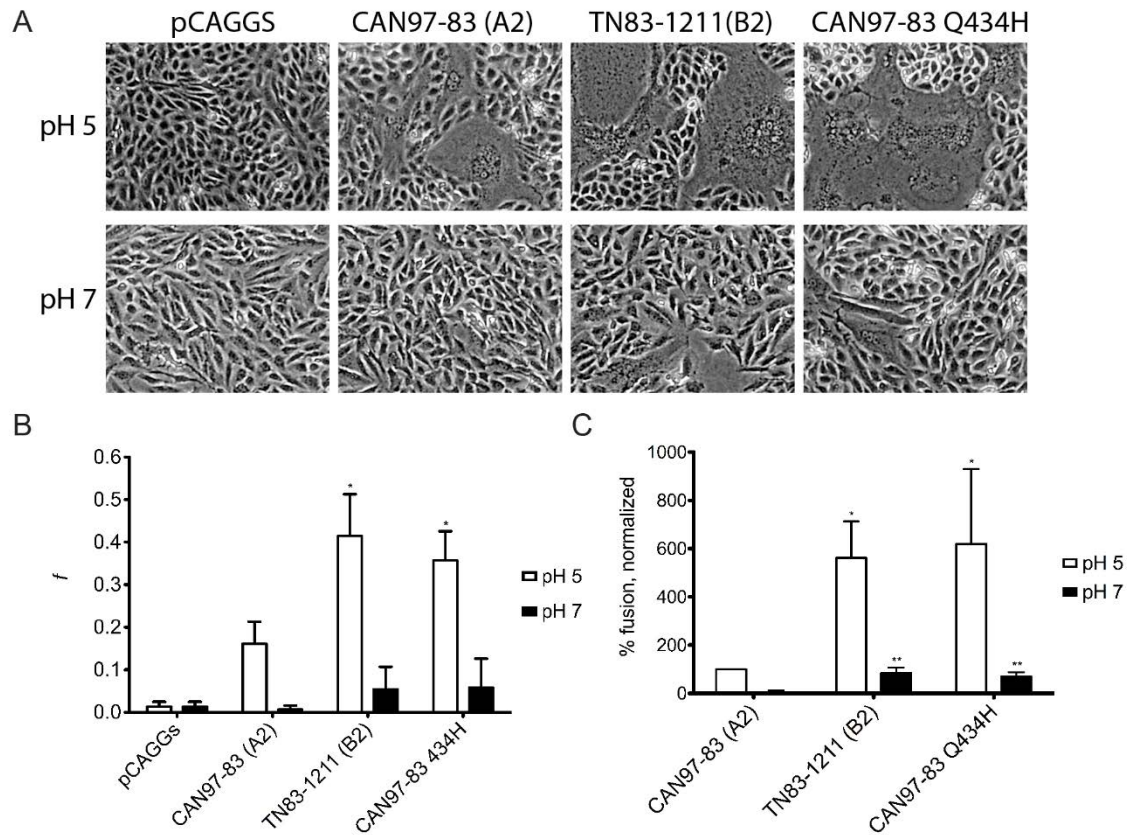


Figure 9. Q434H mutation results in hyperfusogenic activity in CAN97-83 F promoted by low pH.

(A) Representative images of syncytium formation of cells expressing the HMPV F proteins after pulses at pH 5 or pH 7 (n = 3) (B) The fusion index was calculated using the equation $f = [1 - (C / N)]$ where c is the number of cells in a field after fusion and n the number of nuclei. Six fields were scored per condition representative of 3 independent experiments. * Indicates statistically significant compared to f for CAN97-83 (A2) F after pH 5 pulses (n = 3) (C) Luciferase reporter gene assay of Vero cells transfected with HMPV F that were used to overlay BSR cells and subjected to two pH pulses. Data are presented as percentages of CAN97-83 (A2) F luminosity (fusion) at pH 5 (n = 3) +/- standard deviation. * Indicates statistically significant compared to f for CAN97-83 (A2) F after pH 5 pulses, ** indicates statistically significant compared to f for CAN97-83 (A2) F after pH 7 pulses.

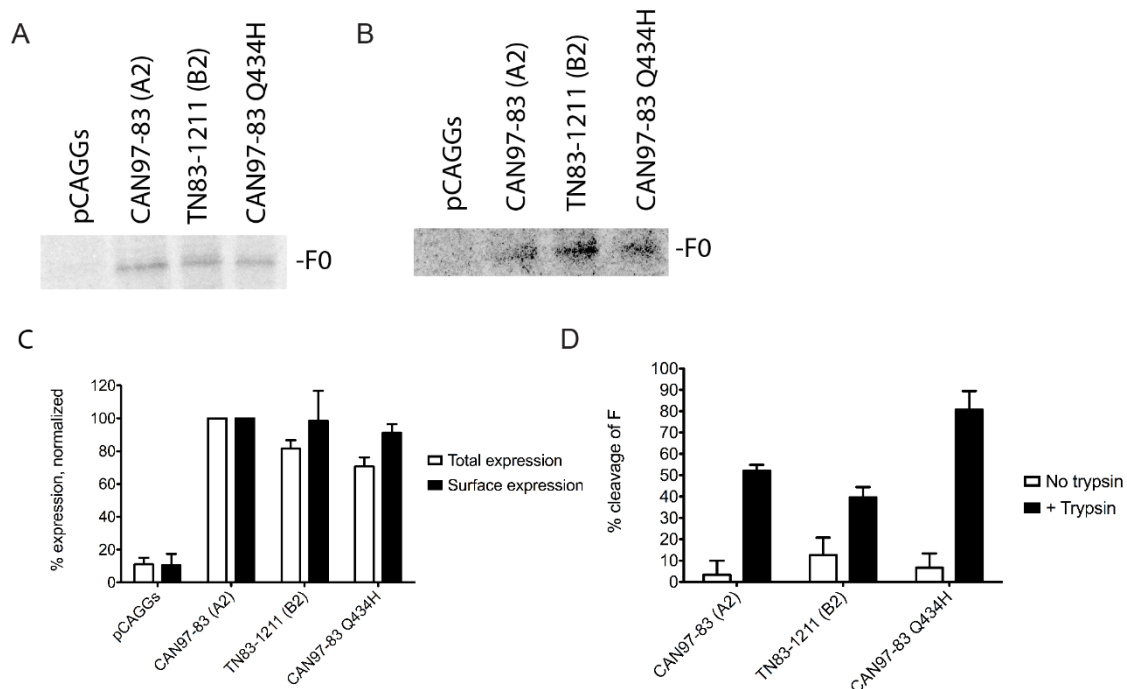


Figure 10. Mutant F protein expression and cleavage by exogenous trypsin.

Representative gel of (A) total and (B) surface protein expression in metabolically labeled Vero cells expressing CAN97-83 (A2) F, TN83-1211 (B2) F and mutant CAN97-83 Q434H F. (C) Quantification of the total and surface expression of the F₀ form in metabolically labeled Vero cells expressing CAN97-83 (A2) F, TN83-1211 (B2) F and mutant CAN97-83 Q434H F. C. Data are presented as percentages of CAN97-83 (A2) F expression, which was set to 100% (n = 3). (D) Trypsin cleavage efficiency of surface expression of CAN97-83 (A2) F, TN83-1211 (B2) F and mutant CAN97-83 Q434H F in the presence or absence of 0.3 μg/ml of TPCK-trypsin was calculated with the following equation: percent cleavage = F₁/(F₁ + F₀) (n= 3). Error bars show standard deviation.

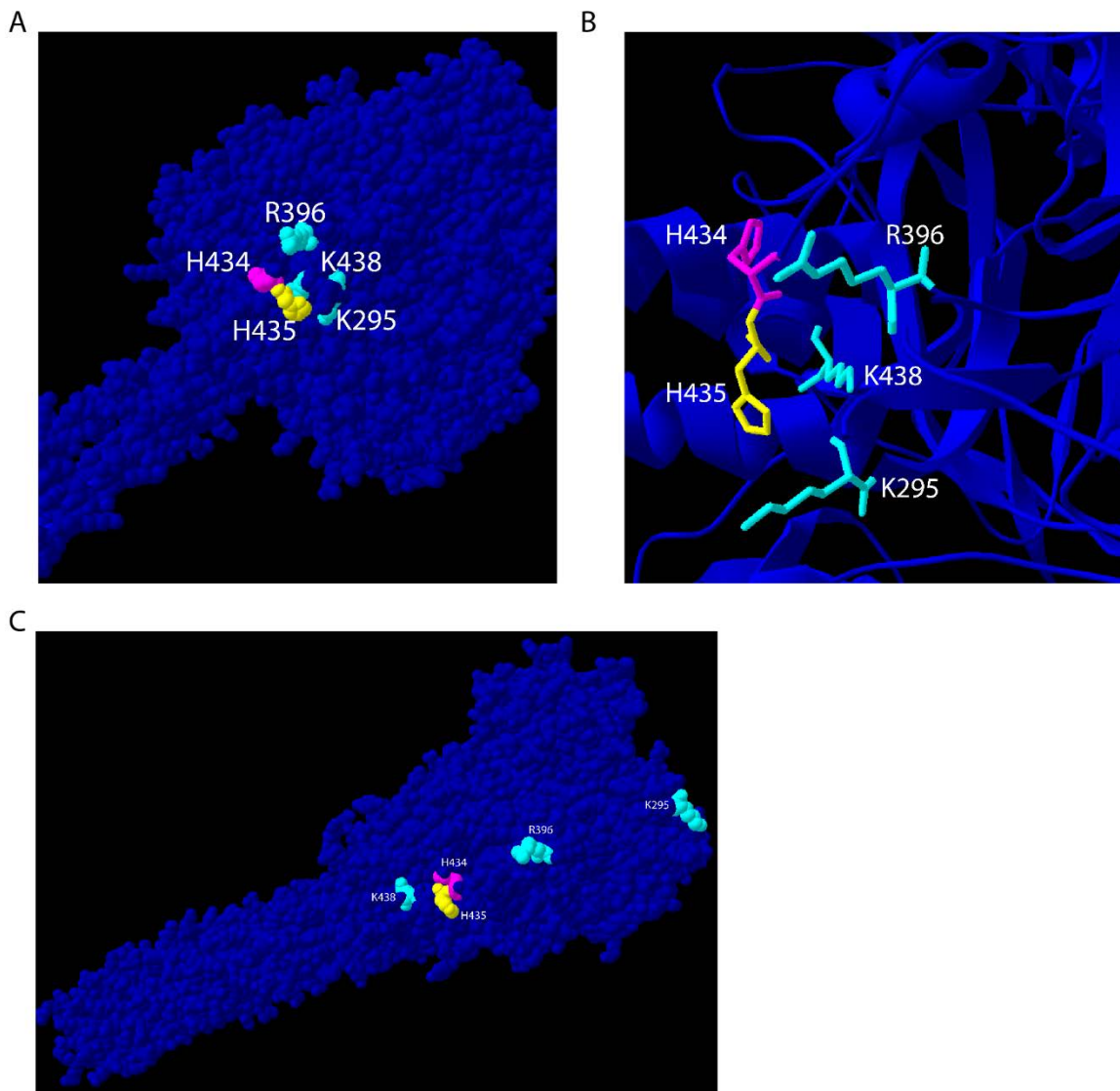


Figure 11. HMPV F structure homology models highlighting key residues surrounding H435.

(A) The amino acid sequence of HMPV F was threaded onto the crystal structure of PIV5 F in its metastable prefusion form (222). In a model of the HMPV F prefusion conformation (B) residues H434 and H435 are exposed on the surface of the globular region of the protein and are surrounded by basic residues K295, R396, and K438 in close proximity. (C) The postfusion homology model of HMPV F was created by threading the amino acid sequence of HMPV into the crystal structure of Newcastle Disease Virus F in its postfusion conformation (317). In the postfusion homology model of HMVP F, the basic residues are no longer located as close proximity to H434 and H435.

Chapter 4: Inhibition of HMPV infection by blocking binding to heparan sulfate

**E. coli* K5 polysaccharide derivatives were supplied by David Lembo (Department of Clinical and Biological Sciences, University of Turin, S. Luigi Gonzaga Hospital, 10043, Orbassano, Turin, Italy) and Pasqua Oreste (Glycores 2000 S.r.l. 20155 Milan, Italy). The human airway epithelium (HAE) tissue experiments using PIV5 and a single experiment using HMPV with iota-carrageenan treatment were completed by Stacy E. Smith.

Introduction

Acute viral respiratory tract infection is the most frequently observed illness in humans worldwide (327). Human metapneumovirus (HMPV), an enveloped, negative-sense, single-stranded RNA virus in the Paramyxoviridae family, is a common cause of both upper and lower respiratory tract infections (30, 31, 321). First identified in 2001 in the Netherlands, HMPV is now known to be the cause of respiratory infections in humans since at least 1958 (31). Nearly every person is exposed to HMPV in the first decade of life; sero-conversion occurs on average by the age of five, and nearly 100% of individuals test seropositive for antibody reactivity to HMPV antigens by the age of ten (7). In children, HMPV infection is the second most common cause of hospitalization due to respiratory infection after the closely related respiratory syncytial virus (RSV) (37, 38). While infants are considered the most vulnerable population to illness from HMPV, adults can foster severe respiratory disease as well, especially the elderly, immunocompromised patients, and individuals with chronic underlying diseases (43-45). In addition to upper respiratory involvement with symptoms typically associated with the common cold, HMPV infection can result in serious lower respiratory syndromes such as pneumonia, bronchitis, and bronchiolitis (321, 322). Due to the recent ability to routinely detect this virus through the inclusion of HMPV in multiplex detection assays, HMPV has been associated with disease outside of the respiratory tract in some cases, including viral encephalopathy (62, 64, 328) and acute myocarditis (69), from initial respiratory involvement. Despite this tremendous clinical burden, there is no known vaccine to prevent HMPV infection, and treatment options are limited to administering ribavirin, which does not have established efficacy against HMPV infection (329).

Key features of HMPV entry into target cells to establish infection have been characterized recently. HMPV utilizes heparan sulfate (HS) present on the cell surface to bind to

target cells (79), followed by clathrin-mediated endocytosis and membrane fusion in endosomes (282). HS is a negatively charged polysaccharide belonging to the family of glycosaminoglycans composed of repeating disaccharide units formed by glucosamine and glucuronic acid, which can undergo a series of modifications during the biosynthesis, leading to very heterogeneous chains. In HS the glucosamine can be N-acetylated, or N-sulfated and O-sulfated in various positions and to varying degrees. Glucuronic acid can also be modified by epimerization. Additionally, integrin $\alpha V\beta 1$ has also been shown to play a role for efficient HMPV entry (79, 119) and has been proposed to be involved in attachment (120).

HSPGs have been implicated in virus-cell interactions for other enveloped viruses, including RSV (163, 330, 331), human papilloma virus (HPV) (162), herpes simplex virus (HSV) (173, 174, 177, 332), human immunodeficiency virus (HIV) (159, 161, 169), and others (reviewed in (333)). We have previously shown that nearly complete reduction in binding and infection results when HS is removed from the cell surface using heparinases, while cells that are able to synthesize only HS, and not any other GAGs, are fully able to bind HMPV (79). Unlike other paramyxoviruses that require two distinct viral glycoproteins to mediate attachment and binding, the fusion protein (F) of HMPV is sufficient for binding and infection (76, 77, 136). Recombinant HMPV that does not have the attachment protein (G) or small hydrophobic protein (SH) is able to bind cells at wild-type levels via HS (79). Thus, the putative interaction between the HMPV F and HS provides an opportunity for antiviral development.

In this study, we describe the potent anti-HMPV effects of the sulfated polysaccharide, iota-carrageenan, in models of respiratory epithelial cells and polarized airway tissues, indicating that the HS-F interaction is important in physiologically relevant models. To further characterize structural features of HS important for binding by HMPV F, we utilized a mini-library of variably sulfated derivatives of *Escherichia coli* K5 polysaccharide, which revealed that the critical common feature required for effective inhibition of binding and infection, is the O-sulfation. In addition, we showed that occluding heparan sulfate with peptide dendrimer SB105-A10 inhibits the binding interaction between HMPV F and target cells and airway tissues. These results provide critical support for a role for HS-HMPV F protein interactions in physiologically relevant models, and identify key features of the interaction between HMPV and HS that have implications for infection *in vivo* and may serve for antiviral development.

Results

Iota-carrageenan inhibits HMPV infection in human respiratory cells

We have previously shown that specific removal of cell surface HS (Fig. 12A) inhibits HMPV binding and infection in a number of cell types (79). In addition, CHO cell lines with altered GAG metabolism were used to further demonstrate that HMPV specifically requires HS for infectivity (79). To dissect how interaction with HS regulates HMPV infection in physiologically relevant models and to determine if blocking this interaction could be a potential antiviral approach, we utilized a sulfated polysaccharide, heparan sulfate mimetics and a compound that occludes HS in combination with infection studies in human bronchial epithelial cells (BEAS-2B) or human airway epithelial (HAE) models.

Sulfated polysaccharides have been previously employed to target viral infection, including a number of studies with carrageenans, which are isolated from red seaweed (334). Carrageenans are composed of sulfated repeating galactose units (Fig. 12B). The three types of known carrageenans (iota, lambda, and kappa) differ in number and positions of sulfate groups (reviewed in (334)). Carrageenans have shown antiviral activity against a number of viral pathogens, including human papilloma virus (HPV) (335), HIV (336), dengue virus (337) and influenza A virus (338). Importantly, iota-carrageenan (Fig. 12B) has been used safely in human trials in the form of a nasal spray to reduce viral infection (339-341).

To verify that sulfated polysaccharides would inhibit HMPV infection in a relevant cell culture model, we first determined the anti-HMPV activity of iota-carrageenan, a well characterized sulfated polysaccharide that has been shown to inhibit infection of other viruses that bind heparan sulfate. Infection of BEAS-2B cells was performed using a recombinant HMPV (strain CAN97-83, clade A2) that results in green fluorescent protein (GFP) expression upon viral infection, which was quantified by flow cytometry. Pretreatment of HMPV with iota-carrageenan resulted in inhibition of infection, with nearly a complete reduction in infection achieved with 10 $\mu\text{g}/\text{mL}$ of iota-carrageenan (Fig. 13A and 13C). To determine if iota-carrageenan had a nonspecific antiviral effect, the paramyxovirus parainfluenza virus 5 (PIV5), which does not utilize heparan sulfate for binding, was used. Incubating rgPIV5, a recombinant PIV5 virus that results in GFP expression, with iota-carrageenan prior to infection did not inhibit infection of BEAS-2B cells at any of the concentrations used compared to the untreated control (Fig. 13B and 13C). Furthermore, treatment of BEAS-2B cells with the highest concentration of iota-carrageenan

tested in the infection assays did not reduce cell viability, as measured by 3-(4, 5-Dimethylthiazol-2-yl)-2, 5-diphenyl-2H-tetrazolium bromide (MTT) cell viability assay (Fig. 14A). Similar effects of iota-carrageenan on rgHMPV and rgPIV5 infection were observed in Vero cells (data not shown). These results indicate that HS-HMPV interactions are critical in BEAS-2B cells, and that iota-carrageenan has anti-HMPV activity, most likely attributed to its sulfated structure.

Our previous studies suggested that HMPV binds to heparan sulfate via the F protein, and we hypothesized that iota-carrageenan is inhibiting HMPV infection by competing with HS binding sites located in HMPV F. To test this, HMPV was added to BEAS-2B cells at 4°C, allowing for binding to occur but not infection, and the amount of bound virus was quantified by detection of the HMPV matrix protein present in cell lysates with β -actin as a loading control, by Western blot. Pretreating HMPV at an MOI of 1 with 40 μ g/mL carrageenan for 30 minutes at 4°C prior to addition to the cells resulted in about 85% inhibition of particle binding, compared to the untreated control (Fig. 13D and 13E), demonstrating that iota-carrageenan competes with the binding of HMPV to HS. Of the three glycoproteins in the viral envelope of HMPV, the attachment protein G, small hydrophobic protein SH, and F, only F is required by HMPV to be infectious; recombinant HMPV without G or SH, HMPV Δ G and Δ G Δ SH respectively, are able to bind cells at wild-type levels (79) and are replication competent in a nonhuman primate model of infection (77). To test whether iota-carrageenan inhibition of HMPV binding and infection is dependent exclusively on F, we pretreated the recombinant HMPV Δ G and Δ G Δ SH with iota-carrageenan and determined the effects on overall infection and binding in BEAS-2B cells. Iota-carrageenan inhibited HMPV Δ G and Δ G Δ SH binding to a similar degree as wild-type HMPV (Fig. 13D and 13E), which supports the hypothesis that interaction between HMPV and heparan sulfate is mediated by F. Interestingly, Δ G and Δ G Δ SH HMPV binding to BEAS-2B cells was more efficient than WT HMPV, as a greater fraction of input particles of Δ G and Δ G Δ SH HMPV bound to BEAS-2B cells than WT HMPV. The input for all three virus samples was determined for each experiment, and was not statistically different across all binding assays completed (data not shown). The potential role of G and SH in regulating HMPV binding is further addressed in Chapter 5. However, despite increased binding at baseline, iota-carrageenan did inhibit binding of Δ G and Δ G Δ SH HMPV to the same degree as WT HMPV, leading to the conclusion that F mediates the interaction with HS (Fig. 13E).

The results in a monolayer respiratory cell model support the hypothesis that HMPV F mediates a key binding interaction to heparan sulfate, and this event can be inhibited using the highly sulfated polysaccharide, iota-carrageenan. However, a monolayer cell culture model is

limited in the ability to recapitulate the complex features of the respiratory epithelium, which include moving cilia, mucus, distinct cell types with important physiological roles, and polarity maintained by tight junctions. Furthermore, immortalized cells highly express HSPGs in a pattern that may be different than complex organized tissues found *in vivo*, and immunohistochemistry studies have not detected significant amounts of HS on the apical surface of human airway, raising concerns that HS interactions may be less important in an airway model (143). We therefore examined the effect of sulfated polysaccharides in a polarized human airway tissue model (HAE; MatTek) that more closely recapitulates the complexity of the human airway, which is the primary site of HMPV infection. HAE tissues have been previously used as models of respiratory virus infection, including human parainfluenza virus 3 (325), rhinovirus (342), human bocavirus 1 (343), and RSV (307).

To test whether iota-carrageenan inhibits HMPV infection in the HAE model, iota-carrageenan treated rgHMPV was used to inoculate the apical surface of the HAE tissues, and a significant reduction in infection of approximately 75% was observed (Fig. 13F and 13G). Unlike rgHMPV, treatment of rgPIV5 with iota-carrageenan had no effect on infection in the airway tissues (Fig. 13F and 13G). These findings indicate that HMPV interactions with heparan sulfate are also important in complex polarized airway tissues that histologically resemble the human respiratory tract, and support the hypothesis that HMPV requires heparan sulfate to establish infection at the apical surface of the respiratory epithelium.

O-sulfated K5 polysaccharide derivatives inhibit HMPV infection

While our preliminary results strongly support a key role for HS in HMPV infection, the specific features of HS required remain to be determined. A class of molecules mimicking HS and thus possible inhibitors of heparan sulfate-virus interactions is represented by the sulfated derivatives of the *Escherichia coli* capsular K5 polysaccharide (Fig. 12D). K5 polysaccharide derivatives are heparan-like molecules devoid of anticoagulant activity obtained by the sulfation of the *E. coli* capsular K5 polysaccharide that has the same structure of the biosynthetic precursor of HS, N-acetyl heparosan. A small library of derivatives with different degrees of sulfation has been synthesized using chemical and enzymatic modifications (318). Sulfated K5 derivatives have been shown to inhibit infection in other viruses in a specific manner, including HPV (335), RSV (344), Dengue (345), CMV (346), HSV-1 and HSV-2 (347), and HIV (348). Analysis of the anti-HMPV activity of these compounds can therefore be used to identify structural features that are

important for recognition by HMPV F and potentially help to identify a potent heparan sulfate mimic.

Because heparan sulfate is negatively charged due to sulfate modifications on the disaccharide units, we hypothesized that charge-charge interactions are contributing to the binding between F and this polysaccharide. Therefore, we predicted that the most highly sulfated K5 derivatives, mainly K5-N,OS(H), and K5-OS(H), would have the greatest inhibitory effect on HMPV infection. To test this, rgHMPV at an MOI of 1 pretreated with the derivatives at 1 μ M was used to inoculate BEAS-2B cells. As predicted, the highly sulfated K5 derivatives, K5-N,OS(H), and K5-OS(H), dramatically inhibited infection (Fig. 15A). Among the lower sulfated derivatives, K5 and K5-NS did not have an observable effect on HMPV infection when examined by microscopy (Fig. 15A), while K5-N,OS(L) and K5-OS(L), also inhibited HMPV infection dramatically (Fig. 15A). K5-NS, which has a single N-linked sulfate group in position 2 of glucosamine, had no effect on HMPV infection (Fig. 15A), indicating a key role of O-sulfate groups in the observed inhibition. When HMPV was treated with variable concentrations (10nm to 1 μ M) of the K5 derivatives and used to infect BEAS-2B cells, flow cytometry analysis of infected cells revealed a dose dependent inhibition of HMPV infection by all the O-sulfated K5 derivatives (Fig. 15B). K5-NS had no effect on HMPV infection, while some inhibition resulted from K5, although only at the highest concentration (Fig. 15B). The reduction of infection by the K5 polysaccharide was not expected, and the mechanism of this action remains unclear as it did not affect HMPV binding (Fig. 15D and 15E). None of the K5 polysaccharide derivatives had an effect on PIV5 infection (Fig. 15C). Additionally, treatment of BEAS-2B cells with the 10 μ M of K5 polysaccharide derivatives, the concentration used in HAE infection experiments and 10-fold higher than the highest concentration used in cell infection assays, did not reduce cell viability, as measured by MTT cell viability assay (Fig. 14A). To determine whether the K5 compounds inhibit HMPV infection by competition, the same binding assay as described in the carrageenan studies was used. rgHMPV was treated with 1 μ M of each of the K5 polysaccharide derivatives prior to incubation with BEAS-2B cells at 4°C at an MOI of 1 to allow for binding to take place. While unmodified K5 and K5-NS, which has a single N-linked sulfation modification, had no effect on viral binding, the higher sulfated compounds, K5-N,OS(L) and K5-OS(L), and the highly sulfated compounds K5-N,OS(H), and K5-OS(H), reduced HMPV binding to BEAS-2B cells significantly (Fig. 15D and 15E).

To confirm these findings in a physiologically relevant tissue model, we determined the effect of K5-N,OS(H) and K5-OS(H), which had the greatest inhibition of HMPV infection in

monolayer cells, in polarized airway tissues. HAE tissues were infected at the apical surface with rgHMPV at an MOI of 5 pretreated with 10 μ M K5-N,OS(H) or K5-OS(H), or Opti-MEM. Forty-eight hours post-infection, we observed a dramatic reduction in infected cells at the apical surface (Fig. 16A). Quantification of GFP-expressing cells revealed approximately a 70% reduction in HMPV infection compared to the control (Fig. 16B). Taken together, these data suggest that highly sulfated K5 derivatives effectively inhibit binding and infection of HMPV, and that O-sulfation is an important structural feature required for the interaction to occur, and strongly support the hypothesis that HMPV interaction with HS plays a significant role during apical infection.

Heparan sulfate occlusion inhibits HMPV infection and binding

We have shown that HMPV F mediates a binding interaction to HS that can be inhibited both in cell culture and tissue models using iota-carrageenan and a small library of K5 polysaccharide derivatives. As an alternative mechanism to characterize the interaction between HMPV and HS, we examined the effect of blocking HS moieties on the target cell, thus making heparan sulfate unavailable for binding. There is two-fold logic to investigating the effect of a heparan sulfate-occluding compound on HMPV binding. Removal of HS caused a robust block in HMPV infection (79); however, HSPGs have critical constitutive and induced interactions with other cellular proteins (reviewed in (349)), and removing HS may interrupt these interactions, causing cellular changes. HS occluding compounds that prevent further ligand binding are less likely to disrupt preexisting HS interactions, and therefore, serve as an alternative approach to address the direct interaction of HMPV with HS. Furthermore, a compound that occludes HS and inhibits HMPV infection may serve as potential building block for antiviral development for HMPV and other viruses that are known to bind HS.

To accomplish this, we utilized a previously characterized heparan sulfate occluding compound, peptide dendrimer SB105-A10 (139, 307, 350). Peptide dendrimers, branched synthetic molecules which consist of a peptidyl branching core and covalently attached surface peptide units, have a number of potential applications, especially in relation to the development of antiviral agents. The peptide dendrimer SB105-A10 (Fig. 12C), which has a branched peptide core with clusters of basic residues that bind to negatively charged sulfate and carboxyl groups, has been shown to specifically occlude ligand binding from HSPGs (139, 350). Furthermore, SB105-A10 has previously been reported to exhibit antiviral activity against RSV (307), CMV (350), HIV (139), HPV (351), HSV-1 and HSV-2 (352), as well as some filoviruses (170).

To determine if SB105-A10 reduces HMPV infection in human lung epithelial cells, BEAS-2B cells were treated with SB105-A10 at 1 μ M prior to infection with rgHMPV at an MOI of 1 and cells were imaged 24 hours later for GFP expression; rgPIV5 was used in control studies to determine specificity. SB105-A10 treatment resulted in dramatic inhibition of HMPV infection, whereas PIV5 infection was not reduced (Fig. 17A). We performed quantification of the effects of SB105-A10 on rgHMPV or rgPIV5 infection by flow cytometry for GFP expression 24 hr post-infection. In these experiments both BEAS-2B and A549 cells were used to determine if the effect of SB105-A10 is cell type-dependent, as this compound is mediating its effects by interacting with the target cell. In BEAS-2B cells, a dose-dependent inhibition of approximately 70% of rgHMPV infection resulted with SB105-A10 treatment, whereas rgPIV5 infection was not affected (Fig. 17B). Similar results were seen in A549 cells (Fig. 17C). Additionally, treatment of BEAS-2B cells with the 2 μ M of SB105-A10, the concentration used in HAE infection experiments and 2-fold higher than the highest concentration used in cell infection assays, did not reduce cell viability, as measured by MTT cell viability assay (Fig. 14B). Based on our hypothesis of HMPV attachment, we predicted that SB105-A10 inhibits infection by blocking particle binding, specifically by preventing the interaction between heparan sulfate and F. To address this, we utilized a binding assay with WT HMPV, Δ G HMPV, and Δ G Δ SH HMPV to determine the effects of SB105-A10. BEAS-2B cells were treated with 1 μ M SB105-A10 or Opti-MEM prior to addition of HMPV at an MOI of 1. The cells were incubated at 4°C for 2 hr to allow for binding and then cell lysates were analyzed for M by Western blot to determine binding. A significant reduction of viral binding was observed in WT HMPV and the recombinant Δ G HMPV and Δ G Δ SH HMPV with SB105-A10 treatment (Fig. 17D and 17E). As was observed in binding assays with iota-carrageenan (Fig. 13D), greater baseline binding was observed for Δ G HMPV and Δ G Δ SH HMPV compared to WT (Fig. 17D), although the same levels of reduction in binding were observed with SB105-A10 (Fig. 17E). To determine the effect of SB105-A10 in polarized tissues, the apical surface of HAE tissues was treated with SB105-A10 at 2 μ M prior to infection with rgHMPV at an MOI of 5. Treatment with SB105-A10 resulted in a reduction of infected cells 48 hours post-infection (Fig. 18A). Quantification of infected cells revealed greater than 50% reduction in HMPV infection at the apical surface with SB105-A10 treatment, compared to vehicle treated control tissues (Fig. 18B). Altogether, these results indicate that occlusion of HS moieties on target cells inhibits HMPV binding and infection mediated by HMPV F and further support that HS is available for viral binding at the apical surface

of the airway. Furthermore, based on our results, occlusion of HS could potentially be used as an antiviral strategy against HMPV.

Discussion

Heparan sulfate is a key attachment factor for HMPV binding to the cell surface. In this study we used compounds that modulate the attachment event to characterize the interaction between HMPV and HS. Our results support a model (Fig. 19) where HMPV F mediates a direct binding interaction to HS, which can be inhibited by sulfated polysaccharides, specifically sulfated in *O*-position (Fig. 15), and HS occluding compounds (Fig. 17). Our results further indicate that HS in the airway epithelium serves as a binding factor during infection at the apical surface, and suggest that HS modulating compounds may serve as a platform for potential HMPV antiviral development.

Iota-carrageenan treatment of HMPV resulted in inhibition of attachment (Fig. 13D) and infection (Fig. 13A and 13C) in bronchial epithelial cells and polarized airway tissues (Fig. 13F). The anti-HMPV activity of a sulfated polysaccharide has been previously reported using native and depolymerized galactans isolated from the red seaweed *Cryptonemia seminervis* (353). While iota-carrageenan is a highly heterogeneous polysaccharide with regard to size, it is unclear if its molecular weight is important in the inhibition of the viral interaction with heparan sulfate. It has been shown that depolymerized galactans ranging in molecular weights from 52-64 kDa were able to inhibit HMPV infection as well as the intact polysaccharide, suggesting low molecular weight sulfated polysaccharides can have potent antiviral activity (353). The potent anti-HMPV effect of iota-carrageenan on HMPV infection in both cells and tissue models has potential as a respiratory therapy, especially as iota-carrageenan has been shown to be safe to use in humans (338, 341, 354). Iota-carrageenan application in the form of a nasal spray in a randomized clinical trial showed reduction in viral titers and fewer days of symptomatic illness (341). Its efficacy to specifically reduce HMPV infection in humans remains to be determined.

To better understand the structural features of heparan sulfate required for recognition by HMPV, we used a mini-library of variably sulfated heparan-like K5 polysaccharide derivatives. Interestingly, our results highlight that variations in the structure of the K5 derivatives, namely the position and degree of sulfation, can modulate the selectivity and potency of their activities against HMPV (Fig. 15B). The highly sulfated K5 polysaccharides exhibited the greatest inhibition of HMPV infection, suggesting negative charges play a role in interacting with F (Fig. 15B). The

highly sulfated K5-OS(H) and K5-N,OS(H) have been shown to inhibit Dengue virus attachment to microvascular endothelial cells by interacting with the viral envelope protein, as shown by surface plasmon resonance (SPR) analysis using the receptor-binding domain III of the E protein (345). Our results support the model that HMPV binding to HS mediated by F involves charge-charge interaction, possibly by a cluster of exposed positively charged residues on F. This is demonstrated by the very high inhibitory activity exerted by K5-OS (H) (Fig. 15B, 15D and 15E). This finding suggests the interaction between HMPV F and HS depends on a specific sulfation pattern, rather than overall negative charges alone. Since the N-sulfated K5 derivatives are less effective in inhibiting the binding of HMPV, we can conclude that O-sulfate groups are important for HMPV F-HS interactions. Interestingly, the most effective fractions of depolymerized galactans to inhibit HMPV infection have the sulfate modifications principally on C-2 and C-6 of the galactose sugars (353). These results further support the importance of O-sulfate groups inhibiting the HS interaction with HMPV F and also suggest that the sugar backbone of the polysaccharide is not the main determinant of the antiviral activity.

Interestingly, binding experiments in this study demonstrated a greater affinity of ΔG and $\Delta G\Delta SH$ HMPV to bind BEAS-2B cells than WT HMPV (Fig. 13D and 17C), as the untreated control bands consistently showed higher levels of particle binding for the recombinant viruses compared to the WT, despite equivalent number of particles added to the cells. We have previously reported that the ΔG and $\Delta G\Delta SH$ recombinant viruses bind and infect at WT levels in other cell types, suggesting that there may be cell-type specific differences in binding. Taken together, these results suggest that SH and G negatively modulate binding in BEAS-2B cells, and thus their absence results in more efficient particle binding. Both HMPV SH and G have been previously reported to modulate events in HMPV entry. Our group has shown SH can modulate fusion activity of F (92). Furthermore, HMPV G and SH have been previously shown to negatively modulate HMPV entry, as particle uptake by micropinocytosis in dendritic cells is enhanced for recombinant HMPV lacking G and SH (93). However, the mechanisms by which G and SH modulate these critical early steps remain to be elucidated.

Treating the cells and tissues with SB105-A10, which specifically occludes any ligand binding to HSPGs, resulted in a significant inhibition of HMPV binding and infection. Our results further support the model that HMPV uses HS as an attachment factor due to a direct binding interaction with F. While adhered immortalized cells readily express accessible heparan sulfate, it is less clear where heparan sulfate localizes in the respiratory epithelium *in vivo*. Based on

detection by immunohistochemistry of human epithelial tissue, heparan sulfate has been previously hypothesized to localize exclusively to the basolateral epithelium (143), making it unclear how a respiratory virus would access heparan sulfate to infect apically. The results in this study demonstrate that HMPV can infect polarized airway tissues at the apical surface and that HS-occlusion inhibits this apical infection, suggesting HS is found at sufficient levels to promote attachment at the apical surface of the airway. HS occlusion with SB105-A10 has also been shown to inhibit RSV infection at the apical surface of HAE tissues (307). HS modification is found on a number of transmembrane proteins, and the two main protein families with HS are syndecans and glypicans. Syndecans have been shown to serve as receptors for other HS-binding viruses, including hepatitis C (172), dengue virus (168) and HIV (161). Anti-syndecan-1 antibodies have recently been shown to block RSV infection at the apical surface of human airway epithelium cultures (355). The role of a specific HSPG, such as one of the syndecan proteins, in HMPV infection remains to be determined, but our results strongly indicate that sufficient levels of HS on HSPGs are exposed at the apical surface of the airway epithelium for viral infection, including HMPV.

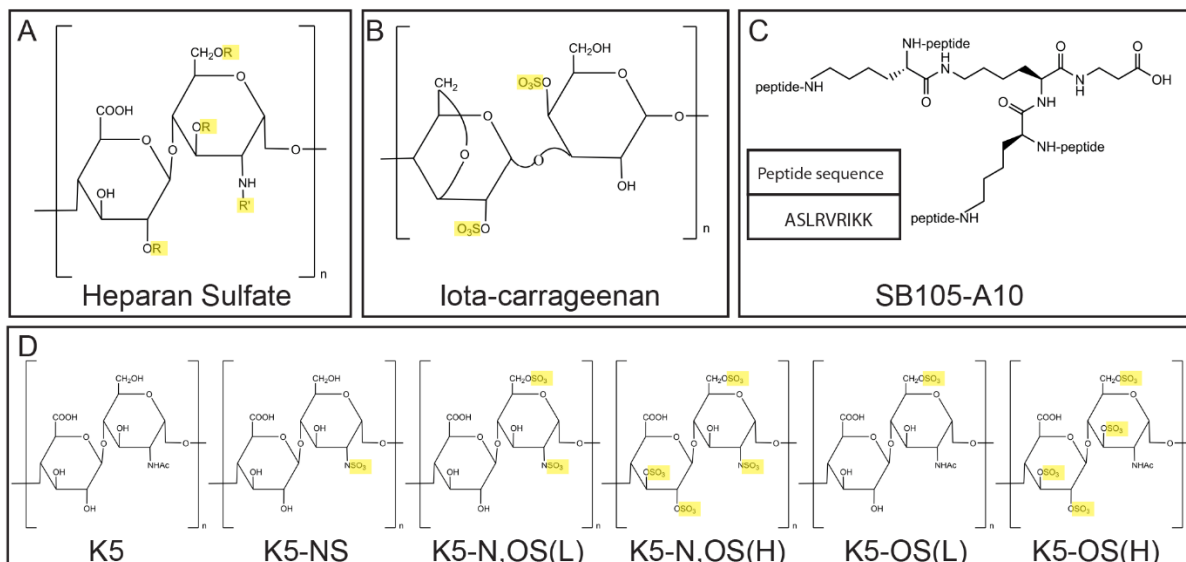


Figure 12. Representative structures of heparan sulfate and related compounds.

(A) Heparan sulfate disaccharides modified by the following possible substitutions: Ac – acetyl, R= H or SO₃⁻; R' = H, Ac, or SO₃⁻. Structures adapted from (349). (B) Iota-carrageenan adapted from (334) (C) SB105-A10 (D) K5 polysaccharide derivatives.

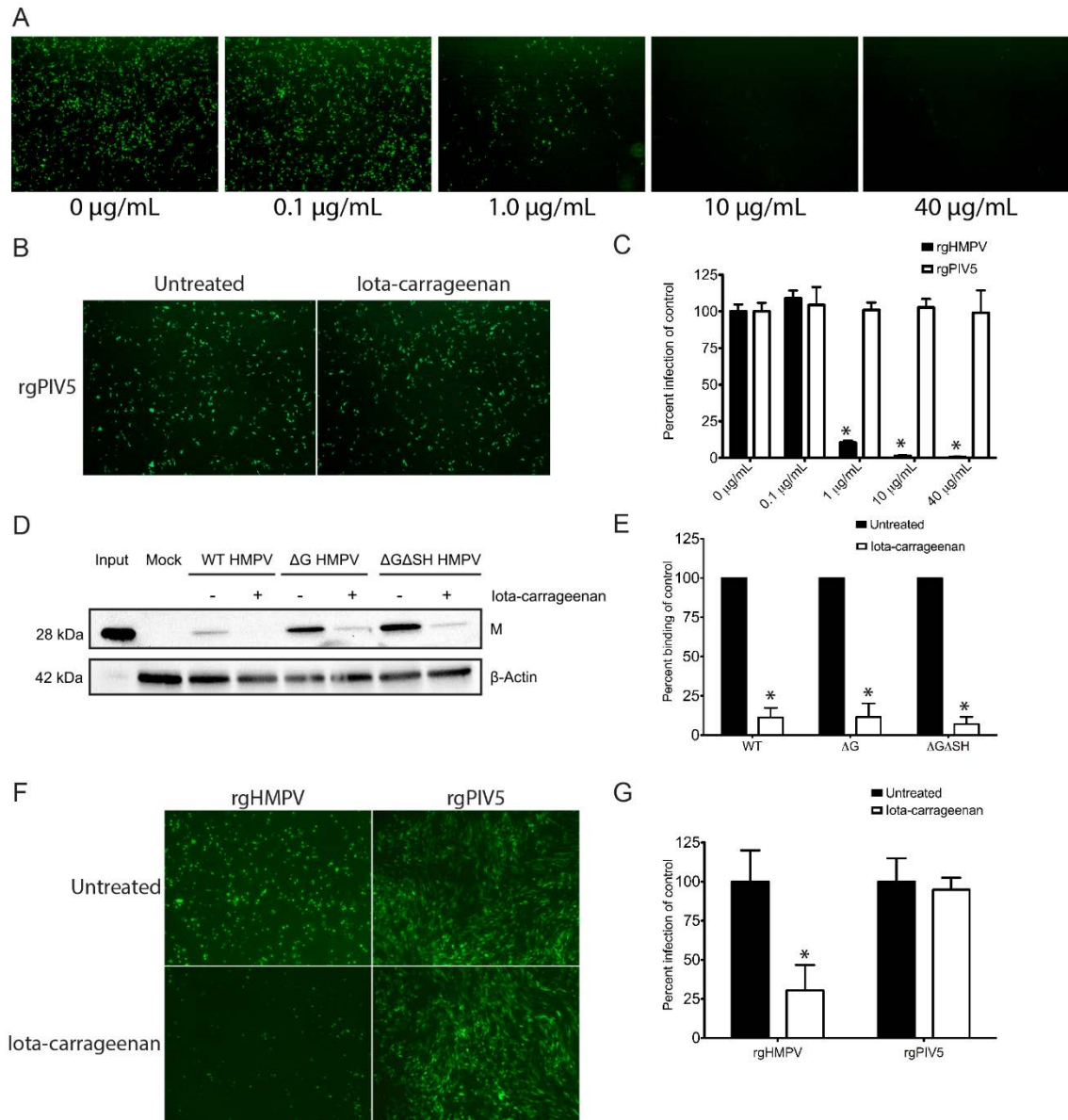


Figure 13. Iota-carrageenan inhibits HMPV infection in cells and tissues by blocking binding.

(A) BEAS-2B cells infected with rgHMPV at an MOI of 1 was treated with variable concentrations of iota-carrageenan. Cells were imaged 24 HPI. (B) BEAS-2B cells were infected with rgPIV5 at an MOI of 1 treated with 40 µg/mL of iota-carrageenan or vehicle. Cells were imaged 24 hours post infection (HPI). (C) Quantification of rgHMPV and rgPIV5 infection in BEAS-2B cells using flow cytometry to detect GFP expressing cells 24 HPI. Data presented as a percent infection of the untreated control (0 µg/mL) for each virus. Data points are means (+/- SD) of duplicate measurements and are representative of a minimum of 3 independent experiments. * Indicates

statistical significance of $P < 0.0001$. (D) HMPV viruses (WT and recombinant mutants ΔG and $\Delta G\Delta SH$) were treated with vehicle or 40 $\mu\text{g}/\text{mL}$ of iota-carrageenan and added to BEAS-2B cells at an MOI of 1 at 4°C for particle binding. Lysates of washed cells were analyzed for HMPV binding by Western blot analysis for M. Input represents 5% of WT HMPV added to the cells for binding. No virus was added to mock infected cells. β -actin served as a loading control. (E) Band intensities of the matrix protein and β -actin were determined for untreated and treated (40 $\mu\text{g}/\text{mL}$ iota-carrageenan) samples. The data are reported as a ratio of M to β -actin normalized to the untreated control for each virus. Data points are means (\pm SD) of measurements representative of 7 independent experiments. * Indicates statistical significance of $P < 0.0001$. (F) HAE tissues were infected with rgHMPV or rgPIV5 at an MOI of 5 treated with 40 $\mu\text{g}/\text{mL}$ of iota-carrageenan or vehicle and imaged 48 hours post-infection at 5X magnification. (G) Quantification of HAE tissue infection. Data points are means (\pm SD) of triplicate measurements and are representative of minimum 3 independent experiments of HMPV infection (rgPIV5 data representative of a single HAE experiment). * Indicates statistical significance of $P < 0.0001$ using Bonferroni's Multiple Comparison Test (Prism).

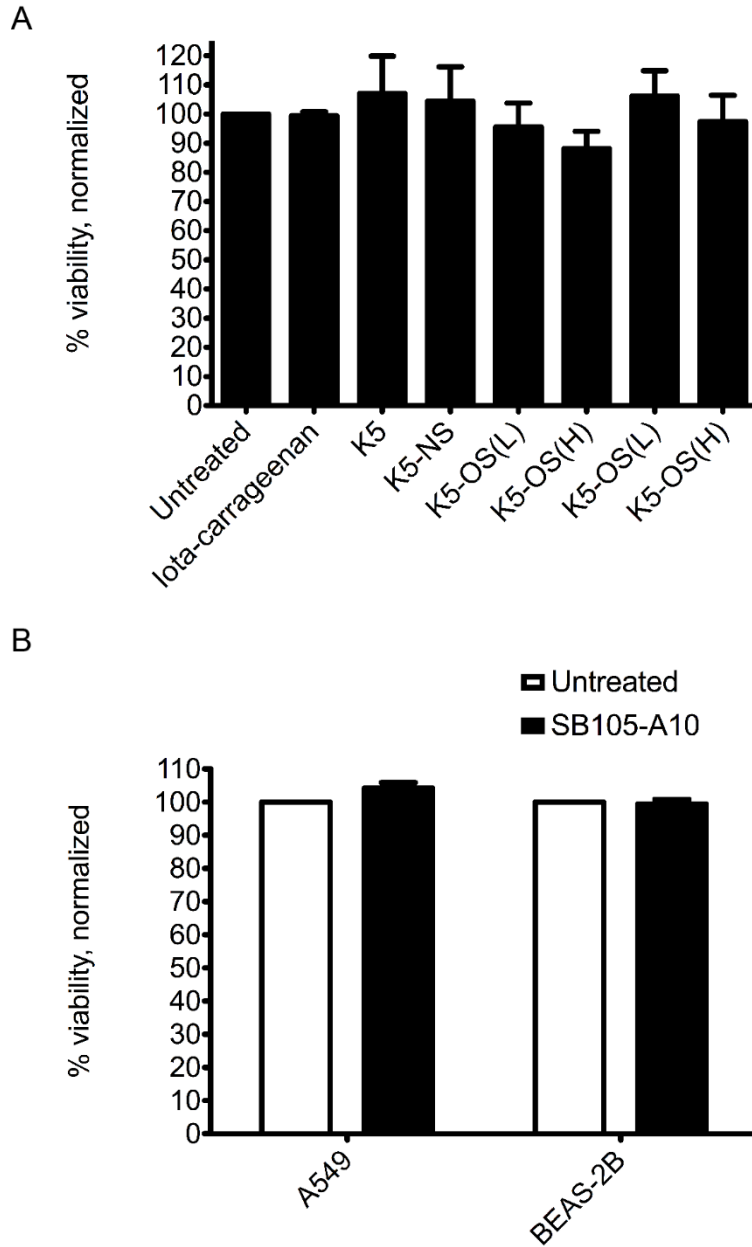


Figure 14. Iota-carrageenan, SB105-A10 and K5 derivatives do not reduce cell viability.

(A) BEAS-2B cells were treated with 40 $\mu\text{g}/\text{mL}$ of iota-carrageenan, 10 μM of each of the K5 polysaccharide derivatives, or vehicle (untreated) in triplicate and assayed for viability by MTT cell viability assay according to manufacturer's protocol. (B) BEAS-2B and A549 cells were treated with 2 μM of SB105-A10 or vehicle (untreated) and assayed for viability by MTT assay. Absorbance at 590 nm is normalized to untreated control. Data points are means (\pm SD) of triplicate measurements and are representative of 3 independent experiments.

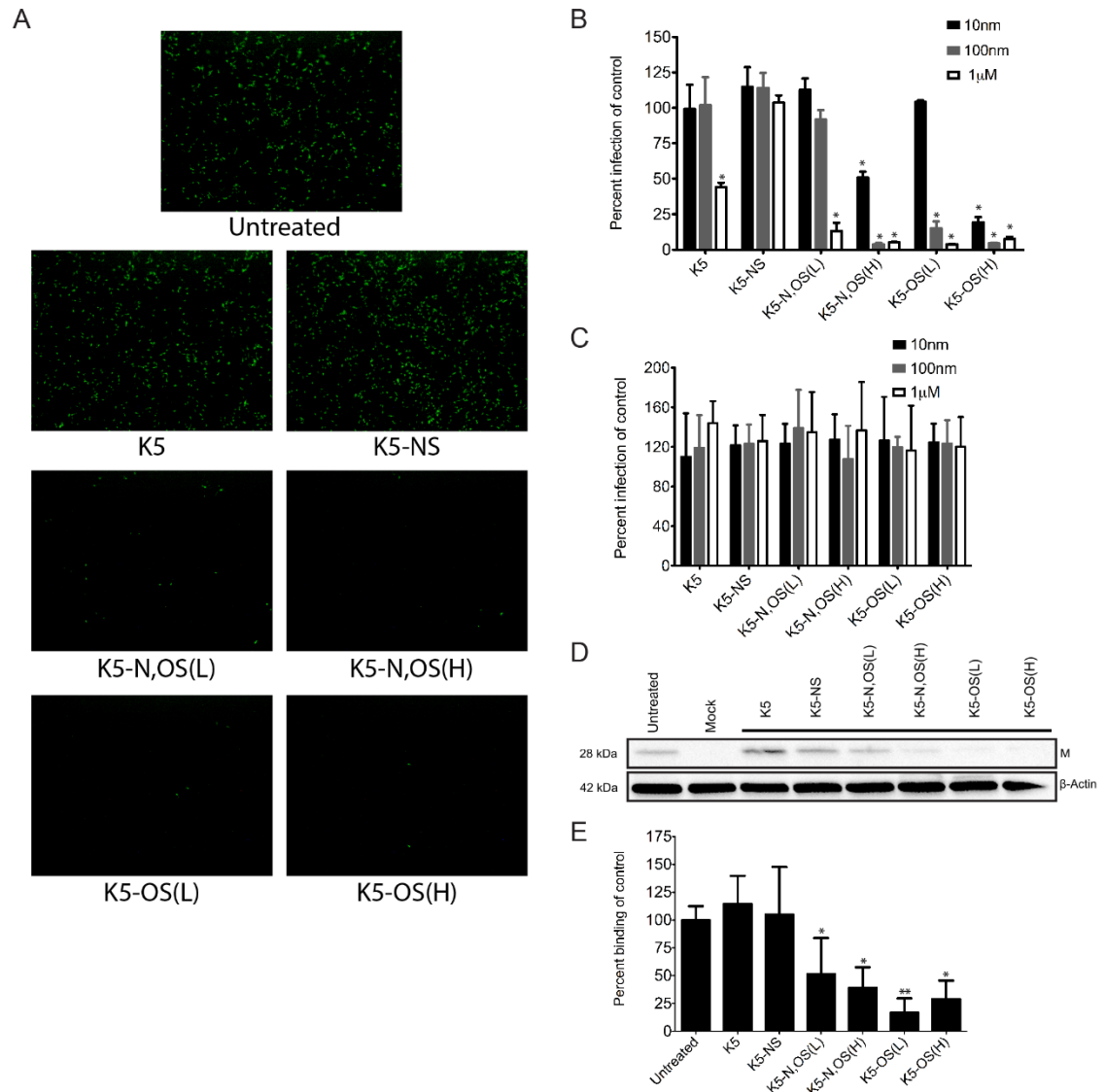


Figure 15. O-sulfated K5 polysaccharide derivatives inhibit HMPV infection in BEAS-2B cells by competing for binding.

(A) BEAS-2B cells were infected with rgHMPV at an MOI of 1 treated with 1 μ M of each K5 polysaccharide derivative or vehicle. Cells were imaged 24 hours post-infection. BEAS-2B cells were infected with rgHMPV (B) or rgPIV5 (C) at an MOI of 1 treated with 10 nM, 100 nM, or 1 μ M of each K5 polysaccharide derivative or vehicle. Infection was quantified by flow cytometry to detect GFP expressing cells 24 HPI. The data is presented as a percent infection of the untreated control. Data points are means (\pm SD) of duplicate measurements and are representative of a minimum of 3 independent experiments. Statistically, * and ** indicate significance of $P < 0.01$ and $P < 0.0001$, respectively. (D) WT HMPV was treated with vehicle (untreated) or a K5

polysaccharide derivative at 1 μM and added to BEAS-2B cells at an MOI of 1 at 4°C for particle binding. Lysates of washed cells were analyzed for HMPV binding by Western blot analysis for M. No virus was added to mock infected cells. β -actin served as a loading control. (E) Band intensities of the matrix protein and β -actin were determined for untreated and treated (1 μM) samples. The data are reported as a ratio of M to β -actin normalized to the untreated control for each virus. Data points are means (+/- SD) of measurements representative of 5 independent experiments. * Indicates statistical significance of $P < 0.001$, and ** indicates statistical significance of $P < 0.0001$ using Bonferroni's Multiple Comparison Test (Prism).

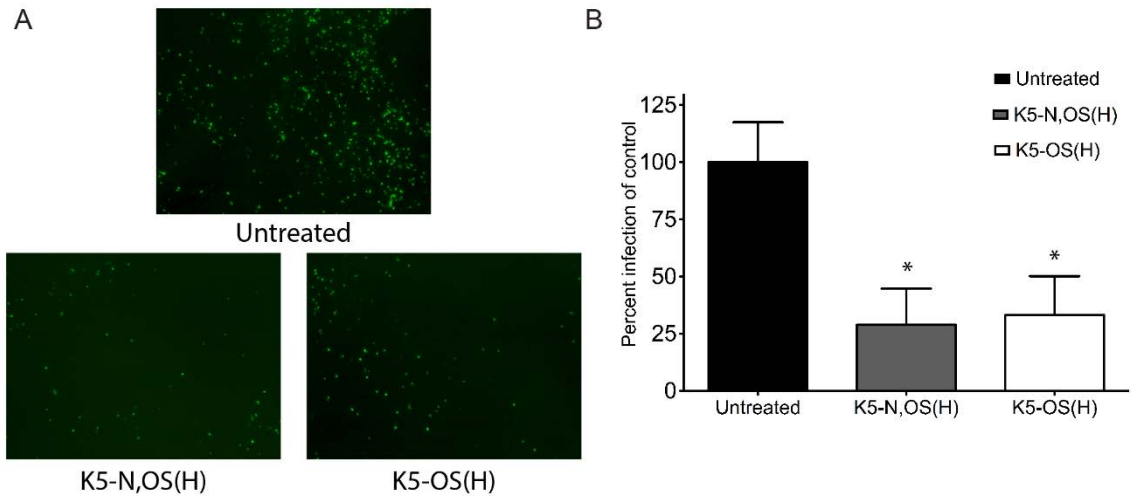


Figure 16. Highly sulfated K5 polysaccharide derivatives inhibit HMPV infection in HAE.

(A) HAE tissues were infected with rgHMPV at an MOI of 5 treated with 10 μ M K5-N,OS(H) or K5-OS(H), or vehicle (untreated) and imaged 48 HPI at 5X magnification. (B) Quantification of HAE tissue infection. Data points are means (\pm SD) of triplicate measurements and are representative of a minimum of 3 independent experiments. * Indicates statistical significance of $P < 0.0001$ using Bonferroni's Multiple Comparison Test (Prism).

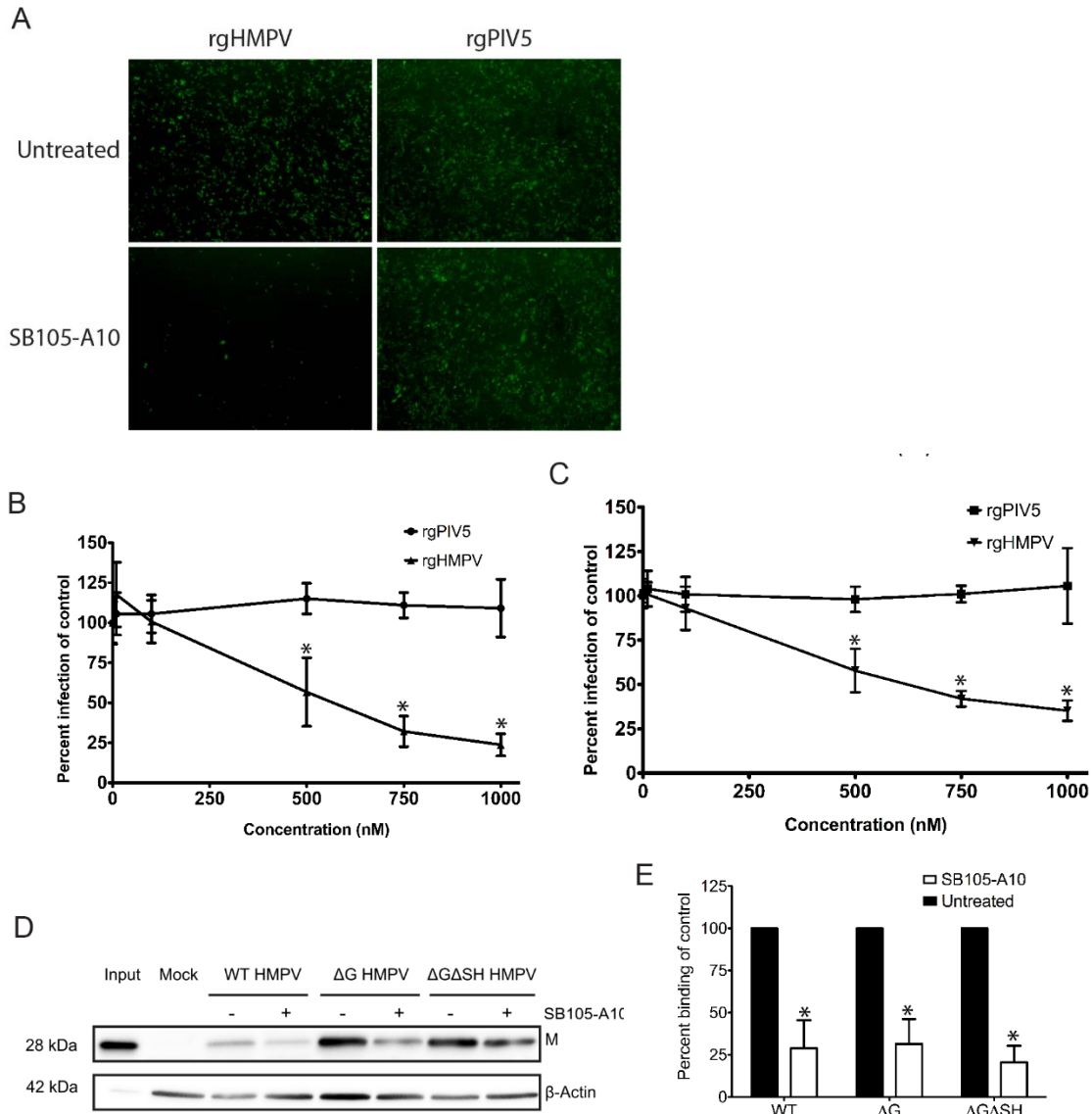


Figure 17. Peptide dendrimer SB105-A10 inhibits HMPV infection in human lung cells by inhibiting binding.

(A) BEAS-2B cells treated with 1 μ M SB105-A10 or vehicle were infected with rgHMPV or rgPIV5 at an MOI of 1. Cells were imaged at 24 hours post-infection. Percent infection of rgHMPV and rgPIV5 at an MOI of 1 treated with variable concentrations of SB105-A10 in BEAS-2B (B) and A549 (C) cells was quantified using flow cytometry. The percent infection is reported normalized to the untreated control for each virus type. Data points are means (+/- SD) of duplicate measurements and are representative of a minimum of 3 independent experiments, * indicating statistical significance $P < 0.0001$. (D) HMPV viruses (WT and recombinant mutants Δ G and Δ G Δ SH) were

added to BEAS-2B cells treated with vehicle or with 1 μ M SB105-A10 at an MOI of 1 at 4°C for particle binding. Lysates of washed cells were analyzed for HMPV binding by Western blot analysis for M. Input represents 5% of WT HMPV added to the cells for binding. No virus was added to mock infected cells. β -actin served as a loading control. (E) Band intensities of the matrix protein and β -actin were determined for untreated and treated (1 μ M SB105-A10) samples. The data are reported as a ratio of M to β -actin normalized to the untreated control for each virus. Data points are means (+/- SD) of measurements representative of 5 independent experiments. * Indicates statistical significance of $P < 0.0002$ using Bonferroni's Multiple Comparison Test (Prism).

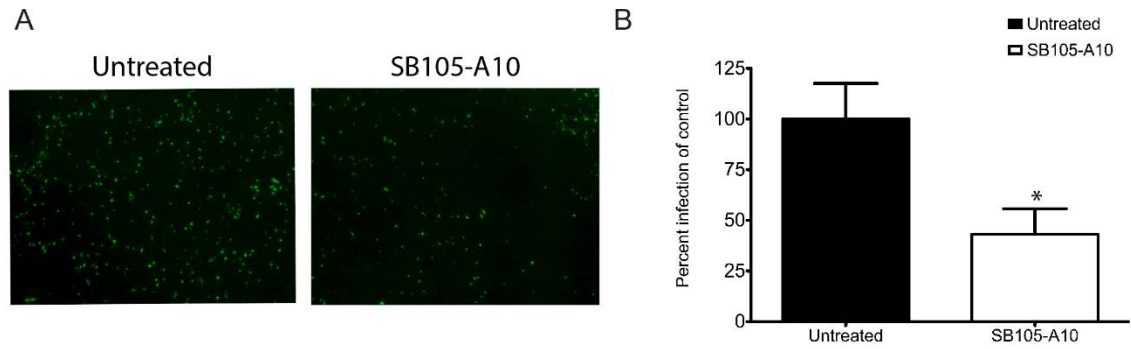


Figure 18. Treatment of HAE tissues with SB105-A10 reduces HMPV infection.

(A) HAE tissues were treated with 2 μ M SB105-A10 or vehicle (untreated) and infected with rgHMPV at an MOI of 5. Tissues were imaged 48 HPI at 5X magnification. (B) Quantification of HAE tissue infection. Data points are means (\pm SD) of triplicate measurements and are representative of a minimum of 3 independent experiments.* Indicates statistical significance of $P < 0.0001$ using Bonferroni's Multiple Comparison Test (Prism).

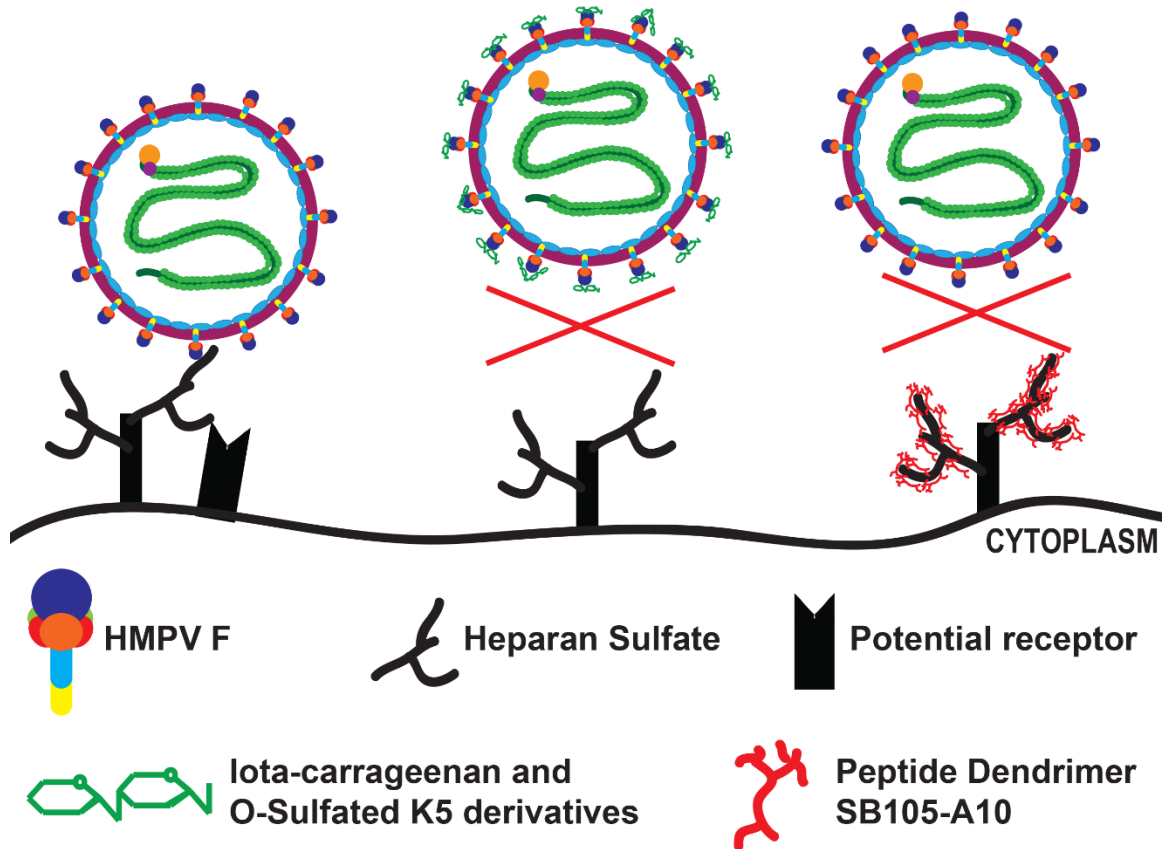


Figure 19. Model for inhibition of HMPV infection by interference between F and heparan sulfate.

HMPV utilizes F for initial attachment to heparan sulfate found on the surface of target cells, with potential involvement of an unidentified receptor necessary to complete entry. Sulfated polysaccharides, iota- carrageenan and the heparan sulfate-like K5 polysaccharide derivatives, inhibit this attachment step. Occluding heparan sulfate with SB105-A10 also blocks HMPV binding by occluding HS from interaction with HMPV F.

Chapter 5: Novel roles of HMPV G and SH during infection in bronchial epithelial cells

*These results were obtained with the help of Nicolás Cifuentes, who obtained images of WT and recombinant HMPV particles using electron microscopy.

Introduction

HMPV is a ubiquitous pathogen that causes respiratory disease worldwide (28-30). First identified in 2001 in the Netherlands, HMPV is now known to be the cause of respiratory infections in humans since at least 1958 (31). Nearly every person is exposed to HMPV in the first decade of life; sero-conversion occurs on average by the age of five and nearly 100% of individuals test seropositive for antibody reactivity to HMPV antigens by age ten (7). HMPV is the second most common cause of lower respiratory infection in children, following the closely related respiratory syncytial virus (RSV) (37, 38). Importantly, up to 70% of infants hospitalized for severe RSV bronchiolitis were also co-infected with HMPV, suggesting HMPV co-infection leads to more severe disease during RSV infection (39-41). While infants are considered the most vulnerable population to developing illness from HMPV, adults can foster severe respiratory infection as well, especially elderly and immunocompromised patients (43-45).

Complications of respiratory infection associated with HMPV include pneumonia, bronchiolitis, and febrile seizures (44, 59). Such complications can be life threatening in these susceptible individuals. It has also been suggested that severe acute respiratory infection from HMPV may have lifelong consequences such as asthma and hyperresponsiveness of the airway (60, 61). While HMPV infection has been thought to be restricted to the respiratory epithelium and lungs, there have been several reports of fatal encephalitis with HMPV the only detected pathogen in both lung and brain tissue (62-64). Even though primary infection occurs during childhood in the majority of cases, repeat infections are common throughout life, likely due to strain variations and incomplete immunity. Despite HMPV prevalence and clinical relevance, there are no specific antiviral treatments or vaccines available.

HMPV is an enveloped virus with a single-stranded, negative sense, non-segmented RNA genome. It is a member of the paramyxovirus family, which includes RSV, measles virus, mumps virus, and parainfluenza virus (PIV), in addition to the emerging zoonotic viruses of high mortality in humans, Hendra and Nipah (356). Phylogenetic amino acid sequence analysis of HMPV isolates

identified multiple strains and two major genetic lineages, A and B (30). In all isolates of HMPV to date, three glycoproteins are present in the viral envelope: the fusion protein (F), the putative attachment protein (G), and the small hydrophobic protein (SH) (90, 357). HMPV F mediates viral membrane fusion and also plays a critical role in binding and infectivity (76, 77, 79). The roles for HMPV G and SH are not as well understood, as they often differ in function from other viruses of the same family.

In most paramyxoviruses the attachment protein typically interacts with a cell receptor upon binding and triggers the fusion protein, which promotes subsequent fusion of viral and cellular membranes. However, HMPV F is the primary factor for viral attachment in addition to its role in membrane fusion. Recombinant HMPV without G was replication competent in cell culture and in multiple animal models, although replication in the lower respiratory tract was modestly attenuated (76, 77). Furthermore, some HMPV F proteins can promote cell-to-cell fusion with acidic pH pulses, without co-expression of G (134, 136, 241-243). These findings suggest HMPV G does not mediate the binding interaction that is typical of attachment proteins found in paramyxoviruses.

In addition to HMPV, SH proteins are found in several other paramyxoviruses, including members of rubulaviruses and pneumoviruses, and the unclassified J virus. The SH protein of most paramyxoviruses is not required for viral replication *in vitro* (78, 358-360). The deletion of the SH proteins of RSV and avian metapneumovirus (AMPV) reduced replication and pathogenicity in animal models (80-82). However, recombinant HMPV lacking the SH gene was found to replicate in both hamster and nonhuman primate models only marginally less efficiently than wild-type (WT) HMPV (76, 83). While these findings suggest HMPV SH has a dispensable role in infection, all HMPV isolates to date have the SH gene, indicating its presence is required for fitness (90). Several functions of HMPV SH have been identified recently. Like the SH of RSV (91), the HMPV SH protein exhibits viroporin, or viral protein channel, activity (92). Furthermore, HMPV SH can regulate the cell-to-cell fusion activity of F (92).

The roles of HMPV G and SH glycoproteins have been recently studied in more detail in the context of HMPV entry. There is direct evidence the HMPV G and SH regulate HMPV entry, which may contribute to immune system modulation of the host. Recent studies using recombinant HMPV lacking G and SH showed that G and SH glycoproteins inhibit macropinocytosis-mediated entry into human dendritic cells and reduce activation of CD4⁺ helper T cells (93). Furthermore, it has been shown that HMPV G, specifically through the cytoplasmic

tail domain, can disrupt mitochondrial signaling in airway epithelial cells that leads to an antiviral response (361). Altogether, there is evidence that HMPV G and SH can affect virus uptake, suggesting these glycoproteins affect F, which is the primary attachment for HMPV. However, the mechanisms of the regulatory effects of G and SH in entry remain to be explored.

In this study, we utilized a model of human bronchial epithelial cells to characterize key differences between WT HMPV and recombinant HMPV lacking G or both G and SH. The results showed G and SH inhibit particle binding to human bronchial epithelial cells, as recombinant HMPV Δ G and Δ G Δ SH were able to bind more efficiently. However, heparan sulfate modulating compounds inhibited the binding of the recombinant and WT HMPV similarly, supporting that F mediates the critical interaction with heparan sulfate. Further analysis revealed increased binding of the recombinant viruses did not result from great F incorporation in particles, and electron microscopy did not reveal any significant differences in morphology between the recombinant and WT HMPV. Interestingly, HMPV lacking G did not incorporate cellular actin into particles, suggesting G may interact with the cell cytoskeleton during trafficking and assembly. These findings demonstrate a potential novel role for HMPV G and further elucidate the complex, regulatory interactions between viral proteins.

Results

Recombinant Δ G and Δ G Δ SH HMPV bind BEAS-2B more efficiently than WT

We previously showed recombinant HMPV Δ G and Δ G Δ SH purified by sucrose cushion binds and infects Vero and CHO cell lines at WT levels (79). This purification process concentrates viral particles of uniform density, which may exclude more variable forms of viruses that may be budding. To better understand what role HMPV glycoproteins G and SH may have in HMPV infection, we utilized human bronchial epithelial (BEAS-2B) cells infected by viruses purified using SPG as a stabilizing agent and for cryoprotection, that does not exclude any particles. To determine if G or SH affect particle binding, viruses purified by SPG were added to BEAS-2B cells at 4°C, allowing for binding to occur but not infection, and the amount of bound virus was quantified by analysis detection of the HMPV matrix protein present in cell lysates with β -actin as a loading control, by Western blot. Five percent of input virus for each virus was also loaded for comparison. Interestingly, HMPV Δ G and Δ G Δ SH had greater binding to BEAS-2B cells than WT HMPV (Fig. 20A and 20B) despite adding the same amount of virus (Fig. 20C). Quantification of binding relative to input revealed enhanced binding of HMPV Δ G Δ SH compared to WT HMPV,

although HMPV ΔG also had a trend for increased binding (Fig. 20D). These results suggest G and SH negatively regulate HMPV binding to BEAS-2B cells. To confirm that the enhanced binding activity of recombinant viruses was still dependent on the interaction between F and heparan sulfate, we utilized iota-carrageenan, a sulfated polysaccharide that has been shown to inhibit HMPV binding and infection (Fig. 13). Pretreatment of WT HMPV and recombinant HMPV ΔG and $\Delta G\Delta SH$ with 40 $\mu\text{g}/\text{mL}$ of iota-carrageenan resulted in an inhibition of binding (Fig. 20A). Furthermore, occlusion of heparan sulfate with 1 μM of peptide dendrimer SB105-A10 also inhibited binding of WT HMPV and recombinant HMPV ΔG and $\Delta G\Delta SH$ (Fig. 20B). Taken together, these results indicate the loss of G and SH results in increased binding to human bronchial epithelial cells, and this binding is dependent on the interaction between F and heparan sulfate as seen in WT HMPV.

We hypothesized that recombinant HMPV ΔG and $\Delta G\Delta SH$ incorporate more F into particles due to the lack of one or both glycoproteins compared to WT HMPV. To test this, we analyzed the relative content in WT and recombinant HMPV viruses of F compared to M (Fig. 21A). Surprisingly, the recombinant HMPV ΔG or $\Delta G\Delta SH$ did not incorporate more F into the particles (Fig. 21B), suggesting more F available for binding is not the mechanism of enhanced binding to BEAS-2B cells.

The viruses used in these studies were purified using SPG, which does not select for particles of uniform density the way concentrating sucrose purification does. It is possible the recombinant HMPV lacking G or G and SH produces different shaped or sized particles than WT HMPV that affect binding. To address this question, we performed electron microscopy on HMPV ΔG (Fig. 22B) and HMPV $\Delta G\Delta SH$ (Fig. 22C), and compared particle appearance and size to WT HMPV (Fig. 22A). Analysis of electron microscopy images did not reveal detectable differences in particle shape as the WT (Fig. 22A) and recombinant HMPV (Fig. 22B and 22C) produced both spherical and pleomorphic particles of variable size. Glycoprotein spikes were observed for WT and recombinant viruses also (Fig. 22). Therefore, we were not able to identify any differences in particle morphology to explain differences in binding, suggesting the glycoproteins G and SH may regulate binding mediated by HMPV F.

Recombinant ΔG and $\Delta G\Delta SH$ HMPV do not incorporate cellular actin

In the binding assays using iota-carrageenan (Fig. 20A) and SB105-A10 (Fig. 20B), β -actin was used as a loading control for cell lysates to ensure the same amount of protein was loaded in

the untreated and untreated samples. Because the input virus samples were also analyzed within the same gel, the amount of β -actin in the virus samples was also detected. Mass spectrometry analysis of WT HMPV has shown cellular cytoskeletal proteins, such as β -actin, are found in purified virus particles, presumably due to incorporation during particle assembly and budding (El Najjar, *et al.*, submitted). Interestingly, we noted WT HMPV incorporated small amounts of β -actin, but there was no β -actin detected in samples of HMPV Δ G or HMPV Δ G Δ SH (Fig. 20A and 20B). To confirm these observations, we analyzed the β -actin content of WT HMPV, recombinant HMPV that results in green fluorescent protein expression (GFP) (rgHMPV), HMPV Δ G, and HMPV Δ G Δ SH by Western blot (Fig. 23A). M was also detected for comparison (Fig. 23A). While similar amounts of M were detected for rgHMPV and the recombinant viruses (Fig. 23B), β -actin incorporation in HMPV Δ G and HMPV Δ G Δ SH was reduced compared to rgHMPV (Fig. 23C). These results suggest HMPV G contributes to β -actin association with HMPV and possible incorporation during assembly. However, what role, if any, recruitment of cellular actin into the viral particles has in assembly and spread is unclear.

Discussion

HMPV F is essential and sufficient for infectivity. Recombinant HMPV without glycoproteins G and SH is infectious *in vitro* and *in vivo*. However, all clinical isolates of HMPV isolated to date contain genomes with all three glycoproteins, indicating that these proteins play an essential role. The results presented here demonstrated HMPV G and SH can affect HMPV binding to human bronchial epithelial cells, as recombinant viruses HMPV Δ G and HMPV Δ G Δ SH demonstrated enhanced binding compared to WT HMPV (Fig. 20). We concluded greater incorporation of F (Fig. 21) or differences in particle morphology (Fig. 22) did not explain the difference in particle binding.

It is possible that HMPV G may regulate binding by direct interaction with F, which is the primary glycoprotein involved in attachment. While expression of HMPV F and M are sufficient for virus-like particle (VLP) formation that resembles HMPV (362), G interacts with F in VLPs when co-expressed with F and M (363). Furthermore, our group has shown SH can regulate cell-to-cell fusion activity of HMPV F expressed at the plasma membrane (92), further supporting a regulatory role. It has been shown HMPV G and SH inhibit uptake by macropinocytosis in dendritic cells (93). Therefore, HMPV G and SH may play a role in numerous aspects in F function: binding, fusion, and mediating entry.

While the results presented here demonstrated enhanced binding of HMPV ΔG and HMPV $\Delta G\Delta SH$ compared to WT HMPV, our group has previously reported that the recombinant viruses bind and infect Vero and CHO cell lines at WT levels (79). There are several possibilities to explain different findings presented here. First, the viruses used in this study were prepared using SPG, which serves as a stabilizing agent. This purification allowed for better preservation of the diversity of viral particles, in contrast to purification by sucrose cushion which utilizes a density barrier at high centrifugation speeds to concentrate particles of similar density and often results in particle breakage. Therefore it is possible this methodology recovered a population of HMPV ΔG and HMPV $\Delta G\Delta SH$ typically excluded by sucrose cushion purification, which allowed for the observation of enhanced binding. Secondly, we utilized a respiratory bronchial epithelial cell line to study the roles of G and SH in binding. BEAS-2B cells are non-cancerous, lung epithelial cells that serve as a physiologically relevant model for respiratory virus infection. It is possible the abundance of specific heparan sulfate proteoglycans (HSPGs) or integrin $\alpha V\beta 1$, both of which contribute to HMPV entry, differ in the airway cells than other cell types. Therefore, regulatory effects of HMPV G and SH on F may become exposed when attachment factors are present in different quantities or ratios. Lastly, it is possible that particle stability is reduced in HMPV ΔG and HMPV $\Delta G\Delta SH$, resulting in more defective particles that are unable to establish infection compared to WT HMPV, although no significant differences were observed by electron microscopy (Fig. 22). Such defective particles may still be able to bind to cells and be detected by Western blot. Preliminary experiments to determine differences in infectivity did not reveal enhanced infection in HMPV lacking G and/or SH compared to WT HMPV. However, further studies are required to confirm this.

We showed HMPV lacking G, both HMPV ΔG and HMPV $\Delta G\Delta SH$, was not associated with cellular actin at levels comparable to that observed with WT HMPV (Fig. 20 and 23). There is no current evidence of direct or indirect interaction of HMPV G with cellular actin. The actin cytoskeleton, which is a central node in cellular pathways, is frequently targeted by various pathogens to modulate cellular responses. The actin cytoskeleton has been shown to play a critical role in the formation of filaments and cellular extensions that serve as HMPV assembly sites and may contribute to cell-to-cell spread (El Najjar, *et al.*, submitted). However, results showed HMPV P induced the cytoskeletal changes, suggesting manipulation of the actin cytoskeleton for spread and actin incorporation into HMPV particles may be unique functions of distinct HMPV proteins. Furthermore, concentrated F-actin localizes to sites of HMPV filament

budding in the plasma membrane and incorporates into filamentous particles (364). Incorporation of cellular actin into particles has been reported for many viruses, including HIV-1 (365) , rabies virus (366), and Newcastle Disease virus (367). For RSV, it is proposed that cellular actin is used as a scaffold to propel filamentous viral to bud and leads to incorporation of cellular actin in the particles (368). However, it is thought cytoplasmic tail of the RSV fusion protein is required for the recruitment into filaments (369, 370). It is not known if the incorporation of cellular actin into viral particles is deliberate and contributes to pathogenicity, or is simply a nuance of assembly.

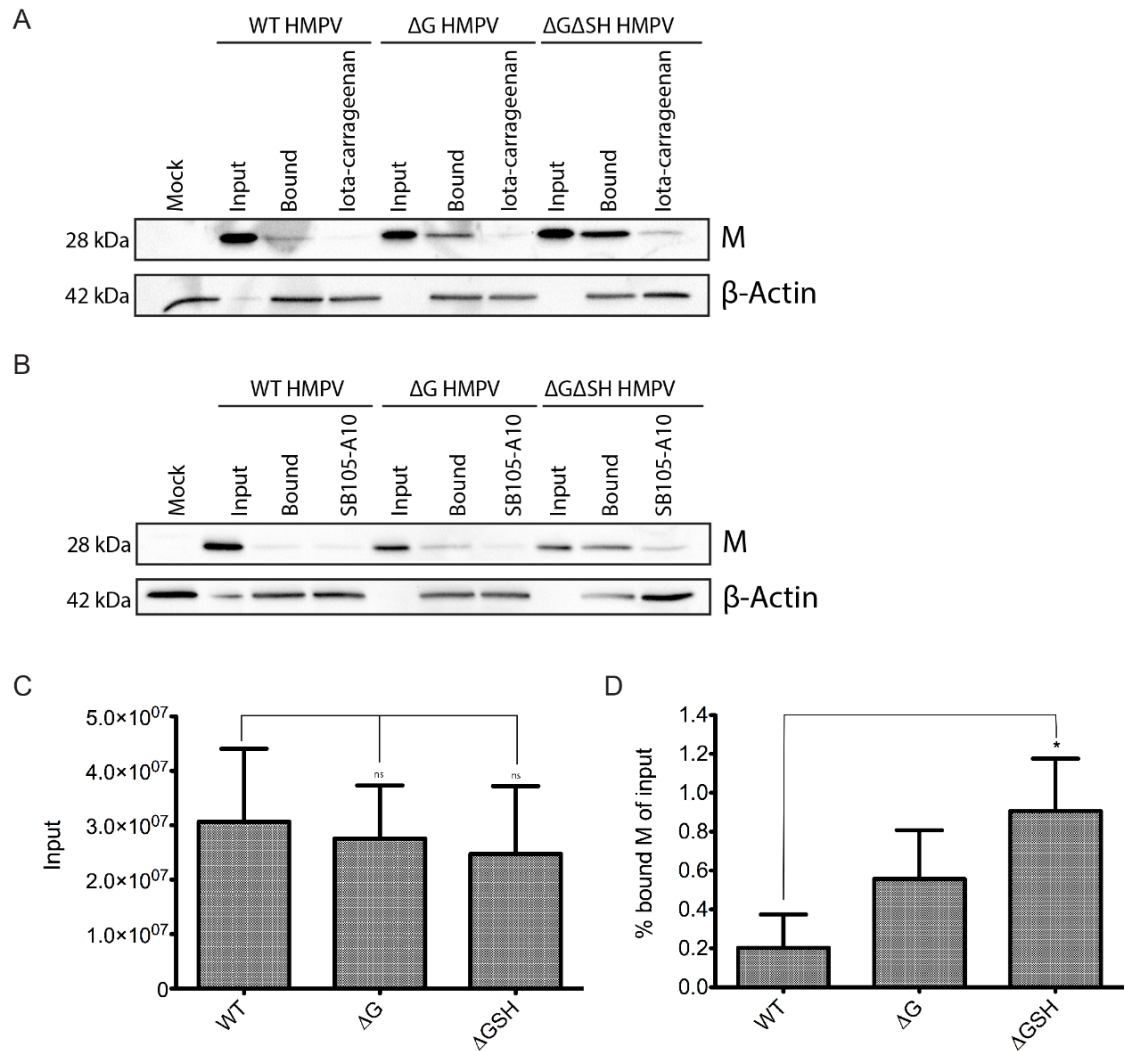


Figure 20. Recombinant HMPV ΔG and $\Delta G\Delta SH$ bind more efficiently to BEAS-2B cells than WT HMPV.

(A) HMPV viruses (WT and recombinant mutants ΔG and $\Delta G\Delta SH$) were treated with 40 $\mu\text{g}/\text{mL}$ of iota-carrageenan and added to BEAS-2B cells at an MOI of 1 at 4°C for particle binding. (B) HMPV viruses (WT and recombinant mutants ΔG and $\Delta G\Delta SH$) were added to BEAS-2B cells treated with vehicle or with 1 μM SB105-A10 at an MOI of 1 at 4°C for particle binding. Lysates of washed cells were analyzed for HMPV binding by Western blot analysis for M. Input represents 5% of WT HMPV added to the cells for binding. No virus was added to mock infected cells. β -actin served as a loading control. (C) Band intensities of the input M of WT and recombinant virus. Data points are means (\pm SD) of measurements representative of 3 independent experiments. (D) Percent bound particles compared to input of WT and recombinant HMPV, determined by quantification

of M. Data points are means (\pm SD) of measurements representative of 5 independent experiments. * Indicates statistical significance of $P < 0.05$.

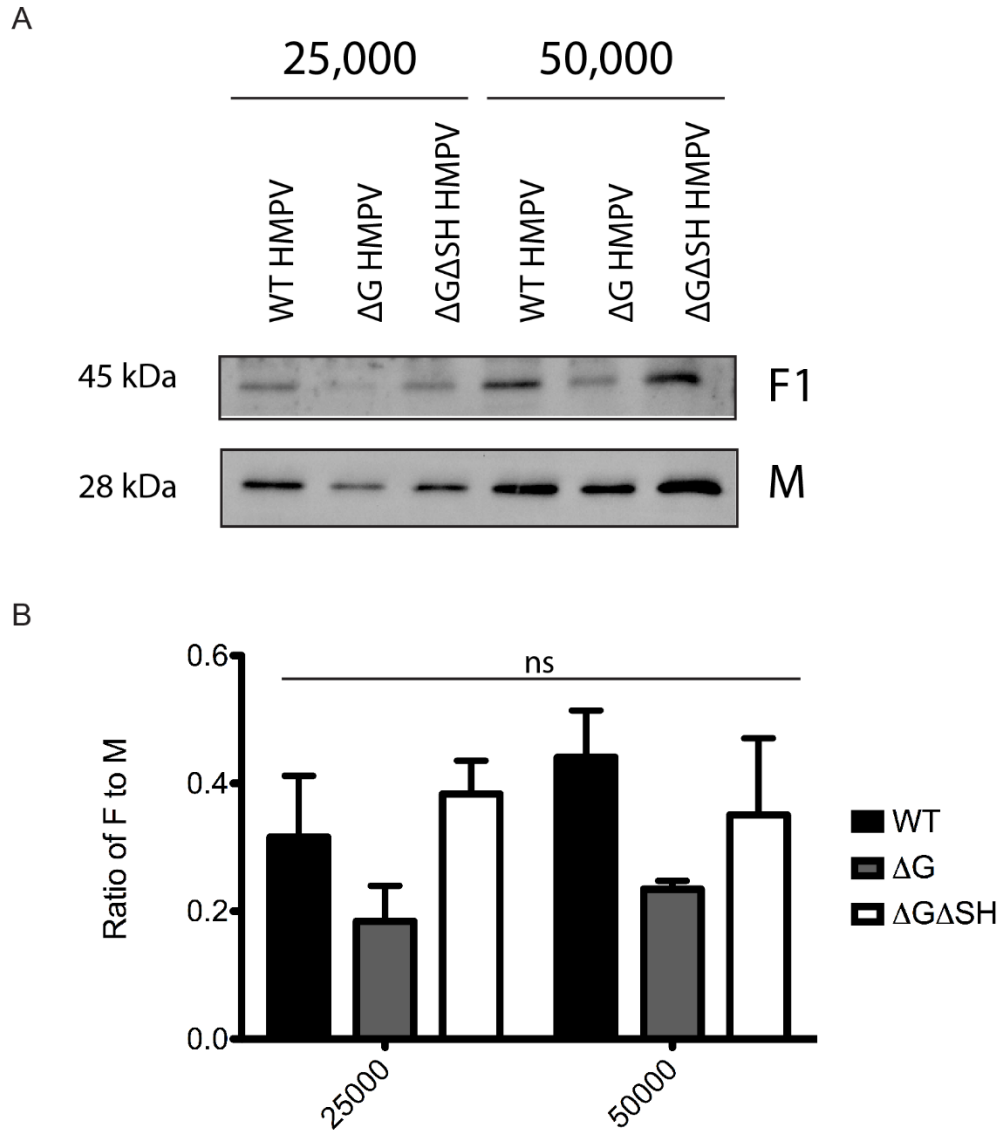
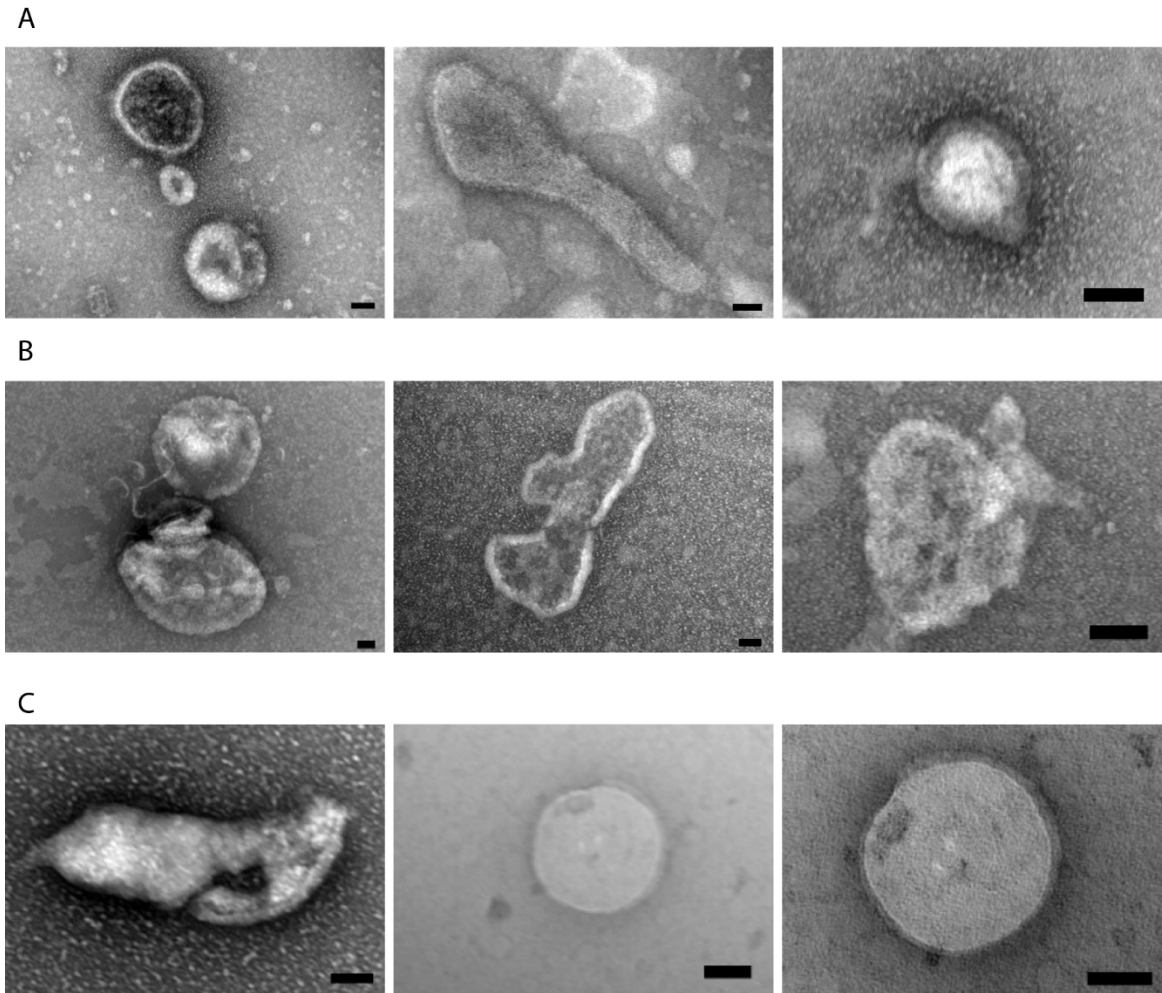


Figure 21. Recombinant HMPV Δ G and Δ G Δ SH do not have greater F incorporation compared to WT HMPV.

(A) Approximately 25,000 and 50,000 particles of WT HMPV, HMPV Δ G, and HMPV Δ G Δ SH were lysed, and proteins were separated by SDS-PAGE followed by Western blot analysis for F1 and M.

(B) Band intensities for F and M were quantified using ImageQuantTL, and the data are presented as a relative ratio of F to M. (n=2)



*scale bar indicates 50 nm

Figure 22. Electron microscopy imaging of viral particles.

(A) WT HMPV, (B) HMPV ΔG , and (C) HMPV $\Delta G\Delta SH$ were propagated in Vero cells for 4-5 days at 37°C and purified using SPG.

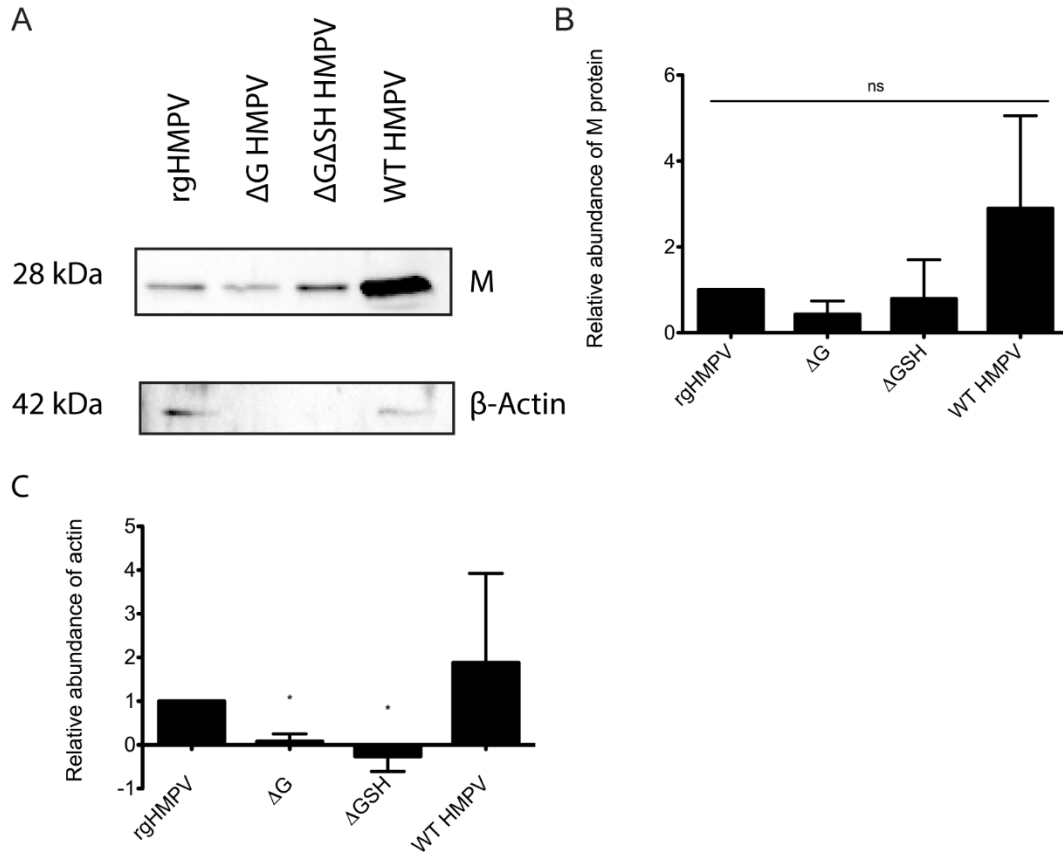


Figure 23. Recombinant HMPV Δ G and Δ G Δ SH are not associated with β -actin.

(A) Recombinant HMPV that results in GFP expression (rgHMPV), HMPV Δ G, HMPV Δ G Δ SH, and WT HMPV aliquots were lysed, and proteins were separated by SDS-PAGE, which was followed by Western blot analysis for HMPV M and β -actin. (B) Band intensities for M and (C) β -actin were quantified using ImageQuantTL, and the data are presented normalized to protein content in rgHMPV. *Indicates statistically significant, $P < 0.05$ ($n = 2$).

Chapter 6: HMPV Infection in a Cystic Fibrosis Model

Introduction

Cystic fibrosis (CF) is an autosomal recessive inherited disorder that affects many organ systems of the body (371-373). Among Caucasians, it is the most common lethal genetic disease with approximately 1 in 2,500 children born with CF in the United States (374). Approximately 1 in 25 Caucasians of European descent are carriers of the allele (375), likely due to heterozygous advantage for the survival of *Vibrio cholera* infection (376, 377). CF is diagnosed by a sweat test and genetic testing for known mutations commonly included in newborn screenings (378). The average life expectancy of individuals with CF has risen to nearly 40 years, compared to only 16 years in the 1970s, due to advances in treatments (379, 380). Cystic fibrosis is characterized by disease in numerous organ systems, including exocrine pancreatic insufficiency, liver and kidney dysfunction, malabsorption in the intestines, infertility in males, and chronic obstructive pulmonary disease. However, complications due to lung dysfunction are responsible for death in 85% of people with CF (381, 382).

The basic genetic defect that causes this disorder, discovered over 25 years ago, resides in the cystic fibrosis transmembrane conductance regulator (CFTR) gene (373). The resulting gene product is a protein kinase A-activated chloride and bicarbonate selective ion channel involved in salt and water transport across apical membranes of epithelial cells. It is expressed in secretory and absorptive epithelial cells in the airway, pancreas, liver, intestine, sweat gland and the vas deferens. CFTR also affects sodium transport through regulation of sodium channels at the plasma membrane. Loss of CFTR function leads to defective anion secretion and sodium hyperabsorption across airway surfaces and submucosal glands. In the lungs, the resulting altered balance of ion transport dehydrates the airway creating viscous mucus and impeding mucociliary clearance (379, 380, 383-386).

Many mutations in the CFTR gene have been identified that result in impaired CFTR function, and a deletion of the 508th amino acid phenylalanine ($\Delta F508$) is the most common, accounting for about 70% of mutations that result in CF (383). CFTR $\Delta F508$ in both copies of the gene results in nearly a total absence of the channel in the membrane, as the misfolded mutant protein fails to progress through the normal biosynthetic pathway from the endoplasmic reticulum to the plasma membrane (387, 388). Other less common mutations, of which over 1,950 have been identified, can result in lower expression CFTR or impaired CFTR function, often leading to

less severe clinical presentation (389). Therefore, CF is a heterogeneous disease that ranges in severity of organ dysfunction, although pulmonary dysfunction affects all individuals with this disease.

The pathophysiology that results from CFTR dysfunction significantly impacts overall lung function and greatly predisposes CF patients to lower respiratory tract disease. Without a proper balance of ions at the apical surface of the airway epithelium, the airway surface liquid is depleted. Retention of airway secretions leads to the hallmarks of CF lung disease, including chronic bacterial airway infection, airway inflammation, and irreversible lung damage (384, 385, 390). The clinical course of this disease is described by chronic inflammation which is punctuated by periods of acute worsening of lung disease that increase with age and declining lung function, eventually leading to lung transplantation or death (57). The most devastating bacterial culprit in CF patients is *Pseudomonas aeruginosa*, as nearly 80% of CF patients are colonized during their lifetimes (391, 392). Once colonized, infection with *P. aeruginosa* becomes a chronic source of inflammation in the lungs and is an indicator of poor prognosis (391, 392). It is thought that exacerbations in airway disease occur due to an imbalance between chronic bacterial infection and host immune response (393). Viral infection may be an important factor that triggers these events. Viral respiratory tract infections are associated with exacerbations in children with CF (394, 395). In a clinical study of viral infection in CF exacerbation, it was shown that virus infection was associated with an increase in *P. aeruginosa* load (396).

Several viruses are well known to cause respiratory disease in CF patients, such as human rhinovirus (HRV) (56, 397-400), parainfluenza virus 3 (397), adenovirus (56), influenza A (56, 399) and respiratory syncytial virus (RSV) (398, 401). The impact of HMPV infection in CF patients has not been addressed in detail. Few studies have examined the incidence and severity of respiratory infection caused by HMPV in these patients. The limited studies that have assessed HMPV infection in CF patients concluded that its prevalence rivals that of RSV and that HMPV is an important clinical pathogen in this patient population (58, 402). In adults, one study found that HMPV was second in prevalence after HRV for viral infection that caused acute exacerbation (398). However, how HMPV infection may differ in the context of CFTR dysfunction compared to healthy lungs is unknown.

Due to the limited knowledge regarding HMPV in the context of CF, we utilized a cystic fibrosis bronchial epithelial (CFBE) cell line derived from a patient with the CFTR homozygous $\Delta F508$ mutation (403) as a model to study HMPV. Infection studies using HMPV and the related

paramyxoviruses RSV and parainfluenza virus 5 (PIV5) revealed CFBE cells were more permissive to specifically HMPV infection compared to other respiratory cell types, suggesting a unique host-virus interaction. Furthermore, CFBE cells were entirely resistant to PIV5 infection. Heparan sulfate modulating compounds that block HMPV binding in respiratory cells inhibited HMPV infection in CFBE cells also, suggesting heparan sulfate serves as an attachment factor in these cells. However, the increased infection of HMPV in CFBE cells could not be attributed to an increase in overall virus binding. These findings suggest CFBE cells and possibly CF lungs are specifically vulnerable to HMPV infection.

Results

CFBE cells more permissive to HMPV but not RSV infection than other human lung cells

Despite the prevalence of HMPV infection in the worldwide population, the impact of HMPV has not been well characterized in patients with CF. The few existing studies have suggested HMPV is a common cause of respiratory disease in these patients, detected at nearly the same incidence as RSV. To examine HMPV infection in the context of CFTR dysfunction, we utilized a cystic fibrosis bronchial epithelial (CFBE) cell line, which contains the most common mutation in the CFTR gene, $\Delta F508$, which leads to nearly a total lack of expression of the protein product at the plasma membrane. To assess permissiveness of CFBE cells to HMPV infection, infection at a specific multiplicity of infection (MOI) was compared to that observed in other human lung cells, A549 and BEAS-2B, as well as Vero cells, which are monkey kidney epithelium cells that lack interferon mediated signaling and are highly permissive to viral infection. The experiments for each cell type were completed at equivalent passage numbers from thawing as prolonged passaging can alter cellular protein expression and affect permissiveness to viral infection. Vero, CFBE, A549 and BEAS-2B cells were cultured overnight, counted, and infected with rgHMPV at MOI 0.1 and 0.5 and the percent of cells with green fluorescent protein (GFP) expression was determined by flow cytometry 24 HPI. A similar efficiency of HMPV infection was observed in A549 and BEAS-2B cells for each MOI, respectively (Fig. 24). As previously observed, Vero cells demonstrated higher HMPV infection (Fig. 24). Interestingly, CFBE cells were similarly permissive to HMPV infection as the Vero cells, and thus showed significantly higher infection rates than both A549 and BEAS-2B cells (Fig. 24).

To determine if CFBE cells are highly permissive to other related respiratory viruses, all four cell types were infected with rgRSV at MOI 0.1 and 0.5 and fluorescent cells were determined

by flow cytometry 48 hours post infection, which is when GFP expression is highest in infected cells. Unlike with HMPV infection, CFBE cells were the least permissive to RSV infection (Fig. 25). A549 and BEAS-2B cells had similar levels of infection and Vero cells were the most permissive to RSV infection (Fig. 25). These results suggest CFBE cells are selectively highly permissive to HMPV compared to the closely related *Pneumoviridae* subfamily member, RSV.

CFBE cells are not permissive to PIV5 infection

Initial studies with paramyxoviruses in the *Pneumoviridae* subfamily, HMPV and RSV, revealed CFBE cells were selectively permissive to HMPV infection compared to other human lung cells. To determine if these cells promote higher infection of other paramyxoviruses, we analyzed the efficiency of PIV5 infection in CFBE, A549, BEAS-2B, and Vero cells. All four cell types were cultured overnight and infected with rgPIV5 at MOI1 and MOI5, and the percent of infected cells was quantified by GFP expression using flow cytometry. Higher MOIs were used in these experiments because no PIV5 infection was observed in CFBE cells in preliminary experiments using MOI 0.1 and 0.5. Therefore, MOI was increased to determine if infection in these cells is simply inefficient or if they were not permissive. Vero, A549 and BEAS-2B cells had similar infection efficiency of PIV5 (Fig. 26). Surprisingly, CFBE cells were highly resistant to PIV5 (Fig. 26). These results indicated viral infection is not enhanced in CFBE cells by a non-specific mechanism.

HMPV infection of CFBE cells inhibited by heparan sulfate modulation

HMPV has been shown to require the proteoglycan heparan sulfate (HS) as a host attachment factor to bind and infect cells (79). We have previously shown that nearly complete reduction in binding and infection results when HS is removed from the cell surface using heparinases, while cells that are able to synthesize only HS, and not any other GAGs, are fully able to bind HMPV (79). It is not known whether HS is required for HMPV binding in CFBE cells, or whether increases in infection relate to increased binding either via HS or another host factor. To test this, CFBE cells were treated with peptide dendrimer SB105-A10 (Fig. 12C), which specifically occludes ligand binding from heparan sulfate proteoglycans (139, 350), and has been shown to inhibit HMPV infection in non-CF human lung cells (Fig. 17). The resulting infection was quantified by counting GFP-expressing cells by flow cytometry. HMPV infection was inhibited by pretreatment of CFBE cells with SB105-A10 by nearly 75% (Fig. 27A), similar to inhibition observed

in A549 (Fig. 17C) and BEAS-2B cells (Fig. 17B). These results suggest HMPV interaction with HS is also required for infection in CFBE cells.

HMPV binding to HS can be inhibited by compounds that mimic HS (Fig. 15). K5 polysaccharide derivatives are heparan-like molecules devoid of anticoagulant activity obtained by the sulfation of the *E. coli* capsular K5 polysaccharide that has the same structure as the biosynthetic precursor of HS, N-acetyl heparosan. A small library of derivatives with different degrees of sulfation has been synthesized using chemical and enzymatic modifications (318). These HS modulating compounds inhibit HMPV infection in healthy bronchial epithelial cells (Fig. 15) and tissues (Fig. 16). To determine if HMPV infection can be inhibited by O-sulfated K5 derivatives in CFBE cells, CFBE cells were infected with HMPV pretreated with the K5 polysaccharide derivatives, and infection was quantified by counting GFP-expressing cells by flow cytometry. As previously shown for BEAS-2B cells (Fig. 15B), the O-sulfated K5 derivatives inhibited HMPV infection CFBE cells (Fig. 27B). Taken together, these results suggest HMPV infection in CFBE cells did depend on interaction with HS as was observed for normal airway cells and HS modulation is a potential antiviral strategy to prevent HMPV infection in CF patients also.

Enhanced HMPV infection is not a result of more particle binding

Greater HMPV infection was observed in CFBE cells compared to other cell types (Fig. 24). This may be a result of increased particle binding or other more complex factors that affect virus infection, such as transcription efficiency or protein trafficking during replication and assembly. HMPV is known to bind HS to infect non-CF cells (79) and our results suggest HS is also a required factor for HMPV infection in CFBE cells (Fig. 27). Increased sulfation and increased concentration of glycosaminoglycans, including HS, have been shown in bronchi-alveolar fluid from children with CF, compared to non-CF controls (404). Thus, it possible CFBE cells express more HS at the plasma membrane, leading to greater HMPV binding and infection. To determine if CFBE cells bind HMPV more efficiently than normal bronchial epithelial cells, HMPV was added to BEAS-2B or CFBE cells at 4°C, allowing for binding to occur but not infection, and the amount of bound virus was quantified by detection of the HMPV matrix protein present in cell lysates and β -actin as a loading control, by Western blot. The detected bound protein was compared to the input. Surprisingly, HMPV binding was about 3-fold less efficient in CFBE cells compared BEAS-2B cells (Fig. 28). Thus, increased binding was not able to account for the greater infectivity observed in the CFBE cells.

Discussion

A comparison of infection efficiency of HMPV, RSV, and PIV5 revealed selective increased permissiveness in CFBE cells to HMPV infection (Fig. 24) and complete resistance to PIV5 infection (Fig. 26). HMPV infection in CFBE cells did require HS (Fig. 27A) and was blocked by O-sulfated K5 polysaccharide derivatives (Fig. 27B). These results suggest loss of CFTR in the plasma membrane results in a unique pathophysiology that primes CFBE cells to HMPV specifically.

It is not clear why HMPV infection is enhanced in CFBE cells compared to normal human lung cells. It is possible that low pH contributes to HMPV infection in CFBE cells. The fusion protein of HMPV carries out an essential step in viral infection to bind and fuse the viral envelope with the target cells, and fusion proteins from many strains of HMPV can be triggered to fuse by low pH (134, 136)(Fig). The rgHMPV virus used in these studies is derived from strain CAN97-83 (A2) and the F protein from this strain is triggered to fuse by low pH. It has been well documented that the apical surface of the airway in CF lungs is acidic (405-407). CFTR itself functions as a chloride and bicarbonate exchanger, and without CFTR, there is a decrease in bicarbonate efflux, contributing to lower pH extracellularly. Furthermore, CFTR has a regulatory influence on the adjacent Na⁺/H⁺ exchanger, resulting in suppression of its activity, thus reducing proton efflux. In the absence of functional CFTR, as is the case in CF, proton efflux is not inhibited resulting in further extracellular acidification. Therefore, it is possible the CFBE cells have an acidic microenvironment that contributes to enhanced HMPV infection. Low pH does not trigger the fusion proteins of RSV or PIV5 (222, 408, 409), providing a potential explanation of the increased permissiveness to HMPV infection.

Calcium signaling can play a role in viral infection (410) and may also contribute to HMPV infection (411). Unlike the matrix (M) proteins of other viruses, HMPV M has two calcium binding sites (412), suggesting cellular calcium plays an important role in HMPV infection. CFBE cells have an increased calcium concentration in the endoplasmic reticulum due to increased SERCA (Sarcoplasmic/Reticulum Ca²⁺ ATPase) pump activity and decreased PMCA (Plasma Membrane Ca²⁺ ATPase) activity (50). As a result, cytoplasmic calcium levels are lower in CFBE cells compared to rescued cells with normal CFTR expression. It remains to be shown if lower cytoplasmic calcium levels contribute to HMPV infection in CFBE cells. Furthermore, it is possible CFBE cells upregulate other calcium transport mechanisms to reach calcium homeostasis, and endocytosis is a means to increase calcium influx without PMCA activity, which is downregulated in CF (413). There is direct evidence HMPV enters cells by endocytosis (136, 282), and increased

endocytic uptake of calcium is a potential mechanism that allows for increased HMPV infection. RSV infects cells via micropinocytosis (304) and PIV5 is thought to fuse at the plasma membrane, both of which are entry mechanisms that would not be enhanced by endocytosis of calcium.

The CFBE cells were not permissive to PIV5 infection (Fig. 26). PIV5 requires sialic acid for binding (414), and CFBE have been shown to have altered sialylation, which may contribute to the resistance to infection. Decreased sialylation has been shown in CFBE cells (415). Furthermore, sialic acid chains expressed on CFBE cells have significantly reduced terminal sialic acid in the alpha-2,6 configuration (416). Viral specificity to bind alpha-2,6 sialic acid is a major determinant of tropism (417-419). Clinically, viruses that utilize sialic acid for binding, such as Influenza A and parainfluenza virus 3, have relatively low incidence of infection in CF patients compared to others (56, 397-400). Therefore, the specific reduction in terminal sialic acid in the alpha-2,6 configuration of CFBE cells may be a contributor to viral tropism and infection in CF patients.

HMPV has only recently become recognized as a pathogen of clinical importance. While it was discovered 15 years ago, there is evidence that HMPV has been causing respiratory disease since at least 1948, though it was often clinically mistaken for RSV infection. Results presented here suggest CFTR dysfunction specifically primes cells for HMPV infection, which has implications for CF patients. While there is no vaccine or established effective treatment for HMPV infection, it is important for clinicians to recognize HMPV may be a particularly important pathogen in this patient group.

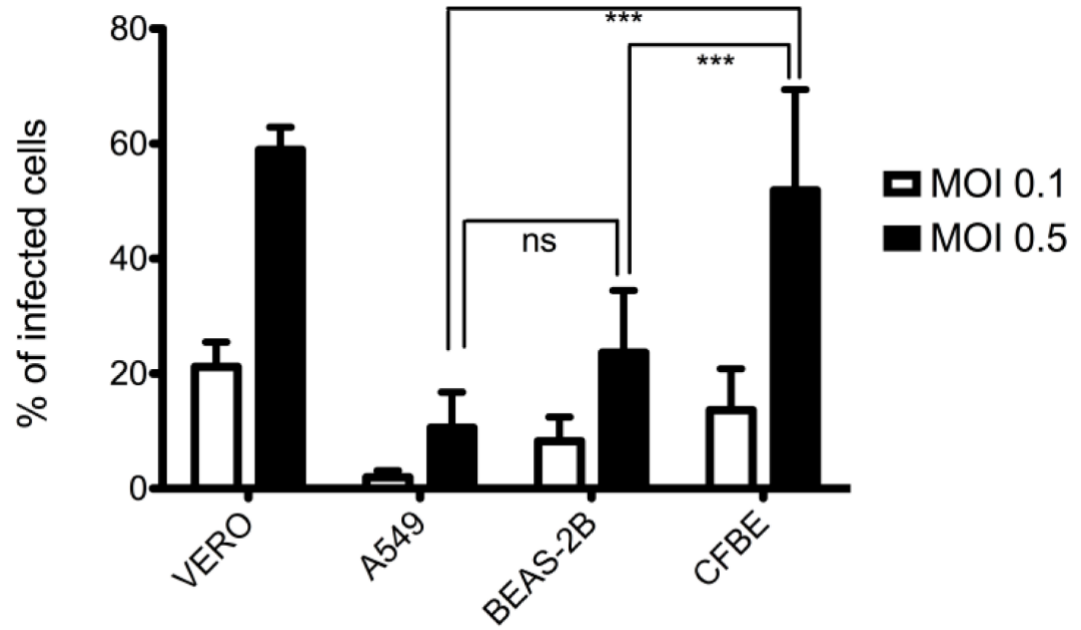


Figure 24. HMPV infection in Vero and human lung cells.

Cells were infected with rgHMPV at MOI 0.1 or 0.5 in duplicate and the percent of infected cells were determined by flow cytometry. Data points are means (+/- SD) of duplicate measurements, *** indicates statistically significant, $P < 0.001$ ($n=3$) using Bonferroni's Multiple Comparison Test (Prism).

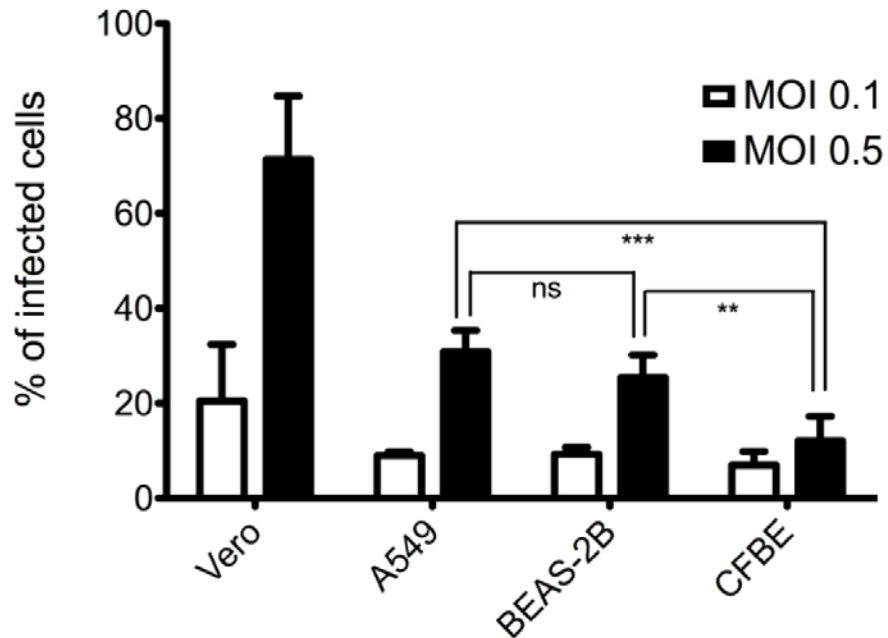


Figure 25. RSV infection in Vero and human lung cells.

Cells were infected with rgRSV at MOI 0.1 or 0.5 in duplicate and the percent of infected cells were determined by flow cytometry. Data points are means (+/- SD) of duplicate measurements, ** and *** indicate statistically significant, $P < 0.01$ and $P < 0.001$, respectively ($n=3$), using Bonferroni's Multiple Comparison Test (Prism).

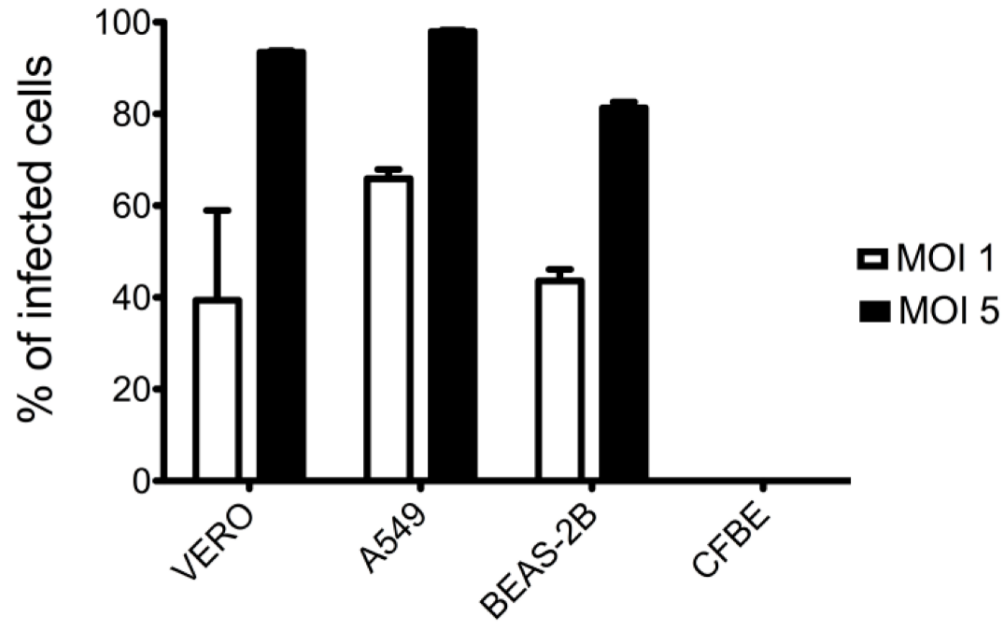


Figure 26. PIV5 infection in Vero and human lung cells.

Cells were infected with rgPIV5 at MOI 1 or 5 in duplicate and the percent of infected cells were determined by flow cytometry. Data points are means (+/- SD) of duplicate measurements (n=3).

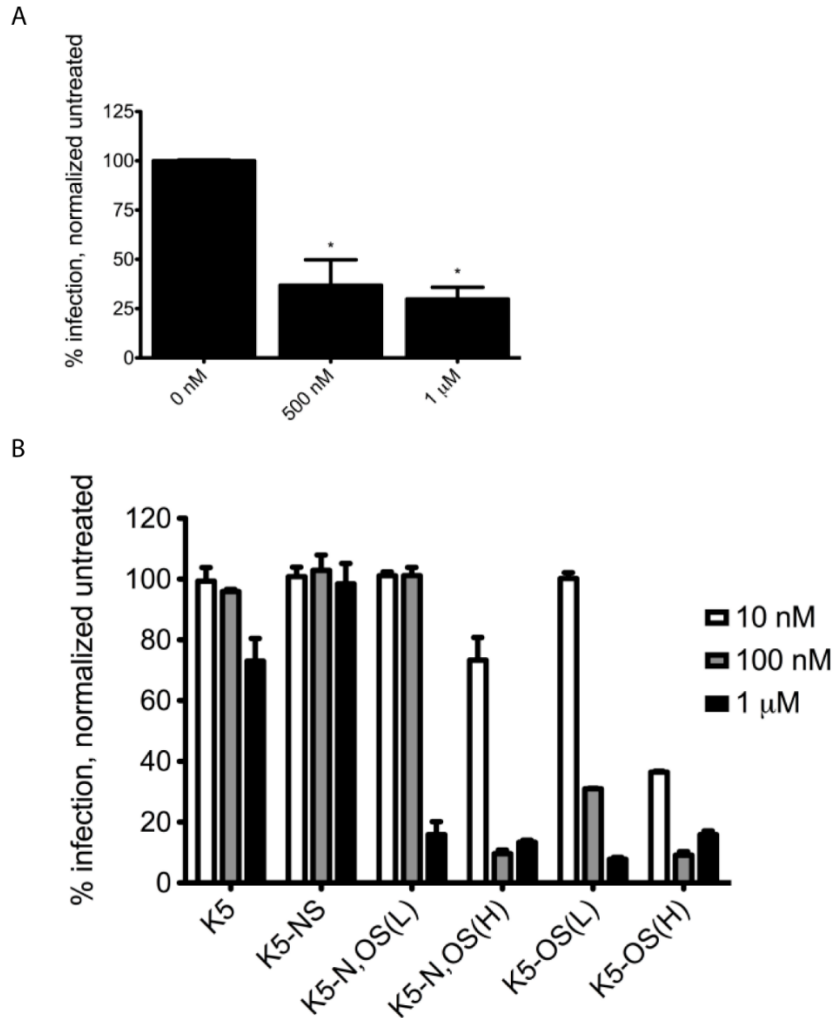


Figure 27. HS modulation inhibits HMPV infection in CFBE cells.

(A) CFBE cells were treated with SB105-A10 or vehicle for 1 hr at 37°C and infected with rgHMPV at MOI 1. Infection was quantified by flow cytometry. Percent infection is reported normalized to the untreated (0 nM). Data points are means (+/- SD) of duplicate measurements, * indicates statistically significant, $P < 0.05$ ($N = 3$). (B) CFBE cells were infected with rgHMPV that was pretreated with K5 polysaccharide derivatives (variable concentrations) or vehicle (untreated), and infection was quantified by flow cytometry. Percent infection is reported normalized to the untreated (0 nM). Data points are means (+/- SD) of duplicate measurements ($n = 2$).

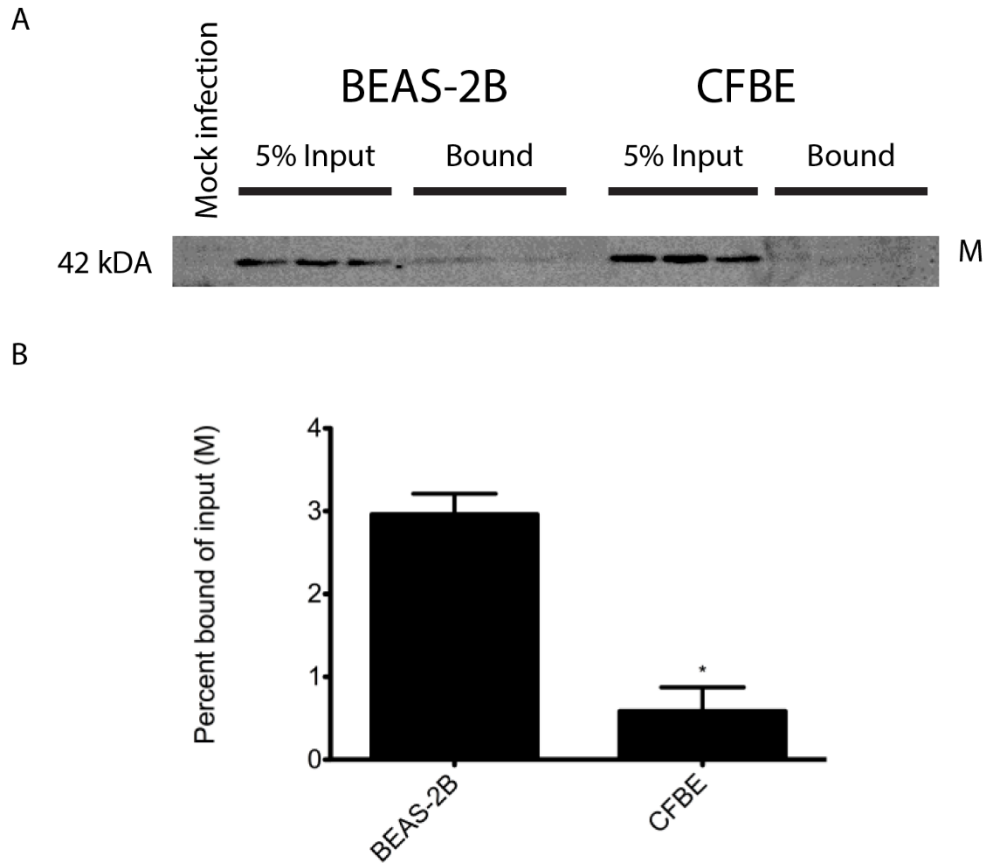


Figure 28. HMPV binding is not more efficient in CFBE cells.

(A) HMPV was added to BEAS-2B and CFBE cells for 2 hr at 4°C at MOI 1 in triplicate. After incubation, the cells were washed and lysed. Cell lysates were analyzed for HMPV matrix (M) protein by Western blot and compared to input virus. (B) Quantification of Western blot results, shown as percent bound M of input. * indicates statistically significant, $P < 0.05$ ($n=1$).

Chapter 7: Discussion and Future Directions

The body of work presented here contributes to our understanding of HMPV binding, fusion, and infection in humans. These results in this thesis provide new insight into some of the complexities of HMPV fusion protein function and characterized critical binding interactions. Finally, the work described has direct translational ramifications. Characterization of HMPV infection in cystic fibrosis revealed a potential vulnerability of this patient group to this pathogen. Taken together, these findings elucidate key features of the HMPV viral cycle, provide a foundation for antiviral development, and identify a vulnerable clinical population.

Complexity of fusion protein regulation and implications of acidic pH promoted fusion

Prior to the work in this thesis, a total of five HMPV F proteins had been analyzed for pH requirements to promote fusion (134, 136, 241, 242), and only CAN97-83 (A2) F has been characterized to be independent of its associated G protein (134), while the others were not evaluated for fusion activity in the presence of HMPV G. Cumulatively, low pH dependence, low pH independence, and failure to promote cell-to-cell fusion were all documented for different HMPV F proteins. Site directed mutagenesis at specific residues resulted in loss of fusion activity or changes from low pH dependence to independence, or vice versa. These results led to a hypothesis that low pH promoted fusion among HMPV F proteins is rare, unique to certain clade A, and requires the presence of specific residues, such as glycine 294 (241, 242). However, the results shown here demonstrate that HMPV F requirements for acidic pH are more complex (Chapter 3). We demonstrated cell-to-cell fusion promoted by TN83-1211 (B2) F and TN94-49 (A2), which does not have a glycine at position 294, can be triggered by low pH. These results demonstrate the challenges of understanding what contributes to low pH triggered fusion and its significance among all HMPV strains. Furthermore, two HMPV F proteins, from TN96-12 (A1) and NL/17/100 (A2) (241, 242), have been identified that fail to promote cell-to-cell fusion when expressed at the plasma membrane. However, both virus strains are capable of establishing productive infection (241, 242, 282), which suggests these F proteins require either additional viral factors, such as HMPV G or HMPV SH, or additional cellular factors, such as a specific receptor factor or unique lipid membrane composition available only in certain compartments (420), that are not present when the F proteins are expressed at the plasma membrane to promote fusion. These factors may regulate HMPV F activity through a number of potential mechanisms, and

acidic pH may still contribute to the triggering of these proteins, but is not sufficient when F is the only viral protein expressed at the plasma membrane. Because we are not able to determine if the HMPV F proteins that failed to promote cell-to-cell fusion were in the metastable prefusion conformation or the postfusion conformation, it is not clear if they require a stabilizing or triggering factor. The presence of an additional viral protein may contribute to either stabilizing the F protein to prevent premature triggering, or contribute to the triggering of the F protein. We plan to determine if HMPV G promotes cell-to-cell fusion of the HMPV F proteins analyzed in this thesis as a starting point to determine if G is required for other HMPV F.

Until recently, there was a simple, binary understanding of viral fusion and entry that was linked by the pH of fusion protein triggering. It was thought viruses with fusion proteins that are triggered independent of pH, at neutral pH, bind cell surface receptors and fuse the viral membrane with the plasma membrane (421). Viruses belonging to the *Retroviridae*, *Paramyxoviridae*, *Herpesviridae*, and *Coronaviridae* families typically initiate fusion in a pH-independent manner (215). On the other hand viruses with fusion proteins that can be triggered by exposure to acidic pH were thought to bind cell surface receptors and be taken up by endocytosis, where exposure to acidic pH in the maturing endosome would provide the necessary trigger to promote the fusion protein activity (421). Viruses belonging to the *Orthomyxoviridae*, *Togaviridae*, *Rhabdoviridae*, *Bunyaviridae*, and *Arenaviridae* families typically require a low-pH-mediated event for efficient fusion of viral and host cellular membranes (215). Because the fusion proteins of most paramyxoviruses to date can be triggered independently of pH, the entire *Paramyxoviridae* family of viruses was previously thought to fuse at the plasma membrane (421). However, this association has been challenged with our group's identification for the role of low pH in HMPV fusion protein activity (134, 136) as well as recent reports of more complex routes of entry for several viruses in the family. RSV can enter cells by macropinocytosis (304) and evidence suggests that New Castle Disease virus is taken up by endocytosis (286, 287). Recent studies also indicate that HMPV fusion can take place in endosomal compartments (282) after complex entry mediated in a dynamin- and clathrin- dependent endocytosis (136, 282). These findings have provided a biological context for the acidic pH to trigger HMPV F. Cox *et al.* reported that prototype strains in each clade (A1, A2, B1, B2) utilize endocytosis, however infection of only some strains was modestly inhibited by chemical interference of endosomal acidification (282). Interestingly, some of the same strains were used in these entry studies that we used to characterize fusion protein activity in Chapter 3. Treatment of cells with ammonium chloride, a

weak base that blocks vacuolar acidification, resulted in as much as a 50% reduction in infection of the A2 virus, which is TN94-49. Our analysis of TN94-49 F revealed acidic pH can promote the fusion activity of this HMPV F. However, ammonium chloride treatment failed to inhibit infection of the A1 virus, TN96-12. Low pH is insufficient to trigger the fusion activity of TN96-12 F, suggesting other factors are required which have not yet been identified. (We do not have information regarding the fusion proteins of the B1 and B2 viruses used in the endocytosis studies.) Therefore, there may be a correlation between low pH trigger during endocytosis and low pH promoted fusion in cell based assays that isolate the fusion protein. However, more complex regulation may be at play in the case of HMPV, than some other low pH-triggered viruses, such as VSV and influenza A, which can be completely blocked by ammonium chloride treatment (282, 315, 422, 423). Of the strains that have been analyzed, all HMPV particles require endocytosis to infect bronchial epithelial cells (282), however not all of the F proteins require low pH for fusion and infection of only some strains is inhibited by blocking acidification. Taken together, this suggests HMPV particles may escape the maturing endosome into the cytosol at different times depending on the requirement for low pH. Following endocytosis and pinching off the membrane, the endosomes travel towards the nucleus while the pH begins to decrease (424). Depending on pH requirements of the fusion protein of that virus particle, it is possible fusion can occur anywhere from early endosomes to endosomes. However, there is an advantage to viral escape in late endosomes closer to the nucleus, as this delays the antiviral response of the cell and has been shown to promote viral infection for other viruses that utilize endocytosis for entry. Furthermore, preliminary imaging of HMPV replication bodies has shown perinuclear localization.

Other HMPV glycoproteins, G and SH, may have more of a regulatory activity role in F activity than initially hypothesized from animal studies using recombinant HMPV lacking one or both of these proteins, as the strain employed in those studies utilized a low pH triggered F. Thus, the biological requirement for low pH in HMPV may vary depending on the interactions between the unique glycoproteins present in each strain of this virus. We hypothesize HMPV strains with F proteins that function independently from their complementary G may be more dependent on acidic pH to trigger fusion to escape the endosome, whereas those that require additional viral or cellular factors, such as TN96-12 (A2) F, not depend on acidic pH in the endosome to facilitate fusion. Whether this hypothesis holds true for HMPV entry remains to be determined.

Heparan sulfate proteoglycans as a potential receptor for HMPV

Heparan sulfate has been identified as a receptor for numerous viruses, whereas the other glycosaminoglycans are rarely implicated in virus-host interactions. HS is the most negatively charged due to the addition of sulfate groups, which has led to a hypothesis that nonspecific charge-charge interactions drive the attraction between diverse viral proteins and the sulfated polysaccharide on the surface of cells. However, our findings that O-sulfation is required to compete with HMVP binding to HS, suggest this is not entirely a simple charge interaction. Furthermore, it has been shown RSV has entirely different sulfation requirements for binding to HS, as N-sulfation is required while O-sulfation is dispensable (425). Thus, although a number of different viruses bind HS, likely due to prevalence of expression among mammalian tissues, they may not share the same mechanism mediating this interaction.

HS is found mainly on two families of cell surface proteins: syndecans and glypicans, and thus it is possible that a specific protein in one of these families may serve as a receptor for HMPV. Glypicans had not previously been identified as a receptor for a human virus until recently, when it was shown GPC-5 serves as a receptor for hepatitis B and hepatitis D viruses (204). Syndecans, on the other hand, have been identified to serve as an attachment factor for numerous viruses that bind HS. SDC-1 has been identified as an attachment factor for hepatitis C (172). SDC-2 and SDC-3 have been identified as receptors for Dengue virus (168) and HIV-1 (161), respectively. Because the different syndecan proteins are expressed in a cell-specific and tissue-specific manner, SDC-1 and SDC-4 are more likely to serve as an attachment factor for a respiratory virus due to their abundance in bronchial epithelial cells, among other tissues. On the other hand, SDC-2 and SDC-3 are enriched in the thymus and neurological tissues. Due to its expression in the human airway, SDC-1 serves a potential receptor or coreceptor HMPV. Anti-SDC-1 antibodies have shown to reduce RSV infection at the apical surface of HAE tissues (355). This is an approach that could be used to determine if SDC-1 also is specific for HMPV binding. SDC-4 is also a potential receptor for HMPV, based on its tissue expression and roles in endocytosis and integrin recycling. Ligand binding to SDC-4 has been shown to orchestrate the activation of GTPases to initiate endocytosis in a dynamin-dependent manner and recycling of $\alpha_5\beta_1$ -integrin (426). SDC-4 has been associated with cell-extracellular matrix junctions, suggesting these HSPGs may not be readily available for interaction with a virus particle.

In apical infection of HAE tissues, a critical step in the preparation of the tissues for infection was washes using lysophosphatidic choline (LPC). LPC is a complex, inverted cone-

shaped lipid naturally found in plasma membranes and as a pulmonary surfactant in low quantities (427, 428). LPC washes prior to HAE infection have been used for a number of viruses, and were first used for HMPV by another group (320). Without LPC, HMPV infection is delayed and less efficient in tissues. *In vivo*, LPC enhanced infection of adenovirus was observed in mouse (429), rabbit (430) and baboon lungs (431), acting as an adjuvant to increase lentivirus gene expression (432, 433). Treatment with LPC results in a decrease or loss of trans-epithelial resistance, potentially by disrupting cell-to-cell junctions (434). Taken together, this suggests LPC increases virus access to the airway cell surface receptors, which may only be available for binding at the apical surface at low levels prior to LPC treatment. Furthermore, transient disturbance of the epithelial barrier function may permit virus access to basolateral receptors or basal cells not normally exposed. For HMPV, apical infection of HAE tissues is enhanced by LPC, but apical infection can still occur without LPC washes of the apical surface. Even with LPC treatment, HMPV infection is primarily limited to the apical layer of HAE tissues. This suggests the required receptors are present at low numbers at the apical surface and disruption of the integrity of the epithelium with LPC increases their availability for binding, leading to greater efficiency of infection.

Sulfated polysaccharides as an antiviral strategy

Our results demonstrate the efficacy of sulfated polysaccharides to block binding and inhibit infection of HMPV. We propose such compounds may serve as a platform for antiviral development. Sulfated derivatives have been previously employed as an antiviral strategy in humans with limited success. Sulfated polysaccharides were first applied clinically to prevent infection of sexually transmitted viruses, such as HIV-1, HSV, and HPV. The phase III clinical trial for carrageenan-based Carraguard showed it did not reduce the risk of HIV infection (435, 436). However, Carraguard has been shown to protect women against high risk-HPV infection (437). Furthermore, carrageenan-based microbicides also appear to be promising to protect against HSV-2 infection (438). Therefore, carrageenan-based antivirals show great potential for clinical value.

Iota-carrageenan has been safely delivered in humans as a nasal spray to reduce viral infection in several clinical trials (341). Although the results did not demonstrate a reduction in symptoms or duration of illness, the delivery was limited to nasal epithelium and subjects began using the carrageenan spray only after experiencing the onset of symptoms. Therefore, it is likely viral infection had already spread to the upper respiratory tract beyond the nasal respiratory

epithelium. However, reduction in viral titer was observed in the treatment group, suggesting iota-carrageenan was efficacious to reduce viral replication. We propose such an antiviral strategy would be most effective as prophylaxis, before the onset of respiratory symptoms. While this would not be a practical approach for most individuals, those at risk to severe illness from HMPV may benefit greatly. This includes patients in elderly care facilities, hospitals, as well as immunocompromised patients, such as bone marrow or organ transplant recipients. Furthermore, aerosolized delivery of a sulfated polysaccharide such as iota-carrageenan would increase delivery to the lower respiratory tract. Thus, treatment of at-risk patients experiencing symptoms of upper respiratory tract infection may prevent the spread of virus to the lower airway, which is the main contributor of morbidity and mortality due to respiratory infection. Treatment with sulfated polysaccharides could protect at risk patients not only from HMPV infection, but potentially other respiratory viruses that utilize heparan sulfate for binding, including RSV (163, 176, 425), the leading cause of respiratory infection in children. Currently, there are no approved vaccines for either RSV or HMPV. Furthermore, high-risk premature infants receive monoclonal antibody therapy as prophylaxis for RSV infection, which is both costly and does not have established efficacy in clinical settings outside of controlled trials (439, 440), where the efficacy of palivizumab has been shown (441). Therefore, there are multiple patient groups that would benefit from a prophylactic therapy to reduce HMPV and RSV infection. Furthermore, iota-carrageenan has shown efficacy to inhibit influenza A (338) and rhinovirus infection (354).

Although our results suggest individuals with cystic fibrosis would benefit from HMPV prophylaxis, the consequences of sulfated polysaccharide delivery to upper or lower respiratory tract in these patients may propose unique risks. Sulfated polysaccharides contribute to chronic colonization and antibiotic resistance of *Pseudomonas aeruginosa* in cystic fibrosis patients. Heparan sulfate inhibits the killing of *P. aeruginosa* (442), possibly because heparan sulfate is incorporated in biofilms that protect the bacterial pathogen (384, 391, 394). However, other formulations may circumvent some of the unique challenges posed by introducing polysaccharides to cystic fibrosis lungs. Sulfated polysaccharides have been delivered in liposomes with efficacy to inhibit replication of some respiratory viruses (443). Thus, further studies are necessary, perhaps in the swine animal model of cystic fibrosis, to determine if sulfated polysaccharides would reduce viral infection or simply contribute to *P. aeruginosa* colonization.

The role of HMPV G in cellular actin recruitment

Cellular actin is often detected inside or associated with viral particles, suggesting it is packed during assembly. Incorporation of cellular actin into particles has been reported for many viruses, including HIV-1 (365), rabies virus (366), and Newcastle Disease virus (367). For RSV, β -actin and number of actin-related proteins have been found in the same sucrose gradient-purified fractions as RSV particles (444, 445), which has led to the hypothesis that cellular actin is used as a scaffold to propel filamentous viral to bud (368). However, RSV filament analysis for presence of actin associated proteins in the particles did not show incorporation of the proteins examined, although they were not analyzed for β -actin content (370). Numerous proteins of the actin cytoskeleton were found by mass spectrometry analysis of ultra-purified WT HMPV particles (El Najjar, *et al.*, submitted). There are sufficient levels of β -actin present that it can be visualized by Western blot analysis of virus samples. It was somewhat of an incidental finding when we observed no β -actin is present in samples of HMPV Δ G or HMPV Δ G Δ SH. These findings are still preliminary and further analysis is required to determine if this has any significant effect on infection or viral fitness. Recent work by Farah El Najjar has highlighted the role of the actin cytoskeleton in formation of cellular filaments and extensions thought to function as a mechanism of cell-to-cell spread. Thus, HMPV G may play a role in driving or regulating some of these processes. Previous studies with the recombinant HMPV Δ G or HMPV Δ G Δ SH in both *in vivo* and *in vitro* models have emphasized that they function similarly to WT HMPV, leading to questions about the roles of these additional proteins. The work presented here, both in regulation of binding and effects in actin incorporation, brings to attention some of the fine tuning these proteins may do during HMPV infection and essentially preserve their own necessity among HMPV viruses. Subtle effects on mediating binding, fusion, entry, particle assembly, and immune modulation under experimental conditions may translate to substantial advantages to maintain fitness in the population.

HMPV infection in cystic fibrosis

Our results showed a cystic fibrosis bronchial epithelial cell line had greater permissiveness to HMPV infection than RSV or PIV5. These findings suggest the loss of CFTR expression in the plasma membrane results in cellular changes that specifically enhance HMPV infection *in vitro*. To determine that it is the specific loss of CFTR expression that contributes to HMPV infectivity in this cell line, utilization of a cell line that has rescued CFTR should be explored.

We would expect to see a decrease in HMPV infection in these cells compared to the native CFBE cells. Furthermore, we can use silencing RNA approaches to knock-down CFTR expression in healthy human bronchial epithelial cells to determine if HMPV infection is enhanced. Several hypotheses are discussed in Chapter 6 for potential mechanisms of increased HMPV infection, including acidic microenvironments, calcium dysregulation and uptake, and increased expression of HSPGs. Additionally, there is evidence loss of CFTR leads to deregulation of the actin cytoskeleton (446). HMPV utilizes the actin cytoskeleton to promote egress and spread (El Najjar, submitted). It is possible that actin cytoskeleton deregulation in CFBE cells contributes to more efficient HMPV infection.

While our results suggested increased binding was not the mechanism of increased infectivity in CFBE cells compared to normal bronchial epithelial cells, it is not clear what the mechanism of increased infectivity may be. We plan to examine replication of HMPV in CFBE cells using a novel technique developed by Nicolás Cifuentes to visualize replication bodies using fluorescent *in situ* hybridization (FISH) to detect viral genomes and messenger RNA transcripts. HMPV infection in BEAS-2B cells results in formation of perinuclear replication bodies where viral genomes are being replicated and transcribed (unpublished data). These replication bodies vary in size and number, from one to several per cell, and can travel between cells through intercellular extensions (unpublished data). It is possible HMPV genome transcription and replication is more efficient in CFBE cells, which may result in detection of replication bodies at earlier time points post-infection, more replication bodies per cell, or larger replication bodies. It also remains to be determined if HMPV may replicate to higher titers in CFBE cells.

The studies in CFBE cells were done with a recombinant virus that results in GFP expression that is based on strain CAN97-83 (A2). It is not known at this time if CFBE permissiveness will be observed to other strains of HMPV. Furthermore, the fusion protein of CAN97-83 can be promoted to fuse by acidic pH. It is not known what role this may have in enhanced infection in CFBE cells, which have acidic pH at the plasma membrane. Additionally, one of the paramyxoviruses used in these studies, PIV5, does not cause disease in humans, although most individuals have antibodies to this virus (18). However, it typically infects human cell lines efficiently, which contributed to the unexpected findings in CFBE cells. Thus, it would contribute to our understanding of viral infection in cystic fibrosis to additionally characterize other viruses commonly linked to cystic fibrosis exacerbation, including HRV, parainfluenza viruses 1 and 3, and influenza A. We hypothesize alteration in terminal sialic acid composition

results in resistance to PIV5 infection in CFBE cells, which could have implications for other sialic acid-binding viruses in endogenous infection in these patients.

HMPV propagation *in vitro* and future analysis of clinical strains

RNA viruses rapidly adapt to the available host environment, often due to error prone polymerases that lack proof-reading mechanisms. As a result, *in vitro* propagation of RNA viruses originally isolated from ill patients may result in changes that promote efficient growth and replication in immortalized cells. We have identified critical virus-host interactions using primarily HMPV strain CAN97-83, one of the best characterized strains of HMPV. In order to broaden the understanding of HMPV life cycle and identify any strain-to-strain differences, we plan to incorporate not only additional strains, some of which have been already noted in this dissertation, but also new clinical isolates of HMPV from sick children at the University of Kentucky Children's Hospital. To date, we have confirmed the presence of HMPV in 15 clinical isolates. Future studies with these novel strains include sequence analysis of genomes, characterization of dependency of HS for binding, and efficacy of apical infection in HAE tissues.

Conclusion

This body of work contributes to our understanding of the life cycle of HMPV. We characterized critical aspects HMPV F protein triggering by low pH, which has biological relevance for endocytic entry. Analysis of F proteins from phylogenetically diverse HMPV strains demonstrated low pH triggered fusion, challenging previously thought requirements, and led to the identification of a critical residue that enhances low pH promoted fusion. These results support our hypothesis that electrostatic interactions play a key role in HMPV F triggering by low pH and further elucidate the complexity of viral fusion proteins. We characterized the key features of the binding interaction between HMPV and HSPGs using heparan sulfate mimetics, identifying an important sulfate modification, and demonstrate that these interactions occur at the apical surface of polarize airways tissues. These results significantly advance our understanding of HMPV infection in the human airway and identify an antiviral strategy. Furthermore, in our analysis of HMPV F mediated binding to HSPGs, we identified regulatory roles of HMPV glycoproteins G and SH that affect binding mediated by F and a potential novel function for HMPV G in actin recruitment. These results contribute to our understanding of the HMPV G and SH, which often do not share the same functional roles of analogous proteins found in viruses of the same family.

Furthermore, our results identified a potential specific susceptibility to HMPV infection in cystic fibrosis cells, which has not been previously reported. Therefore, the work presented here contributes to our understanding of HMPV infection over a broad breadth, from mechanisms of early events of entry to a clinical model of chronic respiratory disease.

Appendix I: Abbreviations Used in this Document

6-HB	Six-helix bundle
AMPV	Avian metapneumovirus
ATCC	American Type Culture Collection
CF	Cystic fibrosis
CFBE	Cystic fibrosis bronchial epithelium
CFTR	Cystic fibrosis conductance regulator
ER	Endoplasmic Reticulum
F	Fusion
FBS	Fetal Bovine Serum
FP	Fusion peptide
GAG	Glycosaminoglycan
GFP	Green fluorescent protein
GPI	Glycophosphatidylinositol
HAE	Human airway epithelium
HeV	Hendra virus
HEV	Hepatitis E virus
HIV	Human immunodeficiency virus
HMPV	Human metapneumovirus
HN/G/H	Paramyxovirus attachment protein
HPI	Hours post-infection
HPIV1	Human parainfluenza virus 1
HPV	Human papilloma virus
HRA	Heptad repeat A
HRB	Heptad repeat B
HRV	Human rhinovirus
HS	Heparan sulfate
HSPG	Heparan sulfate proteoglycans
HSV-1	Herpes simplex virus 1
HTLV-1	Human T-cell leukemia virus 1
M	Matrix protein
MeV	Measles virus
MOI	Multiplicity of infection
MTT	(3-(4,5-Dimethylthiazol-2-yl)-2,5-Diphenyltetrazolium Bromide)

NiV	Nipah virus
P	Phosphoprotein
P/S	Penicillin/Streptomycin
PAGE	Polyacrylamide gel electrophoresis
PI3K	Phosphoinositide 3 – kinase
PIV3	Parainfluenza virus 3
PIV5	Parainfluenza virus 5
PKC	Protein kinase C
PMCA	Plasma membrane calcium ATPase
PVDF	Polyvinylidene flouride
RSV	Respiratory Syncytial virus
SDC	Syndecan
SERCA	Sarco/endoplasmic reticulum calcium ATPase
SeV	Sendai virus
SH	Small hydrophobic protein
SPG	Sucrose phosphate glutamate
TM	Transmembrane domain
VLP	Virus-like particle
VSV	Vesicular stomatitis virus
WT	Wild type

References

1. **Phadke VK, Bednarczyk RA, Salmon DA, Omer SB.** 2016. Association between vaccine refusal and vaccine-preventable diseases in the united states: A review of measles and pertussis. *JAMA* **315**:1149-1158.
2. **Nair H, Nokes DJ, Gessner BD, Dherani M, Madhi SA, Singleton RJ, O'Brien KL, Roca A, Wright PF, Bruce N, Chandran A, Theodoratou E, Sutanto A, Sedyaningsih ER, Ngama M, Munywoki PK, Kartasasmita C, Simões EAF, Rudan I, Weber MW, Campbell H.** 2010. Global burden of acute lower respiratory infections due to respiratory syncytial virus in young children: a systematic review and meta-analysis. *The Lancet* **375**:1545-1555.
3. **Hall CB, Weinberg GA, Iwane MK, Blumkin AK, Edwards KM, Staat MA, Auinger P, Griffin MR, Poehling KA, Erdman D, Grijalva CG, Zhu Y, Szilagyi P.** 2009. The Burden of Respiratory Syncytial Virus Infection in Young Children. *New England Journal of Medicine* **360**:588-598.
4. **Lozano R, Naghavi M, Foreman K, Lim S, Shibuya K, Aboyans V, Abraham J, Adair T, Aggarwal R, Ahn SY, Alvarado M, Anderson HR, Anderson LM, Andrews KG, Atkinson C, Baddour LM, Barker-Collo S, Bartels DH, Bell ML, Benjamin EJ, Bennett D, Bhalla K, Bikbov B, Bin Abdulhak A, Birbeck G, Blyth F, Bolliger I, Boufous S, Bucello C, Burch M, Burney P, Carapetis J, Chen H, Chou D, Chugh SS, Coffeng LE, Colan SD, Colquhoun S, Colson KE, Condon J, Connor MD, Cooper LT, Corriere M, Cortinovis M, de Vaccaro KC, Couser W, Cowie BC, Criqui MH, Cross M, Dabhadkar KC, Dahodwala N, De Leo D, Degenhardt L, Delossantos A, Denenberg J, Des Jarlais DC, Dharmaratne SD, Dorsey ER, Driscoll T, Duber H, Ebel B, Erwin PJ, Espindola P, Ezzati M, Feigin V, Flaxman AD, Forouzanfar MH, Fowkes FG, Franklin R, Fransen M, Freeman MK, Gabriel SE, Gakidou E, Gaspari F, Gillum RF, Gonzalez-Medina D, Halasa YA, Haring D, Harrison JE, Havmoeller R, Hay RJ, Hoen B, Hotez PJ, Hoy D, Jacobsen KH, James SL, Jasrasaria R, Jayaraman S, Johns N, Karthikeyan G, Kassebaum N, Keren A, Khoo JP, Knowlton LM, Kobusingye O, Koranteng A, Krishnamurthi R, Lipnick M, Lipshultz SE, Ohno SL, Mabweijano J, MacIntyre MF, Mallinger L, March L, Marks GB, Marks R, Matsumori A, Matzopoulos R, Mayosi BM, McAnulty JH, McDermott MM, McGrath J, Mensah GA, Merriman TR, Michaud C, Miller M, Miller TR, Mock C, Mocumbi AO, Mokdad AA, Moran A, Mulholland K, Nair MN, Naldi L, Narayan KM, Nasseri K, Norman P, O'Donnell M, Omer SB, Ortblad K, Osborne R, Ozgediz D, Pahari B, Pandian JD, Rivero AP, Padilla RP, Perez-Ruiz F, Perico N, Phillips D, Pierce K, Pope CA, 3rd, Porrini E, Pourmalek F, Raju M, Ranganathan D, Rehm JT, Rein DB, Remuzzi G, Rivara FP, Roberts T, De Leon FR, Rosenfeld LC, Rushton L, Sacco RL, Salomon JA, Sampson U, Sanman E, Schwebel DC, Segui-Gomez M, Shepard DS, Singh D, Singleton J, Sliwa K, Smith E, Steer A, Taylor JA, Thomas B, Tleyjeh IM, Towbin JA, Truelsen T, Undurraga EA, Venketasubramanian N, Vijayakumar L, Vos T, Wagner GR, Wang M, Wang W, Watt K, Weinstock MA, Weintraub R, Wilkinson JD, Woolf AD, Wulf S, Yeh PH, Yip P, Zabetian A, Zheng ZJ, Lopez AD, Murray CJ, AlMazroa MA, Memish ZA.** 2012. Global and regional mortality from 235 causes of death for 20 age groups in 1990 and 2010: a systematic analysis for the Global Burden of Disease Study 2010. *Lancet* **380**:2095-2128.
5. **Nair H, Nokes DJ, Gessner BD, Dherani M, Madhi SA, Singleton RJ, O'Brien KL, Roca A, Wright PF, Bruce N, Chandran A, Theodoratou E, Sutanto A, Sedyaningsih ER, Ngama M, Munywoki PK, Kartasasmita C, Simoes EA, Rudan I, Weber MW, Campbell H.** 2010.

- Global burden of acute lower respiratory infections due to respiratory syncytial virus in young children: a systematic review and meta-analysis. *Lancet* **375**:1545-1555.
6. **Apalsch AM, Green M, Ledesma-Medina J, Nour B, Wald ER.** 1995. Parainfluenza and influenza virus infections in pediatric organ transplant recipients. *Clin Infect Dis* **20**:394-399.
 7. **Don M, Korppi M, Valent F, Vainionpaa R, Canciani M.** 2008. Human metapneumovirus pneumonia in children: results of an Italian study and mini-review. *Scandinavian journal of infectious diseases* **40**:821-826.
 8. **Vainionpaa R, Hyypia T.** 1994. Biology of parainfluenza viruses. *Clin Microbiol Rev* **7**:265-275.
 9. **Young PL, Halpin K, Selleck PW, Field H, Gravel JL, Kelly MA, Mackenzie JS.** 1996. Serologic evidence for the presence in Pteropus bats of a paramyxovirus related to equine morbillivirus. *Emerg Infect Dis* **2**:239-240.
 10. **Olson JG, Rupprecht C, Rollin PE, An US, Niezgodka M, Clemins T, Walston J, Ksiazek TG.** 2002. Antibodies to Nipah-like virus in bats (*Pteropus lylei*), Cambodia. *Emerg Infect Dis* **8**:987-988.
 11. **Selvey LA, Wells RM, McCormack JG, Ansford AJ, Murray K, Rogers RJ, Lavercombe PS, Selleck P, Sheridan JW.** 1995. Infection of humans and horses by a newly described morbillivirus. *The Medical journal of Australia* **162**:642-645.
 12. **Rockx B, Winegar R, Freiberg AN.** 2012. Recent progress in henipavirus research: molecular biology, genetic diversity, animal models. *Antiviral Res* **95**:135-149.
 13. **Bellini WJ, Harcourt BH, Bowden N, Rota PA.** 2005. Nipah virus: an emergent paramyxovirus causing severe encephalitis in humans. *J Neurovirol* **11**:481-487.
 14. **Sherrini BA, Chong TT.** 2014. Nipah encephalitis - an update. *The Medical journal of Malaysia* **69 Suppl A**:103-111.
 15. **Wong K.** 2010. Emerging epidemic viral encephalitides with a special focus on henipaviruses. *Acta Neuropathologica* **120**:317-325.
 16. **Hsiung GD.** 1972. Parainfluenza-5 virus. Infection of man and animal. *Progress in medical virology. Fortschritte der medizinischen Virusforschung. Progres en virologie medicale* **14**:241-274.
 17. **Tribe GW.** 1966. An investigation of the incidence, epidemiology and control of Simian virus 5. *British journal of experimental pathology* **47**:472-479.
 18. **Chatziandreou N, Stock N, Young D, Andrejeva J, Hagmaier K, McGeoch DJ, Randall RE.** 2004. Relationships and host range of human, canine, simian and porcine isolates of simian virus 5 (parainfluenza virus 5). *J Gen Virol* **85**:3007-3016.
 19. **Faisca P, Desmecht D.** 2007. Sendai virus, the mouse parainfluenza type 1: A longstanding pathogen that remains up-to-date. *Research in Veterinary Science* **82**:115-125.
 20. **Mebatsion T, Koolen MJM, de Vaan LTC, de Haas N, Braber M, Romer-Oberdorfer A, van den Elzen P, van der Marel P.** 2002. Newcastle Disease Virus (NDV) Marker Vaccine: an Immunodominant Epitope on the Nucleoprotein Gene of NDV Can Be Deleted or Replaced by a Foreign Epitope. *J. Virol.* **76**:10138-10146.
 21. **Govindarajan D, Buchholz UJ, Samal SK.** 2006. Recovery of Avian Metapneumovirus Subgroup C from cDNA: Cross-Recognition of Avian and Human Metapneumovirus Support Proteins. *J. Virol.* **80**:5790-5797.

22. **Larsen L, Tegtmeier C, Pedersen E.** 2001. Bovine Respiratory Syncytial Virus (BRSV) Pneumonia in Beef Calf Herds Despite Vaccination. *Acta Veterinaria Scandinavica* **42**:113 - 121.
23. **Maganga GD, Bourgarel M, Obame Nkoghe J, N'Dilimabaka N, Drosten C, Paupy C, Morand S, Drexler JF, Leroy EM.** 2014. Identification of an unclassified paramyxovirus in *Coleura afra*: a potential case of host specificity. *PLoS One* **9**:e115588.
24. **Lamb RA, Parks GD.** 2007. *Paramyxoviridae*: the viruses and their replication, p. 1449 - 1646. In Knipe DM, Howley PM (ed.), *Fields Virology* (Fifth Edition), vol. 1. Lippincott Williams & Wilkins, Philadelphia, PA.
25. **Clark HF, Lief FS, Lunger PD, Waters D, Leloup P, Foelsch DW, Wyler RW.** 1979. Fer de Lance virus (FDLV): a probable paramyxovirus isolated from a reptile. *J Gen Virol* **44**:405-418.
26. **Kurath G, Batts WN, Ahne W, Winton JR.** 2004. Complete genome sequence of Fer-de-Lance virus reveals a novel gene in reptilian paramyxoviruses. *J Virol* **78**:2045-2056.
27. **Papp T, Gal J, Abbas MD, Marschang RE, Farkas SL.** 2013. A novel type of paramyxovirus found in Hungary in a masked water snake (*Homalopsis buccata*) with pneumonia supports the suggested new taxonomy within the Ferlavirus genus. *Veterinary microbiology* **162**:195-200.
28. **Hamelin ME, Abed Y, Boivin G.** 2004. Human metapneumovirus: a new player among respiratory viruses. *Clin Infect Dis* **38**:983-990.
29. **Mejias A, Chavez-Bueno S, Ramilo O.** 2004. Human metapneumovirus: a not so new virus. *Pediatr Infect Dis J* **23**:1-7; quiz 8-10.
30. **van den Hoogen BG, Osterhaus DM, Fouchier RA.** 2004. Clinical impact and diagnosis of human metapneumovirus infection. *The Pediatric infectious disease journal* **23**:S25-32.
31. **van den Hoogen BG, de Jong JC, Groen J, Kuiken T, de Groot R, Fouchier RA, Osterhaus AD.** 2001. A newly discovered human pneumovirus isolated from young children with respiratory tract disease. *Nature medicine* **7**:719-724.
32. **van den Hoogen BG, Herfst S, Sprong L, Cane PA, Forleo-Neto E, de Swart RL, Osterhaus AD, Fouchier RA.** 2004. Antigenic and genetic variability of human metapneumoviruses. *Emerg Infect Dis* **10**:658-666.
33. **Huck B, Gesa Scharf, Dieter Neumann-Haefelin, Wolfram Puppe, Josef Weigl, and Valeria Falcone.** 2006. Novel Human Metapneumovirus Sublineage. *Emerging Infectious Diseases* **12**:147-150.
34. **Peret TC, Boivin G, Li Y, Couillard M, Humphrey C, Osterhaus AD, Erdman DD, Anderson LJ.** 2002. Characterization of human metapneumoviruses isolated from patients in North America. *J Infect Dis* **185**:1660-1663.
35. **Bouscambert-Duchamp M, Lina B, Trompette A, Moret H, Motte J, Andreoletti L.** 2005. Detection of Human Metapneumovirus RNA Sequences in Nasopharyngeal Aspirates of Young French Children with Acute Bronchiolitis by Real-Time Reverse Transcriptase PCR and Phylogenetic Analysis. *J. Clin. Microbiol.* **43**:1411-1414.
36. **Mackay IM, Bialasiewicz S, Jacob KC, McQueen E, Arden KE, Nissen MD, Sloots TP.** 2006. Genetic Diversity of Human Metapneumovirus over 4 Consecutive Years in Australia. *Journal of Infectious Diseases* **193**:1630-1633.
37. **Defrasnes C, Hamelin ME, Boivin G.** 2007. Human metapneumovirus. *Semin Respir Crit Care Med* **28**:213-221.
38. **Kahn JS.** 2006. Epidemiology of human metapneumovirus. *Clin Microbiol Rev* **19**:546-557.

39. **Greensill J, McNamara PS, Dove W, Flanagan B, Smyth RL, Hart CA.** 2003. Human metapneumovirus in severe respiratory syncytial virus bronchiolitis. *Emerg Infect Dis* **9**:372-375.
40. **McNamara PS, Flanagan BF, Smyth RL, Hart CA.** 2007. Impact of human metapneumovirus and respiratory syncytial virus co-infection in severe bronchiolitis. *Pediatr Pulmonol* **42**:740-743.
41. **Seemple MG, Cowell A, Dove W, Greensill J, McNamara PS, Halfhide C, Shears P, Smyth RL, Hart CA.** 2005. Dual infection of infants by human metapneumovirus and human respiratory syncytial virus is strongly associated with severe bronchiolitis. *J Infect Dis* **191**:382-386.
42. **Anderson EJ, Simoes EA, Buttery JP, Dennehy PH, Domachowske JB, Jensen K, Lieberman JM, Losonsky GA, Yogev R.** 2012. Prevalence and Characteristics of Human Metapneumovirus Infection Among Hospitalized Children at High Risk for Severe Lower Respiratory Tract Infection. *Journal of the Pediatric Infectious Diseases Society* **1**:212-222.
43. **Boivin G, De Serres G, Cote S, Gilca R, Abed Y, Rochette L, Bergeron MG, Dery P.** 2003. Human metapneumovirus infections in hospitalized children. *Emerg Infect Dis* **9**:634-640.
44. **Esper F, Boucher D, Weibel C, Martinello RA, Kahn JS.** 2003. Human metapneumovirus infection in the United States: clinical manifestations associated with a newly emerging respiratory infection in children. *Pediatrics* **111**:1407-1410.
45. **Esper F, Martinello RA, Boucher D, Weibel C, Ferguson D, Landry ML, Kahn JS.** 2004. A 1-year experience with human metapneumovirus in children aged <5 years. *J Infect Dis* **189**:1388-1396.
46. **Hasvold J, Sjoding M, Pohl K, Cooke C, Hyzy RC.** 2016. The role of human metapneumovirus in the critically ill adult patient. *Journal of critical care* **31**:233-237.
47. **Nicholson KG, Kent J, Hammersley V, Cancio E.** 1997. Acute viral infections of upper respiratory tract in elderly people living in the community: comparative, prospective, population based study of disease burden. *BMJ* **315**:1060-1064.
48. **Louie JK, Schnurr DP, Pan CY, Kiang D, Carter C, Tougaw S, Ventura J, Norman A, Belmusto V, Rosenberg J, Trochet G.** 2007. A summer outbreak of human metapneumovirus infection in a long-term-care facility. *J Infect Dis* **196**:705-708.
49. **Boivin G, De Serres G, Hamelin ME, Cote S, Argouin M, Tremblay G, Maranda-Aubut R, Sauvageau C, Ouakki M, Boulianne N, Couture C.** 2007. An outbreak of severe respiratory tract infection due to human metapneumovirus in a long-term care facility. *Clin Infect Dis* **44**:1152-1158.
50. **Falsey AR, Erdman D, Anderson LJ, Walsh EE.** 2003. Human metapneumovirus infections in young and elderly adults. *J Infect Dis* **187**:785-790.
51. **Falsey AR.** 2008. Human metapneumovirus infection in adults. *Pediatric Infectious Disease Journal* **27**:S80-S83.
52. **Madhi SA, Ludewick H, Kuwanda L, van Niekerk N, Cutland C, Klugman KP.** 2007. Seasonality, incidence, and repeat human metapneumovirus lower respiratory tract infections in an area with a high prevalence of human immunodeficiency virus type-1 infection. *The Pediatric infectious disease journal* **26**:693-699.
53. **Ali M, Baker JM, Richardson SE, Weitzman S, Allen U, Abba O.** 2013. Human metapneumovirus (hMPV) infection in children with cancer. *Journal of pediatric hematology/oncology* **35**:444-446.

54. **Zwaans WA, Mallia P, van Winden ME, Rohde GG.** 2014. The relevance of respiratory viral infections in the exacerbations of chronic obstructive pulmonary disease-A systematic review. *J Clin Virol.*
55. **Ilvan A, Aslan G, Serin MS, Calikoglu M, Yilmaz FM, Tezcan S, Tas D, Ayrik C, Uygungul E, Sezer O, Emekdas G.** 2013. [Investigation of the presence of human metapneumovirus in patients with chronic obstructive pulmonary disease and asthma and its relationship with the attacks]. *Mikrobiyoloji bulteni* **47**:636-649.
56. **Asner S, Waters V, Solomon M, Yau Y, Richardson SE, Grasemann H, Gharabaghi F, Tran D.** 2012. Role of respiratory viruses in pulmonary exacerbations in children with cystic fibrosis. *Journal of cystic fibrosis : official journal of the European Cystic Fibrosis Society* **11**:433-439.
57. **de Boer K, Vandemheen KL, Tullis E, Doucette S, Fergusson D, Freitag A, Paterson N, Jackson M, Loughheed MD, Kumar V, Aaron SD.** 2011. Exacerbation frequency and clinical outcomes in adult patients with cystic fibrosis. *Thorax* **66**:680-685.
58. **Garcia DF, Hiatt PW, Jewell A, Schoonover SL, Cron SG, Riggs M, Grace S, Oermann CM, Piedra PA.** 2007. Human metapneumovirus and respiratory syncytial virus infections in older children with cystic fibrosis. *Pediatric pulmonology* **42**:66-74.
59. **Boivin G, Abed Y, Pelletier G, Ruel L, Moisan D, Cote S, Peret TC, Erdman DD, Anderson LJ.** 2002. Virological features and clinical manifestations associated with human metapneumovirus: a new paramyxovirus responsible for acute respiratory-tract infections in all age groups. *J Infect Dis* **186**:1330-1334.
60. **Hamelin ME, Prince GA, Gomez AM, Kinkead R, Boivin G.** 2006. Human metapneumovirus infection induces long-term pulmonary inflammation associated with airway obstruction and hyperresponsiveness in mice. *J Infect Dis* **193**:1634-1642.
61. **Tsukagoshi H, Ishioka T, Noda M, Kozawa K, Kimura H.** 2013. Molecular epidemiology of respiratory viruses in virus-induced asthma. *Front Microbiol* **4**:278.
62. **Schildgen O, Glatzel T, Geikowski T, Scheibner B, Matz B, Bindl L, Born M, Viazov S, Wilkesmann A, Knopfle G, Roggendorf M, Simon A.** 2005. Human metapneumovirus RNA in encephalitis patient. *Emerg Infect Dis* **11**:467-470.
63. **Hata M, Ito M, Kiyosawa S, Kimpara Y, Tanaka S, Yamashita T, Hasegawa A, Kobayashi S, Koyama N, Minagawa H.** 2007. A fatal case of encephalopathy possibly associated with human metapneumovirus infection. *Jpn J Infect Dis* **60**:328-329.
64. **Niizuma T, Okumura A, Kinoshita K, Shimizu T.** 2014. Acute encephalopathy associated with human metapneumovirus infection. *Jpn J Infect Dis* **67**:213-215.
65. **Fisher DL, Defres S, Solomon T.** 2015. Measles-induced encephalitis. *QJM : monthly journal of the Association of Physicians* **108**:177-182.
66. **Fox A, Hung TM, Wertheim H, Hoa le NM, Vincent A, Lang B, Waters P, Ha NH, Trung NV, Farrar J, Van Kinh N, Horby P.** 2013. Acute measles encephalitis in partially vaccinated adults. *PLoS One* **8**:e71671.
67. **Chakraborty A, Sazzad HM, Hossain MJ, Islam MS, Parveen S, Husain M, Banu SS, Podder G, Afroj S, Rollin PE, Daszak P, Luby SP, Rahman M, Gurley ES.** 2016. Evolving epidemiology of Nipah virus infection in Bangladesh: evidence from outbreaks during 2010-2011. *Epidemiology and infection* **144**:371-380.
68. **Ong KC, Wong KT.** 2015. Henipavirus Encephalitis: Recent Developments and Advances. *Brain pathology* **25**:605-613.

69. **Weinreich MA, Jabbar AY, Malguria N, Haley RW.** 2015. New-Onset Myocarditis in an Immunocompetent Adult with Acute Metapneumovirus Infection. *Case reports in medicine* **2015**:814269.
70. **Kearney MT, Cotton JM, Richardson PJ, Shah AM.** 2001. Viral myocarditis and dilated cardiomyopathy: mechanisms, manifestations, and management. *Postgraduate medical journal* **77**:4-10.
71. **Briand F-X, Henry A, Massin P, Jestin V.** 2012. Complete Genome Sequence of a Novel Avian Paramyxovirus. *Journal of Virology* **86**:7710-7710.
72. **Marschang RE, Papp T, Frost JW.** 2009. Comparison of paramyxovirus isolates from snakes, lizards and a tortoise. *Virus Res* **144**:272-279.
73. **Biacchesi S, Skiadopoulos MH, Boivin G, Hanson CT, Murphy BR, Collins PL, Buchholz UJ.** 2003. Genetic diversity between human metapneumovirus subgroups. *Virology* **315**:1-9.
74. **Karron RA, Buonagurio DA, Georgiu AF, Whitehead SS, Adamus JE, Clements-Mann ML, Harris DO, Randolph VB, Udem SA, Murphy BR, Sidhu MS.** 1997. Respiratory syncytial virus (RSV) SH and G proteins are not essential for viral replication in vitro: Clinical evaluation and molecular characterization of a cold-passaged, attenuated RSV subgroup B mutant. *Proceedings of the National Academy of Sciences* **94**:13961-13966.
75. **Lamb RA, Parks GD.** 2007. *Paramyxoviridae: The viruses and their replication*, p. 1449-1496. In Knipe DM, Howley PM (ed.), *Fields Virology*, Fifth ed. Lippincott, Williams and Wilkins, Philadelphia.
76. **Biacchesi S, Skiadopoulos MH, Yang L, Lamirande EW, Tran KC, Murphy BR, Collins PL, Buchholz UJ.** 2004. Recombinant human Metapneumovirus lacking the small hydrophobic SH and/or attachment G glycoprotein: deletion of G yields a promising vaccine candidate. *J Virol* **78**:12877-12887.
77. **Biacchesi S, Pham QN, Skiadopoulos MH, Murphy BR, Collins PL, Buchholz UJ.** 2005. Infection of nonhuman primates with recombinant human metapneumovirus lacking the SH, G, or M2-2 protein categorizes each as a nonessential accessory protein and identifies vaccine candidates. *J Virol* **79**:12608-12613.
78. **He B, Leser GP, Paterson RG, Lamb RA.** 1998. The paramyxovirus SV5 small hydrophobic (SH) protein is not essential for virus growth in tissue culture cells. *Virology* **250**:30-40.
79. **Chang A, Masante C, Buchholz UJ, Dutch RE.** 2012. Human metapneumovirus (HMPV) binding and infection are mediated by interactions between the HMPV fusion protein and heparan sulfate. *J Virol* **86**:3230-3243.
80. **Ling R, Sinkovic S, Toquin D, Guionie O, Eterradossi N, Easton AJ.** 2008. Deletion of the SH gene from avian metapneumovirus has a greater impact on virus production and immunogenicity in turkeys than deletion of the G gene or M2-2 open reading frame. *J Gen Virol* **89**:525-533.
81. **Bukreyev A, Whitehead SS, Murphy BR, Collins PL.** 1997. Recombinant respiratory syncytial virus from which the entire SH gene has been deleted grows efficiently in cell culture and exhibits site-specific attenuation in the respiratory tract of the mouse. *J. Virol.* **71**:8973-8982.
82. **Whitehead SS, Bukreyev A, Teng MN, Firestone CY, St Claire M, Elkins WR, Collins PL, Murphy BR.** 1999. Recombinant respiratory syncytial virus bearing a deletion of either the NS2 or SH gene is attenuated in chimpanzees. *J Virol* **73**:3438-3442.
83. **Buchholz UJ, Biacchesi S, Pham QN, Tran KC, Yang L, Luongo CL, Skiadopoulos MH, Murphy BR, Collins PL.** 2005. Deletion of M2 gene open reading frames 1 and 2 of

- human metapneumovirus: effects on RNA synthesis, attenuation, and immunogenicity. *J Virol* **79**:6588-6597.
84. **Fuentes S, Tran KC, Luthra P, Teng MN, He B.** 2007. Function of the Respiratory Syncytial Virus Small Hydrophobic Protein. *J. Virol.* **81**:8361-8366.
 85. **He B, Lin GY, Durbin JE, Durbin RK, Lamb RA.** 2001. The SH integral membrane protein of the paramyxovirus simian virus 5 is required to block apoptosis in MDBK cells. *J Virol* **75**:4068-4079.
 86. **Lin Y, Bright AC, Rothermel TA, He B.** 2003. Induction of apoptosis by paramyxovirus simian virus 5 lacking a small hydrophobic gene. *J Virol* **77**:3371-3383.
 87. **Xu P, Li Z, Sun D, Lin Y, Wu J, Rota PA, He B.** 2011. Rescue of wild-type mumps virus from a strain associated with recent outbreaks helps to define the role of the SH ORF in the pathogenesis of mumps virus. *Virology* **417**:126-136.
 88. **Bao X, Kolli D, Liu T, Shan Y, Garofalo RP, Casola A.** 2008. Human Metapneumovirus Small Hydrophobic Protein Inhibits NF- κ B Transcriptional Activity. *J. Virol.* **82**:8224-8229.
 89. **Wilson RL, Fuentes SM, Wang P, Taddeo EC, Klatt A, Henderson AJ, He B.** 2006. Function of Small Hydrophobic Proteins of Paramyxovirus. *J. Virol.* **80**:1700-1709.
 90. **van den Hoogen BG, Bestebroer TM, Osterhaus AD, Fouchier RA.** 2002. Analysis of the genomic sequence of a human metapneumovirus. *Virology* **295**:119-132.
 91. **Gonzalez ME, Carrasco L.** 2003. Viroporins. *FEBS Lett* **552**:28-34.
 92. **Masante C, El Najjar F, Chang A, Jones A, Moncman CL, Dutch RE.** 2014. The human metapneumovirus small hydrophobic protein has properties consistent with those of a viroporin and can modulate viral fusogenic activity. *J Virol* **88**:6423-6433.
 93. **Le Nouen C, Hillyer P, Brock LG, Winter CC, Rabin RL, Collins PL, Buchholz UJ.** 2014. Human metapneumovirus SH and G glycoproteins inhibit macropinocytosis-mediated entry into human dendritic cells and reduce CD4+ T cell activation. *J Virol* **88**:6453-6469.
 94. **Bowden TA, Crispin M, Harvey DJ, Jones EY, Stuart DI.** 2010. Dimeric Architecture of the Hendra Virus Attachment Glycoprotein: Evidence for a Conserved Mode of Assembly. *J. Virol.* **84**:6208-6217.
 95. **Crennell S, Takimoto T, Portner A, Taylor G.** 2000. Crystal structure of the multifunctional paramyxovirus hemagglutinin-neuraminidase. *Nat Struct Mol Biol* **7**:1068-1074.
 96. **Yuan P, Thompson TB, Wurzburg BA, Paterson RG, Lamb RA, Jardetzky TS.** 2005. Structural Studies of the Parainfluenza Virus 5 Hemagglutinin-Neuraminidase Tetramer in Complex with Its Receptor, Sialyllactose. *Structure* **13**:803-815.
 97. **Lawrence MC, Borg NA, Streltsov VA, Pilling PA, Epa VC, Varghese JN, McKimm-Breschkin JL, Colman PM.** 2004. Structure of the Haemagglutinin-neuraminidase from Human Parainfluenza Virus Type III. *Journal of Molecular Biology* **335**:1343-1357.
 98. **Hashiguchi T, Ose T, Kubota M, Maita N, Kamishikiyo J, Maenaka K, Yanagi Y.** 2011. Structure of the measles virus hemagglutinin bound to its cellular receptor SLAM. *Nat Struct Mol Biol* **18**:135-141.
 99. **Xu K, Rajashankar KR, Chan Y-P, Himanen JP, Broder CC, Nikolov DB.** 2008. Host cell recognition by the henipaviruses: Crystal structures of the Nipah G attachment glycoprotein and its complex with ephrin-B3. *Proceedings of the National Academy of Sciences* **105**:9953-9958.
 100. **Bose S, Welch BD, Kors CA, Yuan P, Jardetzky TS, Lamb RA.** 2011. Structure and Mutagenesis of the Parainfluenza Virus 5 Hemagglutinin-Neuraminidase Stalk Domain

- Reveals a Four-Helix Bundle and the Role of the Stalk in Fusion Promotion. *Journal of Virology* **85**:12855-12866.
101. **Plemper RK, Brindley MA, Iorio RM.** 2011. Structural and Mechanistic Studies of Measles Virus Illuminate Paramyxovirus Entry. *PLoS Pathog* **7**:e1002058.
 102. **Deng R, Wang Z, Mahon PJ, Marinello M, Mirza A, Iorio RM.** 1999. Mutations in the Newcastle disease virus hemagglutinin-neuraminidase protein that interfere with its ability to interact with the homologous F protein in the promotion of fusion. *Virology* **253**:43-54.
 103. **Deng R, Wang Z, Mirza AM, Iorio RM.** 1995. Localization of a domain on the paramyxovirus attachment protein required for the promotion of cellular fusion by its homologous fusion protein spike. *Virology* **209**:457-469.
 104. **Tanabayashi K, Compans RW.** 1996. Functional interaction of paramyxovirus glycoproteins: identification of a domain in Sendai virus HN which promotes cell fusion. *J. Virol.* **70**:6112-6118.
 105. **Melanson VR, Iorio RM.** 2006. Addition of N-Glycans in the Stalk of the Newcastle Disease Virus HN Protein Blocks Its Interaction with the F Protein and Prevents Fusion. *J. Virol.* **80**:623-633.
 106. **Zaitsev V, von Itzstein M, Groves D, Kiefel M, Takimoto T, Portner A, Taylor G.** 2004. Second Sialic Acid Binding Site in Newcastle Disease Virus Hemagglutinin-Neuraminidase: Implications for Fusion. *Journal of Virology* **78**:3733-3741.
 107. **Bousse TL, Taylor G, Krishnamurthy S, Portner A, Samal SK, Takimoto T.** 2004. Biological Significance of the Second Receptor Binding Site of Newcastle Disease Virus Hemagglutinin-Neuraminidase Protein. *Journal of Virology* **78**:13351-13355.
 108. **Porotto M, Fornabaio M, Kellogg GE, Moscona A.** 2007. A Second Receptor Binding Site on Human Parainfluenza Virus Type 3 Hemagglutinin-Neuraminidase Contributes to Activation of the Fusion Mechanism. *Journal of Virology* **81**:3216-3228.
 109. **Palermo LM, Porotto M, Greengard O, Moscona A.** 2007. Fusion Promotion by a Paramyxovirus Hemagglutinin-Neuraminidase Protein: pH Modulation of Receptor Avidity of Binding Sites I and II. *Journal of Virology* **81**:9152-9161.
 110. **Porotto M, Fornabaio M, Greengard O, Murrell MT, Kellogg GE, Moscona A.** 2006. Paramyxovirus Receptor-Binding Molecules: Engagement of One Site on the Hemagglutinin-Neuraminidase Protein Modulates Activity at the Second Site. *Journal of Virology* **80**:1204-1213.
 111. **Villar E, Barroso I.** 2006. Role of sialic acid-containing molecules in paramyxovirus entry into the host cell: A minireview. *Glycoconjugate Journal* **23**:5-17.
 112. **Muhlebach MD, Mateo M, Sinn PL, Prufer S, Uhlig KM, Leonard VH, Navaratnarajah CK, Frenzke M, Wong XX, Sawatsky B, Ramachandran S, McCray PB, Jr., Cichutek K, von Messling V, Lopez M, Cattaneo R.** 2011. Adherens junction protein nectin-4 is the epithelial receptor for measles virus. *Nature* **480**:530-533.
 113. **Noyce RS, Bondre DG, Ha MN, Lin LT, Sisson G, Tsao MS, Richardson CD.** 2011. Tumor cell marker PVRL4 (nectin 4) is an epithelial cell receptor for measles virus. *PLoS Pathog* **7**:e1002240.
 114. **Bonaparte MI, Dimitrov AS, Bossart KN, Crameri G, Mungall BA, Bishop KA, Choudhry V, Dimitrov DS, Wang LF, Eaton BT, Broder CC.** 2005. Ephrin-B2 ligand is a functional receptor for Hendra virus and Nipah virus. *Proc Natl Acad Sci U S A* **102**:10652-10657.

115. **Negrete OA, Wolf MC, Aguilar HC, Enterlein S, Wang W, Muhlberger E, Su SV, Bertolotti-Ciarlet A, Flick R, Lee B.** 2006. Two Key Residues in EphrinB3 Are Critical for Its Use as an Alternative Receptor for Nipah Virus. *PLoS Pathog* **2**:e7.
116. **Negrete OA, Levroney EL, Aguilar HC, Bertolotti-Ciarlet A, Nazarian R, Tajyar S, Lee B.** 2005. EphrinB2 is the entry receptor for Nipah virus, an emergent deadly paramyxovirus. *Nature* **436**:401-405.
117. **Krusat T, Streckert HJ.** 1997. Heparin-dependent attachment of respiratory syncytial virus (RSV) to host cells. *Arch Virol* **142**:1247-1254.
118. **Thammawat S, Sadlon TA, Hallsworth PG, Gordon DL.** 2008. Role of cellular glycosaminoglycans and charged regions of viral G protein in human metapneumovirus infection. *J. Virol.* **82**:11767-11774.
119. **Cseke G, Maginnis MS, Cox RG, Tollefson SJ, Podsiad AB, Wright DW, Dermody TS, Williams JV.** 2009. Integrin alphavbeta1 promotes infection by human metapneumovirus. *Proc Natl Acad Sci U S A* **106**:1566-1571.
120. **Cox RG, Livesay SB, Johnson M, Ohi MD, Williams JV.** 2012. The human metapneumovirus fusion protein mediates entry via an interaction with RGD-binding integrins. *J Virol* **86**:12148-12160.
121. **Tayyari F, Marchant D, Moraes TJ, Duan W, Mastrangelo P, Hegele RG.** 2011. Identification of nucleolin as a cellular receptor for human respiratory syncytial virus. *Nature medicine* **17**:1132-1135.
122. **Shingai M, Azuma M, Ebihara T, Sasai M, Funami K, Ayata M, Ogura H, Tsutsumi H, Matsumoto M, Seya T.** 2008. Soluble G protein of respiratory syncytial virus inhibits Toll-like receptor 3/4-mediated IFN-beta induction. *International Immunology* **20**:1169-1180.
123. **Takimoto T, Taylor GL, Connaris HC, Crennell SJ, Portner A.** 2002. Role of the Hemagglutinin-Neuraminidase Protein in the Mechanism of Paramyxovirus-Cell Membrane Fusion. *Journal of Virology* **76**:13028-13033.
124. **Yao Q, Hu X, Compans RW.** 1997. Association of the parainfluenza virus fusion and hemagglutinin-neuraminidase glycoproteins on cell surfaces. *J. Virol.* **71**:650-656.
125. **Stone-Hulslander J, Morrison TG.** 1997. Detection of an interaction between the HN and F proteins in Newcastle disease virus-infected cells. *J. Virol.* **71**:6287-6295.
126. **Lee JK, Prussia A, Paal T, White LK, Snyder JP, Plemper RK.** 2008. Functional Interaction between Paramyxovirus Fusion and Attachment Proteins. *Journal of Biological Chemistry* **283**:16561-16572.
127. **Plemper RK, Hammond AL, Gerlier D, Fielding AK, Cattaneo R.** 2002. Strength of Envelope Protein Interaction Modulates Cytopathicity of Measles Virus. *J. Virol.* **76**:5051-5061.
128. **Aguilar HC, Matreyek KA, Choi DY, Filone CM, Young S, Lee B.** 2007. Polybasic KKR motif in the cytoplasmic tail of Nipah virus fusion protein modulates membrane fusion by inside-out signaling. *J Virol* **81**:4520-4532.
129. **Porotto M, Palmer SG, Palermo LM, Moscona A.** 2012. Mechanism of Fusion Triggering by Human Parainfluenza Virus Type III: Communication Between Viral Glycoproteins During Entry. *Journal of Biological Chemistry* **287**:778-793.
130. **Porotto M, Murrell M, Greengard O, Moscona A.** 2003. Triggering of Human Parainfluenza Virus 3 Fusion Protein (F) by the Hemagglutinin-Neuraminidase (HN) Protein: an HN Mutation Diminishes the Rate of F Activation and Fusion. *Journal of Virology* **77**:3647-3654.

131. **Palermo LM, Porotto M, Yokoyama CC, Palmer SG, Mungall BA, Greengard O, Niewiesk S, Moscona A.** 2009. Human Parainfluenza Virus Infection of the Airway Epithelium: Viral Hemagglutinin-Neuraminidase Regulates Fusion Protein Activation and Modulates Infectivity. *Journal of Virology* **83**:6900-6908.
132. **Teng MN, Whitehead SS, Collins PL.** 2001. Contribution of the respiratory syncytial virus G glycoprotein and its secreted and membrane-bound forms to virus replication in vitro and in vivo. *Virology* **289**:283-296.
133. **Chang A, Masante C, Buchholz UJ, Dutch RE.** 2012. Human Metapneumovirus (HMPV) Binding and Infection Are Mediated by Interactions between the HMPV Fusion Protein and Heparan Sulfate. *Journal of Virology* **86**:3230-3243.
134. **Schowalter RM, Smith SE, Dutch RE.** 2006. Characterization of human metapneumovirus F protein-promoted membrane fusion: critical roles for proteolytic processing and low pH. *J. Virol.* **80**:10931-10941.
135. **Herfst S, Mas V, Ver LS, Wierda RJ, Osterhaus ADME, Fouchier RAM, Melero JA.** 2008. Low-pH-Induced membrane fusion mediated by human metapneumovirus F protein Is a rare, strain-dependent phenomenon. *J. Virol.* **82**:8891-8895.
136. **Schowalter RM, Chang A, Robach JG, Buchholz UJ, Dutch RE.** 2009. Low-pH Triggering of Human Metapneumovirus Fusion: Essential Residues and Importance in Entry. *J. Virol.* **83**:1511-1522.
137. **Lindahl U, Kusche-Gullberg M, Kjellen L.** 1998. Regulated diversity of heparan sulfate. *J Biol Chem* **273**:24979-24982.
138. **Rosenberg RD, Shworak NW, Liu J, Schwartz JJ, Zhang L.** Heparan sulfate proteoglycans of the cardiovascular system. Specific structures emerge but how is synthesis regulated? *The Journal of Clinical Investigation* **99**:2062-2070.
139. **Bon I, Lembo D, Rusnati M, Clo A, Morini S, Miseroocchi A, Bugatti A, Grigolon S, Musumeci G, Landolfo S, Re MC, Gibellini D.** 2013. Peptide-derivatized SB105-A10 dendrimer inhibits the infectivity of R5 and X4 HIV-1 strains in primary PBMCs and cervicovaginal histocultures. *PLoS One* **8**:e76482.
140. **Esko JD, Lindahl U.** 2001. Molecular diversity of heparan sulfate. *J Clin Invest* **108**:169-173.
141. **Esko JD, Stewart TE, Taylor WH.** 1985. Animal cell mutants defective in glycosaminoglycan biosynthesis. *Proc Natl Acad Sci U S A* **82**:3197-3201.
142. **Hallak LK, Kwilas SA, Peeples ME.** 2007. Interaction between respiratory syncytial virus and glycosaminoglycans, including heparan sulfate. *Methods Mol Biol* **379**:15-34.
143. **Hayashi K, Hayashi M, Jalkanen M, Firestone JH, Trelstad RL, Bernfield M.** 1987. Immunocytochemistry of cell surface heparan sulfate proteoglycan in mouse tissues. A light and electron microscopic study. *The journal of histochemistry and cytochemistry : official journal of the Histochemistry Society* **35**:1079-1088.
144. **Iwamoto DV, Calderwood DA.** 2015. Regulation of integrin-mediated adhesions. *Curr Opin Cell Biol* **36**:41-47.
145. **Barczyk M, Carracedo S, Gullberg D.** 2010. Integrins. *Cell and Tissue Research* **339**:269-280.
146. **Hynes RO.** 2002. Integrins: Bidirectional, Allosteric Signaling Machines. *Cell* **110**:673-687.
147. **Caswell PT, Vadrevu S, Norman JC.** 2009. Integrins: masters and slaves of endocytic transport. *Nat Rev Mol Cell Biol* **10**:843-853.

148. **Stewart PL, Nemerow GR.** 2007. Cell integrins: commonly used receptors for diverse viral pathogens. *Trends in Microbiology* **15**:500-507.
149. **Ginsberg MH.** 2014. Integrin activation. *BMB reports* **47**:655-659.
150. **Humphries JD, Byron A, Humphries MJ.** 2006. Integrin ligands at a glance. *Journal of Cell Science* **119**:3901-3903.
151. **Soares MA, Teixeira FC, Fontes M, Areas AL, Leal MG, Pavao MS, Stelling MP.** 2015. Heparan Sulfate Proteoglycans May Promote or Inhibit Cancer Progression by Interacting with Integrins and Affecting Cell Migration. *BioMed research international* **2015**:453801.
152. **Ruoslahti E.** 1996. RGD and other recognition sequences for integrins. *Annual Review of Cell and Developmental Biology* **12**:697-715.
153. **Takada Y, Ye X, Simon S.** 2007. The integrins. *Genome Biology* **8**:215.
154. **del Pozo MA, Balasubramanian N, Alderson NB, Kiosses WB, Grande-Garcia A, Anderson RGW, Schwartz MA.** 2005. Phospho-caveolin-1 mediates integrin-regulated membrane domain internalization. *Nat Cell Biol* **7**:901-908.
155. **Mudhakir D, Harashima H.** 2009. Learning from the viral journey: How to enter cells and how to overcome intracellular barriers to reach the nucleus. *The AAPS Journal* **11**:65-77.
156. **Lyle C, McCormick F.** 2010. Integrin alphavbeta5 is a primary receptor for adenovirus in CAR-negative cells. *Virology Journal* **7**:148.
157. **Gallagher JT, Walker A.** 1985. Molecular distinctions between heparan sulphate and heparin. Analysis of sulphation patterns indicates that heparan sulphate and heparin are separate families of N-sulphated polysaccharides. *Biochemical Journal* **230**:665-674.
158. **Bacsa S, Karasneh G, Dosa S, Liu J, Valyi-Nagy T, Shukla D.** 2011. Syndecan-1 and syndecan-2 play key roles in herpes simplex virus type-1 infection. *J Gen Virol* **92**:733-743.
159. **Crublet E, Andrieu JP, Vives RR, Lortat-Jacob H.** 2008. The HIV-1 envelope glycoprotein gp120 features four heparan sulfate binding domains, including the co-receptor binding site. *J Biol Chem* **283**:15193-15200.
160. **De Francesco MA, Baronio M, Poiesi C.** 2011. HIV-1 p17 matrix protein interacts with heparan sulfate side chain of CD44v3, syndecan-2, and syndecan-4 proteoglycans expressed on human activated CD4+ T cells affecting tumor necrosis factor alpha and interleukin 2 production. *J Biol Chem* **286**:19541-19548.
161. **de Witte L, Bobardt M, Chatterji U, Degeest G, David G, Geijtenbeek TB, Gallay P.** 2007. Syndecan-3 is a dendritic cell-specific attachment receptor for HIV-1. *Proc Natl Acad Sci U S A* **104**:19464-19469.
162. **Giroglou T, Florin L, Schafer F, Streeck RE, Sapp M.** 2001. Human papillomavirus infection requires cell surface heparan sulfate. *J Virol* **75**:1565-1570.
163. **Hallak LK, Collins PL, Knudson W, Peeples ME.** 2000. Iduronic acid-containing glycosaminoglycans on target cells are required for efficient respiratory syncytial virus infection. *Virology* **271**:264-275.
164. **Karasneh GA, Ali M, Shukla D.** 2011. An important role for syndecan-1 in herpes simplex virus type-1 induced cell-to-cell fusion and virus spread. *PLoS One* **6**:e25252.
165. **Lefevre M, Felmlee DJ, Parnot M, Baumert TF, Schuster C.** 2014. Syndecan 4 is involved in mediating HCV entry through interaction with lipoviral particle-associated apolipoprotein E. *PLoS One* **9**:e95550.

166. **Makkonen KE, Turkki P, Laakkonen JP, Yla-Herttuala S, Marjomaki V, Airenne KJ.** 2013. 6-o- and N-sulfated syndecan-1 promotes baculovirus binding and entry into Mammalian cells. *J Virol* **87**:11148-11159.
167. **Misinzo G, Delputte PL, Meerts P, Lefebvre DJ, Nauwynck HJ.** 2006. Porcine circovirus 2 uses heparan sulfate and chondroitin sulfate B glycosaminoglycans as receptors for its attachment to host cells. *J Virol* **80**:3487-3494.
168. **Okamoto K, Kinoshita H, Parquet Mdel C, Raekiansyah M, Kimura D, Yui K, Islam MA, Hasebe F, Morita K.** 2012. Dengue virus strain DEN2 16681 utilizes a specific glycochain of syndecan-2 proteoglycan as a receptor. *J Gen Virol* **93**:761-770.
169. **Patel M, Yanagishita M, Roderiquez G, Bou-Habib DC, Oravec T, Hascall VC, Norcross MA.** 1993. Cell-surface heparan sulfate proteoglycan mediates HIV-1 infection of T-cell lines. *AIDS Res Hum Retroviruses* **9**:167-174.
170. **Salvador B, Sexton NR, Carrion R, Jr., Nunneley J, Patterson JL, Steffen I, Lu K, Muench MO, Lembo D, Simmons G.** 2013. Filoviruses utilize glycosaminoglycans for their attachment to target cells. *J Virol* **87**:3295-3304.
171. **Shafti-Keramat S, Handisurya A, Kriehuber E, Meneguzzi G, Slupetzky K, Kirnbauer R.** 2003. Different heparan sulfate proteoglycans serve as cellular receptors for human papillomaviruses. *J Virol* **77**:13125-13135.
172. **Shi Q, Jiang J, Luo G.** 2013. Syndecan-1 serves as the major receptor for attachment of hepatitis C virus to the surfaces of hepatocytes. *J Virol* **87**:6866-6875.
173. **Shieh MT, WuDunn D, Montgomery RI, Esko JD, Spear PG.** 1992. Cell surface receptors for herpes simplex virus are heparan sulfate proteoglycans. *J Cell Biol* **116**:1273-1281.
174. **Shukla D, Liu J, Blaiklock P, Shworak NW, Bai X, Esko JD, Cohen GH, Eisenberg RJ, Rosenberg RD, Spear PG.** 1999. A novel role for 3-O-sulfated heparan sulfate in herpes simplex virus 1 entry. *Cell* **99**:13-22.
175. **Surviladze Z, Sterk RT, Ozbun MA.** 2015. The interaction of human papillomavirus type 16 particles with heparan sulfate and syndecan-1 molecules in the keratinocyte extracellular matrix plays an active role in infection. *J Gen Virol*.
176. **Techaarpornkul S, Collins PL, Peeples ME.** 2002. Respiratory syncytial virus with the fusion protein as its only viral glycoprotein is less dependent on cellular glycosaminoglycans for attachment than complete virus. *Virology* **294**:296-304.
177. **WuDunn D, Spear PG.** 1989. Initial interaction of herpes simplex virus with cells is binding to heparan sulfate. *J Virol* **63**:52-58.
178. **Lin R, Rosahl TW, Whiting PJ, Fawcett JW, Kwok JC.** 2011. 6-Sulphated chondroitins have a positive influence on axonal regeneration. *PLoS One* **6**:e21499.
179. **Bandtlow CE, Zimmermann DR.** 2000. Proteoglycans in the developing brain: New conceptual insights for old proteins. *Physiological reviews* **80**:1267-1290.
180. **Viapiano MS, Matthews RT.** 2006. From barriers to bridges: chondroitin sulfate proteoglycans in neuropathology. *Trends in molecular medicine* **12**:488-496.
181. **Galtrey CM, Fawcett JW.** 2007. The role of chondroitin sulfate proteoglycans in regeneration and plasticity in the central nervous system. *Brain research reviews* **54**:1-18.
182. **Bergefall K, Trybala E, Johansson M, Uyama T, Naito S, Yamada S, Kitagawa H, Sugahara K, Bergstrom T.** 2005. Chondroitin sulfate characterized by the E-disaccharide unit is a potent inhibitor of herpes simplex virus infectivity and provides the virus binding sites on gro2C cells. *J Biol Chem* **280**:32193-32199.

183. **Kim E, Okumura M, Sawa H, Miyazaki T, Fujikura D, Yamada S, Sugahara K, Sasaki M, Kimura T.** 2011. Paradoxical effects of chondroitin sulfate-E on Japanese encephalitis viral infection. *Biochem Biophys Res Commun* **409**:717-722.
184. **Kato D, Era S, Watanabe I, Arihara M, Sugiura N, Kimata K, Suzuki Y, Morita K, Hidari KI, Suzuki T.** 2010. Antiviral activity of chondroitin sulphate E targeting dengue virus envelope protein. *Antiviral Res* **88**:236-243.
185. **Trowbridge JM, Gallo RL.** 2002. Dermatan sulfate: new functions from an old glycosaminoglycan. *Glycobiology* **12**:117R-125R.
186. **Penc SF, Pomahac B, Eriksson E, Detmar M, Gallo RL.** 1999. Dermatan sulfate activates nuclear factor-kappa b and induces endothelial and circulating intercellular adhesion molecule-1. *Journal of Clinical Investigation* **103**:1329-1335.
187. **Funderburgh JL.** 2002. Keratan Sulfate Biosynthesis. *IUBMB life* **54**:187-194.
188. **Lopes CC, Dietrich CP, Nader HB.** 2006. Specific structural features of syndecans and heparan sulfate chains are needed for cell signaling. *Brazilian journal of medical and biological research = Revista brasileira de pesquisas medicas e biologicas / Sociedade Brasileira de Biofisica ... [et al.]* **39**:157-167.
189. **Sgaramella N, Coates PJ, Strindlund K, Loljung L, Colella G, Laurell G, Rossiello R, Muzio LL, Loizou C, Tartaro G, Olofsson K, Danielsson K, Fahraeus R, Nylander K.** 2015. Expression of p16 in squamous cell carcinoma of the mobile tongue is independent of HPV infection despite presence of the HPV-receptor syndecan-1. *British journal of cancer* **113**:321-326.
190. **Chen E, Hermanson S, Ekker SC.** 2004. Syndecan-2 is essential for angiogenic sprouting during zebrafish development. *Blood* **103**:1710-1719.
191. **Arrington CB, Yost HJ.** 2009. Extra-embryonic syndecan 2 regulates organ primordia migration and fibrillogenesis throughout the zebrafish embryo. *Development* **136**:3143-3152.
192. **Kramer KL, Yost HJ.** Ectodermal Syndecan-2 Mediates Left-Right Axis Formation in Migrating Mesoderm as a Cell-Nonautonomous Vg1 Cofactor. *Developmental cell* **2**:115-124.
193. **Berndt C, Casaroli-Marano RP, Vilaro S, Reina M.** 2001. Cloning and characterization of human syndecan-3. *J Cell Biochem* **82**:246-259.
194. **Renga B, Francisci D, Schiaroli E, Carino A, Cipriani S, D'Amore C, Sidoni A, Sordo RD, Ferri I, Lucattelli M, Lunghi B, Baldelli F, Fiorucci S.** 2014. The HIV matrix protein p17 promotes the activation of human hepatic stellate cells through interactions with CXCR2 and Syndecan-2. *PLoS One* **9**:e94798.
195. **Gallay P.** 2004. Syndecans and HIV-1 pathogenesis. *Microbes and infection / Institut Pasteur* **6**:617-622.
196. **David G, Lories V, Decock B, Marynen P, Cassiman JJ, Van den Berghe H.** 1990. Molecular cloning of a phosphatidylinositol-anchored membrane heparan sulfate proteoglycan from human lung fibroblasts. *J Cell Biol* **111**:3165-3176.
197. **Stipp CS, Litwack ED, Lander AD.** 1994. Cerebroglycan: an integral membrane heparan sulfate proteoglycan that is unique to the developing nervous system and expressed specifically during neuronal differentiation. *J Cell Biol* **124**:149-160.
198. **Watanabe K, Yamada H, Yamaguchi Y.** 1995. K-glypican: a novel GPI-anchored heparan sulfate proteoglycan that is highly expressed in developing brain and kidney. *J Cell Biol* **130**:1207-1218.

199. **Veugelers M, Vermeesch J, Reekmans G, Steinfeld R, Marynen P, David G.** 1997. Characterization of glypican-5 and chromosomal localization of human GPC5, a new member of the glypican gene family. *Genomics* **40**:24-30.
200. **Veugelers M, De Cat B, Ceulemans H, Bruystens AM, Coomans C, Durr J, Vermeesch J, Marynen P, David G.** 1999. Glypican-6, a new member of the glypican family of cell surface heparan sulfate proteoglycans. *J Biol Chem* **274**:26968-26977.
201. **Pilia G, Hughes-Benzie RM, MacKenzie A, Baybayan P, Chen EY, Huber R, Neri G, Cao A, Forabosco A, Schlessinger D.** 1996. Mutations in GPC3, a glypican gene, cause the Simpson-Golabi-Behmel overgrowth syndrome. *Nat Genet* **12**:241-247.
202. **Litwack ED, Stipp CS, Kumbasar A, Lander AD.** 1994. Neuronal expression of glypican, a cell-surface glycosylphosphatidylinositol-anchored heparan sulfate proteoglycan, in the adult rat nervous system. *The Journal of neuroscience : the official journal of the Society for Neuroscience* **14**:3713-3724.
203. **Golabi M, Rosen L.** 1984. A new X-linked mental retardation-overgrowth syndrome. *American journal of medical genetics* **17**:345-358.
204. **Verrier ER, Colpitts CC, Bach C, Heydmann L, Weiss A, Renaud M, Durand SC, Habersetzer F, Durantel D, Abou-Jaoude G, Lopez Ledesma MM, Felmlee DJ, Soumillon M, Croonenborghs T, Pochet N, Nassal M, Schuster C, Brino L, Sureau C, Zeisel MB, Baumert TF.** 2016. A targeted functional RNA interference screen uncovers glypican 5 as an entry factor for hepatitis B and D viruses. *Hepatology* **63**:35-48.
205. **Lamb RA, Jardetzky TS.** 2007. Structural basis of viral invasion: lessons from paramyxovirus F. *Curr Opin Struct Biol* **17**:427-436.
206. **Hosaka M, Nagahama M, Kim WS, Watanabe T, Hatsuzawa K, Ikemizu J, Murakami K, Nakayama K.** 1991. Arg-X-Lys/Arg-Arg motif as a signal for precursor cleavage catalyzed by furin within the constitutive secretory pathway. *J. Biol. Chem.* **266**:12127-12130.
207. **Meulendyke KA, Wurth MA, McCann RO, Dutch RE.** 2005. Endocytosis plays a critical role in proteolytic processing of the Hendra virus fusion protein. *J Virol* **79**:12643-12649.
208. **Ortmann D, Ohuchi M, Angliker H, Shaw E, Garten W, Klenk H-D.** 1994. Proteolytic cleavage of wild type and mutants of the F protein of human parainfluenza virus type 3 by two subtilisin-like endoproteases, furin and KEX2. *J. Virol.* **68**:2772-2776.
209. **Pager CT, Craft WW, Jr., Patch J, Dutch RE.** 2006. A mature and fusogenic form of the Nipah virus fusion protein requires proteolytic processing by cathepsin L. *Virology* **346**:251-257.
210. **Pager CT, Dutch RE.** 2005. Cathepsin L is involved in proteolytic processing of the Hendra virus fusion protein. *J Virol* **79**:12714-12720.
211. **Popa A, Carter JR, Smith SE, Hellman L, Fried MG, Dutch RE.** 2012. Residues in the hendra virus fusion protein transmembrane domain are critical for endocytic recycling. *J Virol* **86**:3014-3026.
212. **Smith EC, Popa A, Chang A, Masante C, Dutch RE.** 2009. Viral entry mechanisms: the increasing diversity of paramyxovirus entry. *FEBS Journal* **276**:7217-7227.
213. **Farzan SF, Palermo LM, Yokoyama CC, Orefice G, Fornabaio M, Sarkar A, Kellogg GE, Greengard O, Porotto M, Moscona A.** 2011. Premature activation of the paramyxovirus fusion protein before target cell attachment with corruption of the viral fusion machinery. *J Biol Chem* **286**:37945-37954.
214. **O'Sullivan JD, Allworth AM, Paterson DL, Snow TM, Boots R, Gleeson LJ, Gould AR, Hyatt AD, Bradfield J.** 1997. Fatal encephalitis due to novel paramyxovirus transmitted from horses. *Lancet* **349**:93-95.

215. **Hernandez LD, Hoffman LR, Wolfsberg TG, White JM.** 1996. Virus-cell and cell-cell fusion. *Annu. Rev. Cell Develop. Biol.* **12**:627-661.
216. **Cseke G, Wright DW, Tollefson SJ, Johnson JE, Crowe JE, Jr., Williams JV.** 2007. Human metapneumovirus fusion protein vaccines that are immunogenic and protective in cotton rats. *J Virol* **81**:698-707.
217. **Skiadopoulos MH, Biacchesi S, Buchholz UJ, Riggs JM, Surman SR, Amaro-Carambot E, McAuliffe JM, Elkins WR, St Claire M, Collins PL, Murphy BR.** 2004. The two major human metapneumovirus genetic lineages are highly related antigenically, and the fusion (F) protein is a major contributor to this antigenic relatedness. *J Virol* **78**:6927-6937.
218. **Tang RS, Mahmood K, Macphail M, Guzzetta JM, Haller AA, Liu H, Kaur J, Lawlor HA, Stillman EA, Schickli JH, Fouchier RA, Osterhaus AD, Spaete RR.** 2005. A host-range restricted parainfluenza virus type 3 (PIV3) expressing the human metapneumovirus (hMPV) fusion protein elicits protective immunity in African green monkeys. *Vaccine* **23**:1657-1667.
219. **Melero JA, Mas V.** 2015. The Pneumovirinae fusion (F) protein: A common target for vaccines and antivirals. *Virus Res* **209**:128-135.
220. **Welch BD, Liu Y, Kors CA, Leser GP, Jardetzky TS, Lamb RA.** 2012. Structure of the cleavage-activated prefusion form of the parainfluenza virus 5 fusion protein. *Proc Natl Acad Sci U S A* **109**:16672-16677.
221. **Wen X, Krause JC, Leser GP, Cox RG, Lamb RA, Williams JV, Crowe JE, Jr., Jardetzky TS.** 2012. Structure of the human metapneumovirus fusion protein with neutralizing antibody identifies a pneumovirus antigenic site. *Nat Struct Mol Biol* **19**:461-463.
222. **Yin HS, Wen X, Paterson RG, Lamb RA, Jardetzky TS.** 2006. Structure of the parainfluenza virus 5 F protein in its metastable, prefusion conformation. *Nature* **439**:38-44.
223. **Yin HS, Paterson RG, Wen X, Lamb RA, Jardetzky TS.** 2005. Structure of the uncleaved ectodomain of the paramyxovirus (hPIV3) fusion protein. *Proc Natl Acad Sci U S A* **102**:9288-9293.
224. **Swanson K, Wen X, Leser GP, Paterson RG, Lamb RA, Jardetzky TS.** 2010. Structure of the Newcastle disease virus F protein in the post-fusion conformation. *Virology* **402**:372-379.
225. **McLellan JS, Yang Y, Graham BS, Kwong PD.** 2011. Structure of Respiratory Syncytial Virus Fusion Glycoprotein in the Postfusion Conformation Reveals Preservation of Neutralizing Epitopes. *Journal of Virology* **85**:7788-7796.
226. **Dutch RE, Joshi SB, Lamb RA.** 1998. Membrane Fusion Promoted by Increasing Surface Densities of the Paramyxovirus F and HN Proteins: Comparison of Fusion Reactions Mediated by Simian Virus 5 F, Human Parainfluenza Virus Type 3 F, and Influenza Virus HA. *J. Virol.* **72**:7745-7753.
227. **Earp LJ, Delos SE, Park HE, White JM.** 2005. The many mechanisms of viral membrane fusion proteins. *Curr Top Microbiol Immunol* **285**:25-66.
228. **Navaratnarajah CK, Oezguen N, Rupp L, Kay L, Leonard VHJ, Braun W, Cattaneo R.** 2011. The heads of the measles virus attachment protein move to transmit the fusion-triggering signal. *Nat Struct Mol Biol* **18**:128-134.
229. **Bishop KA, Stantchev TS, Hickey AC, Khetawat D, Bossart KN, Krasnoperov V, Gill P, Feng YR, Wang L, Eaton BT, Wang LF, Broder CC.** 2007. Identification of hendra virus glycoprotein residues that are critical for receptor binding. *J Virol* **81**:5893-5901.

230. **Porotto M, DeVito I, Palmer SG, Jurgens EM, Yee JL, Yokoyama CC, Pessi A, Moscona A.** 2011. Spring-Loaded Model Revisited: Paramyxovirus Fusion Requires Engagement of a Receptor Binding Protein beyond Initial Triggering of the Fusion Protein. *Journal of Virology* **85**:12867-12880.
231. **Aguilar HC, Ataman ZA, Aspericueta V, Fang AQ, Stroud M, Negrete OA, Kammerer RA, Lee B.** 2009. A Novel Receptor-induced Activation Site in the Nipah Virus Attachment Glycoprotein (G) Involved in Triggering the Fusion Glycoprotein (F). *Journal of Biological Chemistry* **284**:1628-1635.
232. **Mirza AM, Deng R, Iorio RM.** 1994. Site-directed mutagenesis of a conserved hexapeptide in the paramyxovirus hemagglutinin-neuraminidase glycoprotein: effects on antigenic structure and function. *J. Virol.* **68**:5093-5099.
233. **Bishop KA, Hickey AC, Khetawat D, Patch JR, Bossart KN, Zhu Z, Wang L-F, Dimitrov DS, Broder CC.** 2008. Residues in the Stalk Domain of the Hendra Virus G Glycoprotein Modulate Conformational Changes Associated with Receptor Binding. *Journal of Virology* **82**:11398-11409.
234. **McGinnes L, Sergel T, Morrison T.** 1993. Mutations in the transmembrane domain of the HN protein of Newcastle disease virus affect the structure and activity of the protein. *Virology* **196**:101-110.
235. **Bousse T, Takimoto T, Gorman WL, Takahashi T, Portner A.** 1994. Regions on the hemagglutinin-neuraminidase proteins of human parainfluenza virus type-1 and Sendai virus important for membrane fusion. *Virology* **204**:506-514.
236. **Leyrer S, Bitzer M, Lauer U, Kramer J, Neubert WJ, Sedlmeier R.** 1998. Sendai virus-like particles devoid of haemagglutinin-neuraminidase protein infect cells via the human asialoglycoprotein receptor. *J. Gen. Virol.* **79**:683-687.
237. **Paterson RG, Russell CJ, Lamb RA.** 2000. Fusion protein of the paramyxovirus SV5: destabilizing and stabilizing mutants of fusion activation. *Virology* **270**:17-30.
238. **Wharton SA, Skehel JJ, Wiley DC.** 2000. Temperature dependence of fusion by Sendai virus. *Virology* **271**:71-78.
239. **Kahn JS, Schnell MJ, Buonocore L, Rose JK.** 1999. Recombinant vesicular stomatitis virus expressing respiratory syncytial virus (RSV) glycoproteins: RSV fusion protein can mediate infection and cell fusion. *Virology* **254**:81-91.
240. **Techarpornkul S, Barretto N, Peeples ME.** 2001. Functional analysis of recombinant respiratory syncytial virus deletion mutants lacking the small hydrophobic and/or attachment glycoprotein gene. *J Virol* **75**:6825-6834.
241. **Herfst S, Mas V, Ver LS, Wierda RJ, Osterhaus AD, Fouchier RA, Melero JA.** 2008. Low-pH-induced membrane fusion mediated by human metapneumovirus F protein is a rare, strain-dependent phenomenon. *J Virol* **82**:8891-8895.
242. **Mas V, Herfst S, Osterhaus AD, Fouchier RA, Melero JA.** 2011. Residues of the human metapneumovirus fusion (F) protein critical for its strain-related fusion phenotype: implications for the virus replication cycle. *J Virol* **85**:12650-12661.
243. **Chang A, Hackett BA, Winter CC, Buchholz UJ, Dutch RE.** 2012. Potential electrostatic interactions in multiple regions affect human metapneumovirus F-mediated membrane fusion. *J Virol* **86**:9843-9853.
244. **Karger A, Schmidt U, Buchholz UJ.** 2001. Recombinant bovine respiratory syncytial virus with deletions of the G or SH genes: G and F proteins bind heparin. *J Gen Virol* **82**:631-640.

245. **Biacchesi S, Pham QN, Skiadopoulou MH, Murphy BR, Collins PL, Buchholz UJ.** 2006. Modification of the trypsin-dependent cleavage activation site of the human metapneumovirus fusion protein to be trypsin independent does not increase replication or spread in rodents or nonhuman primates. *J Virol* **80**:5798-5806.
246. **Biacchesi S, Skiadopoulou MH, Tran KC, Murphy BR, Collins PL, Buchholz UJ.** 2004. Recovery of human metapneumovirus from cDNA: optimization of growth in vitro and expression of additional genes. *Virology* **321**:247-259.
247. **Shirogane Y, Takeda M, Iwasaki M, Ishiguro N, Takeuchi H, Nakatsu Y, Tahara M, Kikuta H, Yanagi Y.** 2008. Efficient multiplication of human metapneumovirus in Vero cells expressing the transmembrane serine protease TMPRSS2. *J Virol* **82**:8942-8946.
248. **Carr CM, Chaudhry C, Kim PS.** 1997. Influenza hemagglutinin is spring-loaded by a metastable native conformation. *Proc. Natl. Acad. Sci. USA* **94**:14306-14313.
249. **Connolly SA, Leser GP, Yin HS, Jardetzky TS, Lamb RA.** 2006. Refolding of a paramyxovirus F protein from prefusion to postfusion conformations observed by liposome binding and electron microscopy. *Proc Natl Acad Sci U S A* **103**:17903-17908.
250. **Bissonnette ML, Connolly SA, Young DF, Randall RE, Paterson RG, Lamb RA.** 2006. Analysis of the pH requirement for membrane fusion of different isolates of the paramyxovirus parainfluenza virus 5. *J Virol* **80**:3071-3077.
251. **Steinhauer DA, Martin J, Lin YP, Wharton SA, Oldstone MB, Skehel JJ, Wiley DC.** 1996. Studies using double mutants of the conformational transitions in influenza hemagglutinin required for its membrane fusion activity. *Proc Natl Acad Sci U S A* **93**:12873-12878.
252. **Thoennes S, Li Z-N, Lee B-J, Langley WA, Skehel JJ, Russell RJ, Steinhauer DA.** 2008. Analysis of residues near the fusion peptide in the influenza hemagglutinin structure for roles in triggering membrane fusion. *Virology* **370**:403-414.
253. **Stauffer F, De Miranda J, Schechter MC, Carneiro FA, Salgado LT, Machado GF, Da Poian AT.** 2007. Inactivation of vesicular stomatitis virus through inhibition of membrane fusion by chemical modification of the viral glycoprotein. *Antiviral Res* **73**:31-39.
254. **Roche S, Rey FA, Gaudin Y, Bressanelli S.** 2007. Structure of the prefusion form of the vesicular stomatitis virus glycoprotein G. *Science* **315**:843-848.
255. **Harrison SC.** 2008. Viral membrane fusion. *Nat Struct Mol Biol* **15**:690-698.
256. **Huang Q, Sivaramakrishna RP, Ludwig K, Korte T, Bottcher C, Herrmann A.** 2003. Early steps of the conformational change of influenza virus hemagglutinin to a fusion active state: stability and energetics of the hemagglutinin. *Biochim Biophys Acta* **1614**:3-13.
257. **Kampmann T, Mueller DS, Mark AE, Young PR, Kobe B.** 2006. The Role of histidine residues in low-pH-mediated viral membrane fusion. *Structure* **14**:1481-1487.
258. **Fontana J, Steven AC.** 2015. Influenza virus-mediated membrane fusion: Structural insights from electron microscopy. *Arch Biochem Biophys* **581**:86-97.
259. **Lakadamyali M, Rust MJ, Babcock HP, Zhuang X.** 2003. Visualizing infection of individual influenza viruses. *Proc Natl Acad Sci U S A* **100**:9280-9285.
260. **Li S, Sieben C, Ludwig K, Hofer CT, Chiantia S, Herrmann A, Eghiaian F, Schaap IA.** 2014. pH-Controlled two-step uncoating of influenza virus. *Biophys J* **106**:1447-1456.
261. **Blumenthal R, Bali-Puri A, Walter A, Covell D, Eidelman O.** 1987. pH-dependent fusion of vesicular stomatitis virus with Vero cells. Measurement by dequenching of octadecyl rhodamine fluorescence. *J Biol Chem* **262**:13614-13619.

262. **Brown JC, Newcomb WW, Lawrenz-Smith S.** 1988. pH-dependent accumulation of the vesicular stomatitis virus glycoprotein at the ends of intact virions. *Virology* **167**:625-629.
263. **Clague MJ, Schoch C, Zech L, Blumenthal R.** 1990. Gating kinetics of pH-activated membrane fusion of vesicular stomatitis virus with cells: Stopped-flow measurements by dequenching of octadecylrhodamine fluorescence. *Biochemistry* **29**:1303-1308.
264. **Ferlin A, Raux H, Baquero E, Lepault J, Gaudin Y.** 2014. Characterization of pH-sensitive molecular switches that trigger the structural transition of vesicular stomatitis virus glycoprotein from the postfusion state toward the prefusion state. *J Virol* **88**:13396-13409.
265. **Fredericksen BL, Whitt MA.** 1996. Mutations at two conserved acidic amino acids in the glycoprotein of vesicular stomatitis virus affect pH-dependent conformational changes and reduce the pH threshold for membrane fusion. *Virology* **217**:49-57.
266. **Puri A, Winick J, Lowy RJ, Covell D, Eidelman O, Walter A, Blumenthal R.** 1988. Activation of vesicular stomatitis virus fusion with cells by pretreatment at low pH. *J. Biol. Chem.* **263**:4749-4753.
267. **Rucker P, Wieninger SA, Ullmann GM, Sticht H.** 2012. pH-dependent molecular dynamics of vesicular stomatitis virus glycoprotein G. *Proteins* **80**:2601-2613.
268. **Sun X, Roth SL, Bialecki MA, Whittaker GR.** 2010. Internalization and fusion mechanism of vesicular stomatitis virus and related rhabdoviruses. *Future virology* **5**:85-96.
269. **Yao Y, Ghosh K, Epand RF, Epand RM, Ghosh HP.** 2003. Membrane fusion activity of vesicular stomatitis virus glycoprotein G is induced by low pH but not by heat or denaturant. *Virology* **310**:319-332.
270. **Seth S, Vincent A, Compans RW.** 2003. Activation of fusion by the SER virus F protein: a low-pH-dependent paramyxovirus entry process. *J Virol* **77**:6520-6527.
271. **Bissonnette MLZ, Connolly SA, Young DF, Randall RE, Paterson RG, Lamb RA.** 2006. Analysis of the pH Requirement for Membrane Fusion of Different Isolates of the Paramyxovirus Parainfluenza Virus 5. *Journal of Virology* **80**:3071-3077.
272. **Barretto N, Hallak LK, Peebles ME.** 2003. Neuraminidase treatment of respiratory syncytial virus-infected cells or virions, but not target cells, enhances cell-cell fusion and infection. *Virology* **313**:33-43.
273. **Benmerah A, and Christophe Lamaze.** 2007. Clathrin-Coated Pits: Vive La Difference? *Traffic* **8**:970-982.
274. **Wang H, Jiang C.** 2009. Influenza A virus H5N1 entry into host cells is through clathrin-dependent endocytosis. *Science in China. Series C, Life sciences / Chinese Academy of Sciences* **52**:464-469.
275. **Chen C, Zhuang X.** 2008. Epsin 1 is a cargo-specific adaptor for the clathrin-mediated endocytosis of the influenza virus. *Proc Natl Acad Sci U S A* **105**:11790-11795.
276. **Matlin KS, Reggio H, Helenius A, Simons K.** 1981. Infectious entry pathway of influenza virus in a canine kidney cell line. *J. Cell Biol.* **91**:601-613.
277. **Rust MJ, Lakadamyali M, Zhang F, Zhuang X.** 2004. Assembly of endocytic machinery around individual influenza viruses during viral entry. *Nature structural & molecular biology* **11**:567-573.
278. **Sun X, Yau VK, Briggs BJ, Whittaker GR.** 2005. Role of clathrin-mediated endocytosis during vesicular stomatitis virus entry into host cells. *Virology* **338**:53-60.

279. **Acosta EG, Castilla V, Damonte EB.** 2008. Functional entry of dengue virus into *Aedes albopictus* mosquito cells is dependent on clathrin-mediated endocytosis. *J Gen Virol* **89**:474-484.
280. **Peng T, Wang JL, Chen W, Zhang JL, Gao N, Chen ZT, Xu XF, Fan DY, An J.** 2009. Entry of dengue virus serotype 2 into ECV304 cells depends on clathrin-dependent endocytosis, but not on caveolae-dependent endocytosis. *Can J Microbiol* **55**:139-145.
281. **Gutierrez-Ortega A, Sanchez-Hernandez C, Gomez-Garcia B.** 2008. Respiratory syncytial virus glycoproteins uptake occurs through clathrin-mediated endocytosis in a human epithelial cell line. *Virology* **5**:127.
282. **Cox RG, Mainou BA, Johnson M, Hastings AK, Schuster JE, Dermody TS, Williams JV.** 2015. Human Metapneumovirus Is Capable of Entering Cells by Fusion with Endosomal Membranes. *PLoS Pathog* **11**:e1005303.
283. **Mayor S, Pagano RE.** 2007. Pathways of clathrin-independent endocytosis. *Nat Rev Mol Cell Biol* **8**:603-612.
284. **Pelkmans L, Helenius A.** 2002. Endocytosis Via Caveolae. *Traffic* **3**:311-320.
285. **Parton RG, Howes MT.** 2010. Revisiting caveolin trafficking: the end of the caveosome. *The Journal of Cell Biology* **191**:439-441.
286. **Cantin C, Holguera J, Ferreira L, Villar E, Munoz-Barroso I.** 2007. Newcastle disease virus may enter cells by caveolae-mediated endocytosis. *J Gen Virol* **88**:559-569.
287. **Sanchez-Felipe L, Villar E, Munoz-Barroso I.** 2014. Entry of Newcastle Disease Virus into the host cell: role of acidic pH and endocytosis. *Biochim Biophys Acta* **1838**:300-309.
288. **Dugan AS, S. Eash, W.J. Atwood,.** 2006. Update on BK virus entry and intracellular trafficking. *Transplant Infectious Disease* **8**:62-67.
289. **Marsh M, Helenius A.** 2006. Virus entry: open sesame. *Cell* **124**:729-740.
290. **Neu U, Stehle T, Atwood WJ.** 2009. The Polyomaviridae: Contributions of virus structure to our understanding of virus receptors and infectious entry. *Virology* **384**:389-399.
291. **Pelkmans L, Bürli T, Zerial M, Helenius A.** 2004. Caveolin-Stabilized Membrane Domains as Multifunctional Transport and Sorting Devices in Endocytic Membrane Traffic. *Cell* **118**:767-780.
292. **Floyd DL, Ragains JR, Skehel JJ, Harrison SC, van Oijen AM.** 2008. Single-particle kinetics of influenza virus membrane fusion. *Proceedings of the National Academy of Sciences* **105**:15382-15387.
293. **Cureton DK, Massol RH, Saffarian S, Kirchhausen TL, Whelan SPJ.** 2009. Vesicular Stomatitis Virus Enters Cells through Vesicles Incompletely Coated with Clathrin That Depend upon Actin for Internalization. *PLoS Pathog* **5**:e1000394.
294. **Skehel JJ, Wiley DC.** 2000. Receptor binding and membrane fusion in virus entry: the influenza hemagglutinin. *Annu. Rev. Biochem.* **69**:531-569.
295. **Haigler HT, McKanna JA, Cohen S.** 1979. Rapid stimulation of pinocytosis in human carcinoma cells A-431 by epidermal growth factor. *J Cell Biol* **83**:82-90.
296. **Mercer J, Helenius A.** 2012. Gulping rather than sipping: macropinocytosis as a way of virus entry. *Current opinion in microbiology* **15**:490-499.
297. **Lim JP, Gleeson PA.** 2011. Macropinocytosis: an endocytic pathway for internalising large gulps. *Immunology and cell biology* **89**:836-843.
298. **Norbury CC, Hewlett LJ, Prescott AR, Shastri N, Watts C.** 1995. Class I MHC presentation of exogenous soluble antigen via macropinocytosis in bone marrow macrophages. *Immunity* **3**:783-791.

299. **Sallusto F, Cella M, Danieli C, Lanzavecchia A.** 1995. Dendritic cells use macropinocytosis and the mannose receptor to concentrate macromolecules in the major histocompatibility complex class II compartment: downregulation by cytokines and bacterial products. *J Exp Med* **182**:389-400.
300. **Kerr MC, Lindsay MR, Luetterforst R, Hamilton N, Simpson F, Parton RG, Gleeson PA, Teasdale RD.** 2006. Visualisation of macropinosome maturation by the recruitment of sorting nexins. *J Cell Sci* **119**:3967-3980.
301. **Mercer J, Helenius A.** 2008. Vaccinia virus uses macropinocytosis and apoptotic mimicry to enter host cells. *Science* **320**:531-535.
302. **Amstutz B, Gastaldelli M, Kalin S, Imelli N, Boucke K, Wandeler E, Mercer J, Hemmi S, Greber UF.** 2008. Subversion of CtBP1-controlled macropinocytosis by human adenovirus serotype 3. *EMBO J* **27**:956-969.
303. **Rossman JS, Leser GP, Lamb RA.** 2012. Filamentous influenza virus enters cells via macropinocytosis. *J Virol* **86**:10950-10960.
304. **Krzyzaniak MA, Zumstein MT, Gerez JA, Picotti P, Helenius A.** 2013. Host cell entry of respiratory syncytial virus involves macropinocytosis followed by proteolytic activation of the F protein. *PLoS Pathog* **9**:e1003309.
305. **Klausner M, Ayehunie S, Breyfogle BA, Wertz PW, Bacca L, Kubilus J.** 2007. Organotypic human oral tissue models for toxicological studies. *Toxicol In Vitro* **21**:938-949.
306. **Triana-Baltzer GB, Babizki M, Chan MC, Wong AC, Aschenbrenner LM, Campbell ER, Li QX, Chan RW, Peiris JS, Nicholls JM, Fang F.** 2010. DAS181, a sialidase fusion protein, protects human airway epithelium against influenza virus infection: an in vitro pharmacodynamic analysis. *J Antimicrob Chemother* **65**:275-284.
307. **Donalisio M, Rusnati M, Cagno V, Civra A, Bugatti A, Giuliani A, Pirri G, Volante M, Papotti M, Landolfo S, Lembo D.** 2012. Inhibition of human respiratory syncytial virus infectivity by a dendrimeric heparan sulfate-binding peptide. *Antimicrob Agents Chemother* **56**:5278-5288.
308. **Ren D, Nelson KL, Uchakin PN, Smith AL, Gu XX, Daines DA.** 2012. Characterization of extended co-culture of non-typeable *Haemophilus influenzae* with primary human respiratory tissues. *Exp Biol Med (Maywood)* **237**:540-547.
309. **Kwilas S, Liesman RM, Zhang L, Walsh E, Pickles RJ, Peeples ME.** 2009. Respiratory syncytial virus grown in Vero cells contains a truncated attachment protein that alters its infectivity and dependence on glycosaminoglycans. *J Virol* **83**:10710-10718.
310. **Zhang L, Bukreyev A, Thompson CI, Watson B, Peeples ME, Collins PL, Pickles RJ.** 2005. Infection of ciliated cells by human parainfluenza virus type 3 in an in vitro model of human airway epithelium. *J Virol* **79**:1113-1124.
311. **Zhang L, Peeples ME, Boucher RC, Collins PL, Pickles RJ.** 2002. Respiratory syncytial virus infection of human airway epithelial cells is polarized, specific to ciliated cells, and without obvious cytopathology. *J Virol* **76**:5654-5666.
312. **Chang A, Dutch RE.** 2012. Paramyxovirus fusion and entry: multiple paths to a common end. *Viruses* **4**:613-636.
313. **Sabo Y, Ehrlich M, Bacharach E.** 2011. The conserved YAGL motif in human metapneumovirus is required for higher-order cellular assemblies of the matrix protein and for virion production. *J Virol* **85**:6594-6609.
314. **Schwalter RM, Smith SE, Dutch RE.** 2006. Characterization of human metapneumovirus F protein-promoted membrane fusion: critical roles for proteolytic processing and low pH. *J Virol* **80**:10931-10941.

315. **White J, Matlin K, Helenius A.** 1981. Cell fusion by Semliki Forest, influenza, and vesicular stomatitis viruses. *J. Cell Biol.* **89**:674-679.
316. **Paterson RG, Lamb RA.** 1993. The molecular biology of influenza viruses and paramyxoviruses, p. 35-73. *In* Davidson A, Elliott RM (ed.), *Molecular Virology: A Practical Approach*. IRL Oxford University Press, Oxford.
317. **Swanson K, Wen X, Leser GP, Paterson RG, Lamb RA, Jardetzky TS.** 2010. Structure of the Newcastle disease virus F protein in the post-fusion conformation. *Virology* **402**:372-379.
318. **Leali D, Belleri M, Urbinati C, Coltrini D, Oreste P, Zoppetti G, Ribatti D, Rusnati M, Presta M.** 2001. Fibroblast growth factor-2 antagonist activity and angiostatic capacity of sulfated Escherichia coli K5 polysaccharide derivatives. *J Biol Chem* **276**:37900-37908.
319. **Biacchesi S, Murphy BR, Collins PL, Buchholz UJ.** 2007. Frequent frameshift and point mutations in the SH gene of human metapneumovirus passaged in vitro. *J Virol* **81**:6057-6067.
320. **de Graaf M, Herfst S, Aarbiou J, Burgers PC, Zaaraoui-Boutahar F, Bijl M, van Ijcken W, Schrauwen EJ, Osterhaus AD, Luider TM, Scholte BJ, Fouchier RA, Andeweg AC.** 2013. Small hydrophobic protein of human metapneumovirus does not affect virus replication and host gene expression in vitro. *PLoS One* **8**:e58572.
321. **van den Hoogen BG, van Doornum GJ, Fockens JC, Cornelissen JJ, Beyer WE, de Groot R, Osterhaus AD, Fouchier RA.** 2003. Prevalence and clinical symptoms of human metapneumovirus infection in hospitalized patients. *J Infect Dis* **188**:1571-1577.
322. **Feuillet F, Lina B, Rosa-Calatrava M, Boivin G.** 2012. Ten years of human metapneumovirus research. *J Clin Virol* **53**:97-105.
323. **Boivin G, Mackay I, Sloots TP, Madhi S, Freymuth F, Wolf D, Shemer-Avni Y, Ludewick H, Gray GC, LeBlanc E.** 2004. Global genetic diversity of human metapneumovirus fusion gene. *Emerg Infect Dis* **10**:1154-1157.
324. **Lo Presti A, Cammarota R, Apostoli P, Cella E, Fiorentini S, Babakir-Mina M, Ciotti M, Ciccozzi M.** 2011. Genetic variability and circulation pattern of human metapneumovirus isolated in Italy over five epidemic seasons. *The new microbiologica* **34**:337-344.
325. **Palmer SG, Porotto M, Palermo LM, Cunha LF, Greengard O, Moscona A.** 2012. Adaptation of human parainfluenza virus to airway epithelium reveals fusion properties required for growth in host tissue. *MBio* **3**.
326. **Hotard AL, Lee S, Currier MG, Crowe JE, Jr., Sakamoto K, Newcomb DC, Peebles RS, Jr., Plemper RK, Moore ML.** 2015. Identification of residues in the human respiratory syncytial virus fusion protein that modulate fusion activity and pathogenesis. *J Virol* **89**:512-522.
327. **Monto AS.** 2002. Epidemiology of viral respiratory infections. *The American journal of medicine* **112 Suppl 6A**:4S-12S.
328. **Arnold JC, Singh KK, Milder E, Spector SA, Sawyer MH, Gavali S, Glaser C.** 2009. Human metapneumovirus associated with central nervous system infection in children. *The Pediatric infectious disease journal* **28**:1057-1060.
329. **Principi N, Esposito S.** 2014. Paediatric human metapneumovirus infection: epidemiology, prevention and therapy. *J Clin Virol* **59**:141-147.
330. **Feldman SA, Audet S, Beeler JA.** 2000. The fusion glycoprotein of human respiratory syncytial virus facilitates virus attachment and infectivity via an interaction with cellular heparan sulfate. *J Virol* **74**:6442-6447.

331. **Escribano-Romero E, Rawling J, Garcia-Barreno B, Melero JA.** 2004. The soluble form of human respiratory syncytial virus attachment protein differs from the membrane-bound form in its oligomeric state but is still capable of binding to cell surface proteoglycans. *J Virol* **78**:3524-3532.
332. **Herold BC, Visalli RJ, Susmarski N, Brandt CR, Spear PG.** 1994. Glycoprotein C-independent binding of herpes simplex virus to cells requires cell surface heparan sulphate and glycoprotein B. *J Gen Virol* **75**:1211-1222.
333. **Spillmann D.** 2001. Heparan sulfate: anchor for viral intruders? *Biochimie* **83**:811-817.
334. **Ahmadi A, Zorofchian Moghadamtousi S, Abubakar S, Zandi K.** 2015. Antiviral Potential of Algae Polysaccharides Isolated from Marine Sources: A Review. *BioMed research international* **2015**:825203.
335. **Buck CB, Thompson CD, Roberts JN, Muller M, Lowy DR, Schiller JT.** 2006. Carrageenan is a potent inhibitor of papillomavirus infection. *PLoS Pathog* **2**:e69.
336. **Lynch G, Low L, Li S, Sloane A, Adams S, Parish C, Kemp B, Cunningham AL.** 1994. Sulfated polyanions prevent HIV infection of lymphocytes by disruption of the CD4-gp120 interaction, but do not inhibit monocyte infection. *Journal of leukocyte biology* **56**:266-272.
337. **Talarico LB, Noseda MD, Ducatti DR, Duarte ME, Damonte EB.** 2011. Differential inhibition of dengue virus infection in mammalian and mosquito cells by iota-carrageenan. *J Gen Virol* **92**:1332-1342.
338. **Leibbrandt A, Meier C, Konig-Schuster M, Weinmullner R, Kalthoff D, Pflugfelder B, Graf P, Frank-Gehrke B, Beer M, Fazekas T, Unger H, Prieschl-Grassauer E, Grassauer A.** 2010. Iota-carrageenan is a potent inhibitor of influenza A virus infection. *PLoS One* **5**:e14320.
339. **Eccles R, Meier C, Jawad M, Weinmullner R, Grassauer A, Prieschl-Grassauer E.** 2010. Efficacy and safety of an antiviral Iota-Carrageenan nasal spray: a randomized, double-blind, placebo-controlled exploratory study in volunteers with early symptoms of the common cold. *Respiratory research* **11**:108.
340. **Fazekas T, Eickhoff P, Pruckner N, Vollnhofer G, Fischmeister G, Diakos C, Rauch M, Verdianz M, Zoubek A, Gadner H, Lion T.** 2012. Lessons learned from a double-blind randomised placebo-controlled study with a Iota-carrageenan nasal spray as medical device in children with acute symptoms of common cold. *BMC complementary and alternative medicine* **12**:147.
341. **Ludwig M, Enzenhofer E, Schneider S, Rauch M, Bodenteich A, Neumann K, Prieschl-Grassauer E, Grassauer A, Lion T, Mueller CA.** 2013. Efficacy of a carrageenan nasal spray in patients with common cold: a randomized controlled trial. *Respiratory research* **14**:124.
342. **Bai J, Smock SL, Jackson GR, Jr., Maclsaac KD, Huang Y, Mankus C, Oldach J, Roberts B, Ma YL, Klappenbach JA, Crackower MA, Alves SE, Hayden PJ.** 2015. Phenotypic responses of differentiated asthmatic human airway epithelial cultures to rhinovirus. *PLoS One* **10**:e0118286.
343. **Deng X, Li Y, Qiu J.** 2014. Human bocavirus 1 infects commercially available primary human airway epithelium cultures productively. *Journal of virological methods* **195**:112-119.
344. **Cagno V, Donalizio M, Civra A, Volante M, Veccelli E, Oreste P, Rusnati M, Lembo D.** 2014. Highly sulfated K5 Escherichia coli polysaccharide derivatives inhibit respiratory

- syncytial virus infectivity in cell lines and human tracheal-bronchial histocultures. *Antimicrob Agents Chemother* **58**:4782-4794.
345. **Vervaeke P, Alen M, Noppen S, Schols D, Oreste P, Liekens S.** 2013. Sulfated *Escherichia coli* K5 polysaccharide derivatives inhibit dengue virus infection of human microvascular endothelial cells by interacting with the viral envelope protein E domain III. *PLoS One* **8**:e74035.
346. **Mercorelli B, Oreste P, Sinigalia E, Muratore G, Lembo D, Palu G, Loregian A.** 2010. Sulfated derivatives of *Escherichia coli* K5 capsular polysaccharide are potent inhibitors of human cytomegalovirus. *Antimicrob Agents Chemother* **54**:4561-4567.
347. **Pinna D, Oreste P, Coradin T, Kajaste-Rudnitski A, Ghezzi S, Zoppetti G, Rotola A, Argnani R, Poli G, Manservigi R, Vicenzi E.** 2008. Inhibition of herpes simplex virus types 1 and 2 in vitro infection by sulfated derivatives of *Escherichia coli* K5 polysaccharide. *Antimicrob Agents Chemother* **52**:3078-3084.
348. **Vicenzi E, Gatti A, Ghezzi S, Oreste P, Zoppetti G, Poli G.** 2003. Broad spectrum inhibition of HIV-1 infection by sulfated K5 *Escherichia coli* polysaccharide derivatives. *Aids* **17**:177-181.
349. **Esko JD, Selleck SB.** 2002. Order out of chaos: assembly of ligand binding sites in heparan sulfate. *Annu Rev Biochem* **71**:435-471.
350. **Luganini A, Giuliani A, Pirri G, Pizzuto L, Landolfo S, Gribaudo G.** 2010. Peptide-derivatized dendrimers inhibit human cytomegalovirus infection by blocking virus binding to cell surface heparan sulfate. *Antiviral Res* **85**:532-540.
351. **Donalisio M, Rusnati M, Civra A, Bugatti A, Allemand D, Pirri G, Giuliani A, Landolfo S, Lembo D.** 2010. Identification of a dendrimeric heparan sulfate-binding peptide that inhibits infectivity of genital types of human papillomaviruses. *Antimicrob Agents Chemother* **54**:4290-4299.
352. **Luganini A, Nicoletto SF, Pizzuto L, Pirri G, Giuliani A, Landolfo S, Gribaudo G.** 2011. Inhibition of herpes simplex virus type 1 and type 2 infections by peptide-derivatized dendrimers. *Antimicrob Agents Chemother* **55**:3231-3239.
353. **Mendes GS, Duarte ME, Colodi FG, Nosedá MD, Ferreira LG, Berte SD, Cavalcanti JF, Santos N, Romanos MT.** 2014. Structure and anti-metapneumovirus activity of sulfated galactans from the red seaweed *Cryptonemia seminervis*. *Carbohydrate polymers* **101**:313-323.
354. **Grassauer A, Weinmuellner R, Meier C, Pretsch A, Prieschl-Grassauer E, Unger H.** 2008. Iota-Carrageenan is a potent inhibitor of rhinovirus infection. *Virology* **5**:107.
355. **Chirkova T, Lin S, Oomens AG, Gaston KA, Boyoglu-Barnum S, Meng J, Stobart CC, Cotton CU, Hartert TV, Moore ML, Ziady AG, Anderson LJ.** 2015. CX3CR1 is an important surface molecule for respiratory syncytial virus infection in human airway epithelial cells. *J Gen Virol* **96**:2543-2556.
356. **Lamb RAP, G.D.** 2007. *Fields Virology*, 5th ed, vol. 1. Lippincott Williams & Wilkins, Philadelphia, PA.
357. **Ishiguro N, Ebihara T, Endo R, Ma X, Kikuta H, Ishiko H, Kobayashi K.** 2004. High genetic diversity of the attachment (G) protein of human metapneumovirus. *J Clin Microbiol* **42**:3406-3414.
358. **Takeuchi K, Tanabayashi K, Hishiyama M, Yamada A.** 1996. The mumps virus SH protein is a membrane protein and not essential for virus growth. *Virology* **225**:156-162.

359. **Jin H, Cheng X, Zhou HZ, Li S, Seddiqui A.** 2000. Respiratory syncytial virus that lacks open reading frame 2 of the M2 gene (M2-2) has altered growth characteristics and is attenuated in rodents. *J. Virol.* **74**:74-82.
360. **Karron RA, Buonagurio DA, Georgiu AF, Whitehead SS, Adamus JE, Clements-Mann ML, Harris DO, Randolph VB, Udem SA, Murphy BR, Sidhu MS.** 1997. Respiratory syncytial virus (RSV) SH and G proteins are not essential for viral replication in vitro: clinical evaluation and molecular characterization of a cold-passaged, attenuated RSV subgroup B mutant. *Proc. Natl. Acad. Sci. USA* **94**:13961-13966.
361. **Bao X, Kolli D, Ren J, Liu T, Garofalo RP, Casola A.** 2013. Human metapneumovirus glycoprotein G disrupts mitochondrial signaling in airway epithelial cells. *PLoS One* **8**:e62568.
362. **Cox RG, Erickson JJ, Hastings AK, Becker JC, Johnson M, Craven RE, Tollefson SJ, Boyd KL, Williams JV.** 2014. Human metapneumovirus virus-like particles induce protective B and T cell responses in a mouse model. *J Virol* **88**:6368-6379.
363. **Loo LH, Jumat MR, Fu Y, Ayi TC, Wong PS, Tee NW, Tan BH, Sugrue RJ.** 2013. Evidence for the interaction of the human metapneumovirus G and F proteins during virus-like particle formation. *Virol J* **10**:294.
364. **Jumat MR, Nguyen Huong T, Wong P, Loo LH, Tan BH, Fenwick F, Toms GL, Sugrue RJ.** 2014. Imaging analysis of human metapneumovirus-infected cells provides evidence for the involvement of F-actin and the raft-lipid microdomains in virus morphogenesis. *Virol J* **11**:198.
365. **Stauffer S, Rahman SA, de Marco A, Carlson LA, Glass B, Oberwinkler H, Herold N, Briggs JA, Muller B, Grunewald K, Krausslich HG.** 2014. The nucleocapsid domain of Gag is dispensable for actin incorporation into HIV-1 and for association of viral budding sites with cortical F-actin. *J Virol* **88**:7893-7903.
366. **Tu Z, Gong W, Zhang Y, Feng Y, Li N, Tu C.** 2015. [Proteomic Analyses of Purified Particles of the Rabies Virus]. *Bing du xue bao = Chinese journal of virology / [bian ji, Bing du xue bao bian ji wei yuan hui]* **31**:209-216.
367. **Ren X, Xue C, Kong Q, Zhang C, Bi Y, Cao Y.** 2012. Proteomic analysis of purified Newcastle disease virus particles. *Proteome science* **10**:32.
368. **Santangelo PJ, Bao G.** 2007. Dynamics of filamentous viral RNPs prior to egress. *Nucleic Acids Res* **35**:3602-3611.
369. **Shaikh FY, Cox RG, Lifland AW, Hotard AL, Williams JV, Moore ML, Santangelo PJ, Crowe JE, Jr.** 2012. A critical phenylalanine residue in the respiratory syncytial virus fusion protein cytoplasmic tail mediates assembly of internal viral proteins into viral filaments and particles. *MBio* **3**.
370. **Shaikh FY, Utley TJ, Craven RE, Rogers MC, Lapierre LA, Goldenring JR, Crowe JE, Jr.** 2012. Respiratory syncytial virus assembles into structured filamentous virion particles independently of host cytoskeleton and related proteins. *PLoS One* **7**:e40826.
371. **Buchwald M, Tsui LC, Riordan JR.** 1989. The search for the cystic fibrosis gene. *The American journal of physiology* **257**:L47-52.
372. **Collins FS, Riordan JR, Tsui LC.** 1990. The cystic fibrosis gene: isolation and significance. *Hospital practice* **25**:47-57.
373. **Riordan JR, Rommens JM, Kerem B, Alon N, Rozmahel R, Grzelczak Z, Zielenski J, Lok S, Plavsic N, Chou JL, et al.** 1989. Identification of the cystic fibrosis gene: cloning and characterization of complementary DNA. *Science* **245**:1066-1073.

374. **Strom CM, Crossley B, Buller-Buerkle A, Jarvis M, Quan F, Peng M, Muralidharan K, Pratt V, Redman JB, Sun W.** 2011. Cystic fibrosis testing 8 years on: lessons learned from carrier screening and sequencing analysis. *Genetics in medicine : official journal of the American College of Medical Genetics* **13**:166-172.
375. **Zvereff VV, Faruki H, Edwards M, Friedman KJ.** 2014. Cystic fibrosis carrier screening in a North American population. *Genetics in medicine : official journal of the American College of Medical Genetics* **16**:539-546.
376. **Gabriel SE, Brigman KN, Koller BH, Boucher RC, Stutts MJ.** 1994. Cystic fibrosis heterozygote resistance to cholera toxin in the cystic fibrosis mouse model. *Science* **266**:107-109.
377. **Rodman DM, Zamudio S.** 1991. The cystic fibrosis heterozygote--advantage in surviving cholera? *Medical hypotheses* **36**:253-258.
378. **Farrell PM, Mischler EH.** 1992. Newborn screening for cystic fibrosis. The Cystic Fibrosis Neonatal Screening Study Group. *Advances in pediatrics* **39**:35-70.
379. **Ong T, Ramsey BW.** 2015. Update in Cystic Fibrosis 2014. *American journal of respiratory and critical care medicine* **192**:669-675.
380. **Nazareth D, Walshaw M.** 2013. Coming of age in cystic fibrosis - transition from paediatric to adult care. *Clinical medicine* **13**:482-486.
381. **Jones AM, Helm JM.** 2009. Emerging treatments in cystic fibrosis. *Drugs* **69**:1903-1910.
382. **Pettit RS, Johnson CE.** 2011. Airway-rehydrating agents for the treatment of cystic fibrosis: past, present, and future. *The Annals of pharmacotherapy* **45**:49-59.
383. **Kerem B, Rommens JM, Buchanan JA, Markiewicz D, Cox TK, Chakravarti A, Buchwald M, Tsui LC.** 1989. Identification of the cystic fibrosis gene: genetic analysis. *Science* **245**:1073-1080.
384. **Mogayzel PJ, Jr., Flume PA.** 2010. Update in cystic fibrosis 2009. *American journal of respiratory and critical care medicine* **181**:539-544.
385. **Strausbaugh SD, Davis PB.** 2007. Cystic fibrosis: a review of epidemiology and pathobiology. *Clinics in chest medicine* **28**:279-288.
386. **Zielenski J, Rozmahel R, Bozon D, Kerem B, Grzelczak Z, Riordan JR, Rommens J, Tsui LC.** 1991. Genomic DNA sequence of the cystic fibrosis transmembrane conductance regulator (CFTR) gene. *Genomics* **10**:214-228.
387. **Welsh MJ, Denning GM, Ostedgaard LS, Anderson MP.** 1993. Dysfunction of CFTR bearing the delta F508 mutation. *Journal of cell science. Supplement* **17**:235-239.
388. **Brown CR, Hong-Brown LQ, Welch WJ.** 1997. Strategies for correcting the delta F508 CFTR protein-folding defect. *Journal of bioenergetics and biomembranes* **29**:491-502.
389. **Fanen P, Wohlhuter-Haddad A, Hinzpeter A.** 2014. Genetics of cystic fibrosis: CFTR mutation classifications toward genotype-based CF therapies. *The international journal of biochemistry & cell biology* **52**:94-102.
390. **Grasemann H, Ratjen F.** 2010. Emerging therapies for cystic fibrosis lung disease. *Expert opinion on emerging drugs* **15**:653-659.
391. **Nixon GM, Armstrong DS, Carzino R, Carlin JB, Olinsky A, Robertson CF, Grimwood K.** 2001. Clinical outcome after early *Pseudomonas aeruginosa* infection in cystic fibrosis. *The Journal of pediatrics* **138**:699-704.
392. **Konstan MW, Morgan WJ, Butler SM, Pasta DJ, Craib ML, Silva SJ, Stokes DC, Wohl ME, Wagener JS, Regelmann WE, Johnson CA, Scientific Advisory G, the I, Coordinators of the Epidemiologic Study of Cystic F.** 2007. Risk factors for rate of decline in forced

- expiratory volume in one second in children and adolescents with cystic fibrosis. *The Journal of pediatrics* **151**:134-139, 139 e131.
393. **Tang AC, Turvey SE, Alves MP, Regamey N, Tummeler B, Hartl D.** 2014. Current concepts: host-pathogen interactions in cystic fibrosis airways disease. *European respiratory review : an official journal of the European Respiratory Society* **23**:320-332.
394. **Armstrong D, Grimwood K, Carlin JB, Carzino R, Hull J, Olinsky A, Phelan PD.** 1998. Severe viral respiratory infections in infants with cystic fibrosis. *Pediatric pulmonology* **26**:371-379.
395. **Smyth A, Lewis S, Bertenshaw C, Choonara I, McGaw J, Watson A.** 2008. Case-control study of acute renal failure in patients with cystic fibrosis in the UK. *Thorax* **63**:532-535.
396. **Wark PA, Tooze M, Cheese L, Whitehead B, Gibson PG, Wark KF, McDonald VM.** 2012. Viral infections trigger exacerbations of cystic fibrosis in adults and children. *The European respiratory journal* **40**:510-512.
397. **Stelzer-Braid S, Johal H, Skilbeck K, Steller A, Alsubie H, Tovey E, Van Asperen P, McKay K, Rawlinson WD.** 2012. Detection of viral and bacterial respiratory pathogens in patients with cystic fibrosis. *Journal of virological methods* **186**:109-112.
398. **Flight WG, Bright-Thomas RJ, Tilston P, Mutton KJ, Guiver M, Morris J, Webb AK, Jones AM.** 2014. Incidence and clinical impact of respiratory viruses in adults with cystic fibrosis. *Thorax* **69**:247-253.
399. **Ramirez IA, Caverly LJ, Kalikin LM, Goldsmith AM, Lewis TC, Burke DT, LiPuma JJ, Sajjan US, Hershenson MB.** 2014. Differential responses to rhinovirus- and influenza-associated pulmonary exacerbations in patients with cystic fibrosis. *Annals of the American Thoracic Society* **11**:554-561.
400. **Goffard A, Lambert V, Salleron J, Herwegh S, Engelmann I, Pinel C, Pin I, Perrez T, Prevotat A, Dewilde A, Delhaes L.** 2014. Virus and cystic fibrosis: rhinoviruses are associated with exacerbations in adult patients. *J Clin Virol* **60**:147-153.
401. **Kong M, Maeng P, Hong J, Szczesniak R, Sorscher E, Sullender W, Clancy JP.** 2013. Respiratory syncytial virus infection disrupts monolayer integrity and function in cystic fibrosis airway cells. *Viruses* **5**:2260-2271.
402. **Wilkesmann A, Schildgen O, Eis-Hubinger AM, Lentze MJ, Bode U, Simon A.** 2007. [Human Metapneumovirus in hospitalized children - a review]. *Klinische Padiatrie* **219**:58-65.
403. **Zeitlin PL, Lu L, Rhim J, Cutting G, Stetten G, Kieffer KA, Craig R, Guggino WB.** 1991. A cystic fibrosis bronchial epithelial cell line: immortalization by adeno-12-SV40 infection. *American journal of respiratory cell and molecular biology* **4**:313-319.
404. **Reeves EP, Williamson M, Byrne B, Bergin DA, Smith SG, Grealley P, O'Kennedy R, O'Neill SJ, McElvaney NG.** 2010. IL-8 dictates glycosaminoglycan binding and stability of IL-18 in cystic fibrosis. *J Immunol* **184**:1642-1652.
405. **Pezzulo AA, Tang XX, Hoegger MJ, Alaiwa MH, Ramachandran S, Moninger TO, Karp PH, Wohlford-Lenane CL, Haagsman HP, van Eijk M, Banfi B, Horswill AR, Stoltz DA, McCray PB, Jr., Welsh MJ, Zabner J.** 2012. Reduced airway surface pH impairs bacterial killing in the porcine cystic fibrosis lung. *Nature* **487**:109-113.
406. **Ambort D, Johansson ME, Gustafsson JK, Nilsson HE, Ermund A, Johansson BR, Koeck PJ, Hebert H, Hansson GC.** 2012. Calcium and pH-dependent packing and release of the gel-forming MUC2 mucin. *Proc Natl Acad Sci U S A* **109**:5645-5650.
407. **Quinton PM.** 2008. Cystic fibrosis: impaired bicarbonate secretion and mucoviscidosis. *Lancet* **372**:415-417.

408. **Connolly SA, Lamb RA.** 2006. Paramyxovirus fusion: real-time measurement of parainfluenza virus 5 virus-cell fusion. *Virology* **355**:203-212.
409. **Lamb RA, Paterson RG, Jardetzky TS.** 2006. Paramyxovirus membrane fusion: lessons from the F and HN atomic structures. *Virology* **344**:30-37.
410. **Zhou Y, Frey TK, Yang JJ.** 2009. Viral calciomics: interplays between Ca²⁺ and virus. *Cell calcium* **46**:1-17.
411. **Amarasinghe GK, Dutch RE.** 2014. A calcium-fortified viral matrix protein. *Structure* **22**:5-7.
412. **Leyrat C, Renner M, Harlos K, Huiskonen JT, Grimes JM.** 2014. Structure and self-assembly of the calcium binding matrix protein of human metapneumovirus. *Structure* **22**:136-148.
413. **Gerasimenko JV, Tepikin AV, Petersen OH, Gerasimenko OV.** 1998. Calcium uptake via endocytosis with rapid release from acidifying endosomes. *Current biology : CB* **8**:1335-1338.
414. **Yuan P, Thompson TB, Wurzburg BA, Paterson RG, Lamb RA, Jardetzky TS.** 2005. Structural studies of the parainfluenza virus 5 hemagglutinin-neuraminidase tetramer in complex with its receptor, sialyllactose. *Structure* **13**:803-815.
415. **Rhim AD, Kothari VA, Park PJ, Mulberg AE, Glick MC, Scanlin TF.** 2000. Terminal glycosylation of cystic fibrosis airway epithelial cells. *Glycoconjugate journal* **17**:385-391.
416. **Kube D, Adams L, Perez A, Davis PB.** 2001. Terminal sialylation is altered in airway cells with impaired CFTR-mediated chloride transport. *American journal of physiology. Lung cellular and molecular physiology* **280**:L482-492.
417. **Glaser L, Stevens J, Zamarin D, Wilson IA, Garcia-Sastre A, Tumpey TM, Basler CF, Taubenberger JK, Palese P.** 2005. A single amino acid substitution in 1918 influenza virus hemagglutinin changes receptor binding specificity. *J Virol* **79**:11533-11536.
418. **Imai M, Kawaoka Y.** 2012. The role of receptor binding specificity in interspecies transmission of influenza viruses. *Current opinion in virology* **2**:160-167.
419. **Nicholls JM, Chan RW, Russell RJ, Air GM, Peiris JS.** 2008. Evolving complexities of influenza virus and its receptors. *Trends Microbiol* **16**:149-157.
420. **Rossman JS, Jing X, Leser GP, Lamb RA.** 2010. Influenza virus M2 protein mediates ESCRT-independent membrane scission. *Cell* **142**:902-913.
421. **Lamb RA, Kolakofsky, D.** 2001. Paramyxoviridae: The Viruses and Their Replication, p. 1305-1340. *In* Knipe D, Howley, PM., Griffin, DE., et al. (ed.), *Fields Virology*, 4th ed, vol. 2. Lippincott-Raven Press, New York.
422. **Ohnishi S, Yoshimura A.** 1984. [Infectious cell entry mechanism of enveloped viruses]. *Uirusu* **34**:11-24.
423. **Yoshimura A, Kuroda K, Kawasaki K, Yamashina S, Maeda T, Ohnishi S.** 1982. Infectious cell entry mechanism of influenza virus. *J Virol* **43**:284-293.
424. **Mukherjee S, Ghosh RN, Maxfield FR.** 1997. Endocytosis. *Physiological reviews* **77**:759-803.
425. **Hallak LK, Spillmann D, Collins PL, Peeples ME.** 2000. Glycosaminoglycan sulfation requirements for respiratory syncytial virus infection. *J Virol* **74**:10508-10513.
426. **Brooks R, Williamson R, Bass M.** 2012. Syndecan-4 independently regulates multiple small GTPases to promote fibroblast migration during wound healing. *Small GTPases* **3**:73-79.

427. **Epand RM.** 1985. Diacylglycerols, lysolecithin, or hydrocarbons markedly alter the bilayer to hexagonal phase transition temperature of phosphatidylethanolamines. *Biochemistry* **24**:7092-7095.
428. **Holm BA, Wang Z, Notter RH.** 1999. Multiple mechanisms of lung surfactant inhibition. *Pediatric research* **46**:85-93.
429. **Koehler DR, Martin B, Corey M, Palmer D, Ng P, Tanswell AK, Hu J.** 2006. Readministration of helper-dependent adenovirus to mouse lung. *Gene therapy* **13**:773-780.
430. **Koehler DR, Frndova H, Leung K, Louca E, Palmer D, Ng P, McKerlie C, Cox P, Coates AL, Hu J.** 2005. Aerosol delivery of an enhanced helper-dependent adenovirus formulation to rabbit lung using an intratracheal catheter. *The journal of gene medicine* **7**:1409-1420.
431. **Hiatt P, Brunetti-Pierri N, Koehler D, McConnell R, Katkin J, Palmer D, Dimmock D, Hu J, Finegold M, Beaudet A, Carey D, Rice K, Ng P.** 2005. 815. Aerosol Delivery of Helper-Dependent Adenoviral Vector into Nonhuman Primate Lungs Results in High Efficiency Pulmonary Transduction with Minimal Toxicity. *Mol Ther* **11**:S317-S317.
432. **Stocker AG, Kremer KL, Koldej R, Miller DS, Anson DS, Parsons DW.** 2009. Single-dose lentiviral gene transfer for lifetime airway gene expression. *The journal of gene medicine* **11**:861-867.
433. **Kremer KL, Dunning KR, Parsons DW, Anson DS.** 2007. Gene delivery to airway epithelial cells in vivo: a direct comparison of apical and basolateral transduction strategies using pseudotyped lentivirus vectors. *The journal of gene medicine* **9**:362-368.
434. **Cmielewski P, Anson DS, Parsons DW.** 2010. Lysophosphatidylcholine as an adjuvant for lentiviral vector mediated gene transfer to airway epithelium: effect of acyl chain length. *Respiratory research* **11**:84.
435. **Council P** 2008., posting date. Trial shows anti-HIV microbicide is safe, but does not prove it effective. [Online.]
436. **Morris GC, Lacey CJ.** 2010. Microbicides and HIV prevention: lessons from the past, looking to the future. *Current opinion in infectious diseases* **23**:57-63.
437. **Marais D, Gawarecki D, Allan B, Ahmed K, Altini L, Cassim N, Gopolang F, Hoffman M, Ramjee G, Williamson AL.** 2011. The effectiveness of Carraguard, a vaginal microbicide, in protecting women against high-risk human papillomavirus infection. *Antiviral therapy* **16**:1219-1226.
438. **Levendosky K, Mizenina O, Martinelli E, Jean-Pierre N, Kizima L, Rodriguez A, Kleinbeck K, Bonnaire T, Robbiani M, Zydowsky TM, O'Keefe BR, Fernandez-Romero JA.** 2015. Griffithsin and Carrageenan Combination To Target Herpes Simplex Virus 2 and Human Papillomavirus. *Antimicrob Agents Chemother* **59**:7290-7298.
439. **Homaira N, Rawlinson W, Snelling TL, Jaffe A.** 2014. Effectiveness of Palivizumab in Preventing RSV Hospitalization in High Risk Children: A Real-World Perspective. *International journal of pediatrics* **2014**:571609.
440. **Hussman JM, Li A, Paes B, Lanctot KL.** 2012. A review of cost-effectiveness of palivizumab for respiratory syncytial virus. *Expert review of pharmacoeconomics & outcomes research* **12**:553-567.
441. **Resch B.** 2014. Respiratory Syncytial Virus Infection in High-risk Infants - an Update on Palivizumab Prophylaxis. *The open microbiology journal* **8**:71-77.

442. **Jinno A, Park PW.** 2015. Role of glycosaminoglycans in infectious disease. *Methods Mol Biol* **1229**:567-585.
443. **Hendricks GL, Velazquez L, Pham S, Qaisar N, Delaney JC, Viswanathan K, Albers L, Comolli JC, Shriver Z, Knipe DM, Kurt-Jones EA, Fygenon DK, Trevejo JM, Wang JP, Finberg RW.** 2015. Heparin octasaccharide decoy liposomes inhibit replication of multiple viruses. *Antiviral Res* **116**:34-44.
444. **Radhakrishnan A, Yeo D, Brown G, Myaing MZ, Iyer LR, Fleck R, Tan BH, Aitken J, Sanmun D, Tang K, Yarwood A, Brink J, Sugrue RJ.** 2010. Protein analysis of purified respiratory syncytial virus particles reveals an important role for heat shock protein 90 in virus particle assembly. *Molecular & cellular proteomics : MCP* **9**:1829-1848.
445. **Brock SC, Heck JM, McGraw PA, Crowe JE, Jr.** 2005. The transmembrane domain of the respiratory syncytial virus F protein is an orientation-independent apical plasma membrane sorting sequence. *J Virol* **79**:12528-12535.
446. **Monterisi S, Favia M, Guerra L, Cardone RA, Marzulli D, Reshkin SJ, Casavola V, Zaccolo M.** 2012. CFTR regulation in human airway epithelial cells requires integrity of the actin cytoskeleton and compartmentalized cAMP and PKA activity. *J Cell Sci* **125**:1106-1117.

Vita

Edita Klimyte

Birthplace: Kaunas, Lithuania

Education:

B.S., Biochemistry (2010), Michigan State University

B.A., Spanish Language and Literature (2010), Michigan State University

Professional Positions:

Graduate Teaching Assistant (2012), Department of Molecular and Cellular Biochemistry, University of Kentucky

Professorial Assistant (2007-2010), Department of Zoology, Michigan State University

Scholastic and Professional Honors:

MD/PhD Scholarship, University of Kentucky, Lexington, KY, USA, 2010 – 2018

Graduate Student Travel Award, University of Kentucky, Lexington, KY, USA, 2013 – 2016

3MT Competition 3rd Place Winner, University of Kentucky, Lexington, KY, USA, 2015

ACTS Burroughs-Wellcome Fund Trainee Travel Award, Washington, D.C., USA, 2015

American Society for Virology Graduate Student Travel Award, USA and Canada, 2013, 2015

IDSA/NIH Infectious Diseases Research Career Development Meeting Travel Award, Bethesda, MD, USA 2014

American Physician Scientist Association Institutional Travel Award, Chicago, IL, USA, 2014

Best Poster Presentation by a Pre-Doctoral Scholar, Department of Biochemistry Annual Retreat, University of Kentucky, Lexington, KY, USA, 2013

Experimental Biology Travel Award, Boston, MA, USA, 2013

Saha Cardiovascular Research Award, University of Kentucky, Lexington, KY, USA, 2013

Family of Medicine Scholarship for medical Spanish immersion, San José, Costa Rica, 2011

Department of Family Medicine Community Service Recognition Award, University of Kentucky, Lexington, KY, USA, 2011

Larry D. Fowler Undergraduate Research Scholarship, Michigan State University, East Lansing, MI, 2009

MPI Research Grant, Michigan State University, East Lansing, MI, 2008-2009

College of Natural Science Undergraduate Research Support Scholarship, Michigan State University, East Lansing, MI, 2008

Research Support:

National Research Service Award F30 Individual Predoctoral MD/PhD Fellowship, National Institute of Allergy and Infectious Diseases

05/01/2015-05/30/2018

Center for Clinical and Translational Science TL1 Predoctoral Fellowship, University of Kentucky

08/01/2014-04/30/2015

Professional Student Mentored Research Fellowship, University of Kentucky

07/01/2011-05/30/2012

Professional Publications:

Kimyte, E., Smith, S., Oreste, P., Lembo, D., and R. E. Dutch. Inhibition of human metapneumovirus binding to heparan sulfate blocks infection in human lung cells and airway tissues. *Submitted*.

Research Presentations:

Blocking viral access to heparan sulfate reduces HMPV infection in human lung cells. American Society for Virology, London, Ontario, Canada. 2015.

Blocking viral access to heparan sulfate reduces HMPV infection in human lung cells. Gordon Conference, Girona, Spain. 2015.

Potential for therapeutic development: Blocking viral access to heparan sulfate reduces HMPV infection in human lung cells. AOA Groves Memorial Research Day, Lexington, KY, USA. 2015.

Human metapneumovirus F protein histidine 434 associated with a hyperfusogenic phenotype. National Institute of Allergy and Infectious Diseases and Infectious Diseases Society of America Research Career Meeting, Bethesda, MA, USA. 2014.

Variability in fusogenic activity of Human metapneumovirus fusion protein from different strains. American Society for Virology, Hershey, PA, USA. 2013.

Studies of Human Metapneumovirus Fusion and Entry. Clinical and Translational Science Seminar Series, University of Kentucky, Lexington, KY, USA. 2012

Health advocacy across the health professions: How our student-led effort to improve patient access and outcomes evolved into an interprofessional leadership development opportunity. AAFP Global Health Workshop, San Diego, CA, USA. 2011.

Alternative hypothesis concerning human disease and models of compensatory evolution in tRNAs via experiments in *Saccharomyces cerevisiae*. Society of Molecular Biology and Evolution Conference, Iowa City, Iowa. 2009.

Edita Klimyte